# Trace element analysis in precious metals using Time Resolved Emission Spectroscopy

by

**Martha Maria Julsing**

Submitted in partial fulfilment of the requirements for the degree

MAGISTER SCIENTIAE
Chemistry

In the Faculty of Natural and Agricultural Science

University of Pretoria

Pretoria

October 2002

Universiteit van Pretoria
University of Pretoria

# Trace element analysis in precious metals using Time Resolved Emission Spectroscopy

by

Martha Maria Julsing

Leader: Prof. Dr. C. A. Strydom

Department of Chemistry

University of Pretoria

Degree: Magister Scientiae
Chemistry

## SYNOPSIS

Determining the purity of precious metals has received considerable scientific attention, mainly because of the high intrinsic value of these precious metals.
These metals are extremely useful as catalysts in the chemical and petroleum industry. They have been used as exhaust catalysts and as conductors in the electrical industry, in medical and dental applications as well as in the jewellery industry.

Two methods of analysis are used to determine the purity of metals; the direct and indirect method of analysis. During the direct method of analysis, the actual percentage of metal is directly determined. Techniques used are the Fire Assay, gravimetrical wet chemical techniques. However, these techniques are not suitable for characterising individual precious metals and impurities.

Indirect methods, based on spectroscopy, are well suited for the analysis of high purity metals. Using these techniques, the various impurities and their concentrations are determined and the purity of the metal is determined by difference. It is therefore

important that all impurities are determined with the highest degree of precision and accuracy, as this influences the ultimate purity and quality of the product.

A method was developed to determine the impurities in Ruthenium. The limits of detection obtained were in some instances improved up to a factor of ten times, compared to the current techniques used for the determination of the impurities. Elements such as Cd, Se, As and Cr which were previously reported as not detected, due to the difficulty of detecting them at levels below 10–15 ppm, are now measurable using the spark spectrometer. Making use of time resolved spectroscopy has in general increased the sensitivity by a factor of five to ten times, even when compared to normal spark analysis as used for Alloys.

The technique used in this study in the analysis of impurities in precious metals is known as SAFT (Spark Analysis For Traces). SAFT involves the use of time resolved spectroscopy, which is able to reduce background and thus improve signal to background ratios of spectral lines. It makes use of the phenomenon of "atomic afterglow". By switching the photomultiplier detector to observe (measure) only the afterglow, the background radiation can be separated from the atomic radiation.

The technique is very sensitive and analyses of purities at 99.995 % are possible. However, the greatest drawback of the method when used for precious metals is the lack of commercially available standard samples for low concentration of impurity.

# Spoorelementanalise vir platinum metale met behulp van tydontledings Emissiespektroskopie

deur

Martha Maria Julsing

Studieleier: Prof. Dr. C. A. Strydom

Departement Chemie

Universiteit Pretoria

Graad: Magister Scientiae
Chemie

## SAMEVATTING

Suiwerheidbepaling van edelmetale geniet baie wetenskaplike aandag hoofsaaklik as gevolg van hulle hoë intrinsieke waarde. Hierdie metale is baie waardevol en word as katalisators in die chemise en petrochemiese industrie bebruik, asook uitlaat-systeemkatalisatore en as geleiers in die elektriese industrie, mediese- en tandheelkunde en juweliersindustrieë.

Daar is twee tipes analise vir die bepaling van suiwerheid van metale: 'n direkte en indirekte metode van analise. Die direkte metode van analise, bepaal die persentasie waarde van die metaal op 'n direkte wyse. Hierdie metodes sluit in, traditionele essaieering, gravimetriese en nat chemiese tegnieke. Hierdie tegnieke is nie geskik vir karakterisering van individuele edelmetale en onsuiwerhede nie.

Indirekte metodes is gebaseer op spektroskopie en is geskik vir die hoë suiwerheid analise van metale. Hierdie tegnieke bepaal die konsentrasie van die onsuiwerhede. Die suiwerheid van die metal word bepaal deur die verskil. Om hierdie rede is dit baie belangrik dat al die onsuiwerhede bepaal word met die hoogste graad van presisie en akkuraatheid, omdat dit 'n invloed sal hê op die uiteindelike suiwerheid en kwaliteit van die produk.

Die alternatiewe metode is ontwikkel om die onsuiwerhede in Ruthenium te bepaal. Die deteksie limiete in sommige gevalle het met 'n faktor tot tien verbeter, invergelyking met huidige tegnieke wat gebruik word vir die bepaling van onsuiwerhede. Elemente soos Cd, Se, As en Cr was voorheen as onbepaald geraporteer omdat deteksie limiete laer as 10–15 ppm nie moontlik was nie, maar nou wel moontlik is met vonkanaliese.

Die tegniek gebruik vir die analiese van onsuiwerhede in die edelmetale is bekend as SAFT " Spark Analysis For Traces" (Vonkanaliese vir spoorelemente). SAFT maak gebruik van tydontledingsspektroskopie, wat agtergrond kan verminder en daardeur die sein tot agtergrond verhouding van spektrale lyne verbeter.

Dit maak gebruik van die atoomgloei. Deur die fotovermenigvuldigerdetektor te skakel om slegs die atoomgloei waar te neem kan die agtergronduitstraling geskei word van die atoom uitstraling. Die sensitiwiteit is 'n faktor van vyf tot tien keer beter as met normale vonkanalise.

Die tegniek is baie sensitief en analise met suiwerhede van 99.995 % is moontlik, alhoewel die grootste nadeel van die metode vir edelmetale is die gebrek aan kommersieële beskikbare standarde met laë konsentrasie onsuiwerhede in.

**ACKNOWLEDGEMENTS**

My thanks to;

Impala Platinum Refineries, for the opportunity to conduct the experiments and the use of their instrument. Also to the staff of the Precious Metals laboratory for their assistance.

Dr. Pat Butler, for allowing me the opportunity to continue with my studies, his mentorship and valuable discussions over the years.

Spectro Analytical Instruments for the financing of my studies.

Prof. Dr. C. A. Strydom, for her help, guidance and encouragement.

Prof. C.J. Rademeyer, for his help in the initial stages.

My husband, Dr. Herman Julsing and my daughters Claire and Andrea for their love and support.

# CONTENTS

# Chapter 1

## Brief Overview

### *1.1 Introduction*

In this investigation an alternative method for determining the impurities in Ruthenium was developed. The limit of detection for most elements lies between 0.1 and 10 μg/g. The technique has provided producers of the precious metals with a quick turnaround time and an accurate method for production control and certification of their final products.

Determining the purity of precious metals has received considerable scientific attention, mainly because of the high intrinsic value of these precious metals.
These metals are extremely useful as catalysts in the chemical and petroleum industry, as exhaust catalysts, and as conductors in the electrical industry; they have medical and dental applications as well as uses in the jewellery industry. Precious metals include platinum (Pt), palladium (Pd), rhodium, (Rh), ruthenium (Ru) iridium (Ir), osmium (Os); when gold (Au) and silver are included these are often referred to as noble metals.

Traditionally, fire assay methods have been used, and are still being used, especially for the analysis of gold [1]. However, this technique is not suitable for characterising individual precious metals. Gravimetric methods have been used to establish the purity of the metal, but these methods have limitations, not only with regard to precision and accuracy, but also with regard to their inability to identify the impurities and to quantify them.
Problems associated with the determination of impurities by means of wet chemical methods probably encouraged the early application of spectrochemistry [2].

During 1928, Gerlach and Schweizer worked on spectrographic analysis of the platinum metals, and these methods are still used today [3]. They developed the spectral analysis as a quantitative method, using the method of internal reference.

Techniques with good detection ranges such as the packed electrodes (DC and AC arcs), generally for non-metallic powders (e.g. ores), and the globular arc for metallic materials, were introduced [3]. These techniques have been used with considerable success. However, the shortage of photographic plates, the demand for higher speed, precision and accuracy as well as the necessity of determining more elements in the deep ultra violet spectral region have resulted in other methods being developed. The use of photoelectric measurement of spectral line intensities has reduced the turn-around times, eliminating the calculations from photographic plates.

Spectrometers operating with controlled spark discharge and photomultiplier measurement were developed in the 1940s in the USA and were imported to Europe in the 1950s for metal analysis [4]. However, there were some problems associated with this technique. The calibrations were suspect, due to oxidation by air at the spark area. Elements important for steel manufactures are C, P and S, which all have their best analytical lines in the spectral region below 200nm, and air strongly absorbs this radiation. The detection limits range from 10 to 100 μg/g. The technique is based on the principle that the impurities are determined, quantified, and then subtracted from 100 % to determine the purity of the metal. The limits of detection are therefore most significant and the impurities must be determined with the highest degree of precision and accuracy.

In the 1960s the vacuum spectrometer was introduced and argon rather than air was used as discharge atmosphere to overcome some of the abovementioned problems. The spark and arc sources were developed for the analysis of conductive materials. The spark is a more precise emission source than the arc source, but it has been considered to be insensitive for purities in excess of 99,9 %. This is mainly due to the intense background radiation in spark excitation, which adversely affects the signal to background ratio, and in turn, the limit of detection [4].

The technique used for the analysis of impurities (pertaining to this study) in precious metals is known as SAFT (Spark Analysis For Traces). SAFT involves the use of time resolved spectroscopy, which for many years has been known to reduce

background and thus improve line / background ratios of spectral lines. It makes use of the phenomenon of "atomic afterglow". In this study, the excitation characteristics of individual sparks were studied to relate the emission of spectral lines to time. It was observed that the background radiation, due to electron effects, closely followed the electrical discharge. Radiation from ion lines caused severe background. The radiation from atom lines persisted after the electrical discharge had decayed. This was termed the "after glow". By carefully switching the photomultiplier detector to observe (measure) only the after glow, the background radiation can be separated from the atomic radiation. This radiation is integrated and used for the analysis. The sensitivity is a factor of ten times greater than in normal spark analysis [5].

The optimisation of the technique requires developing ideal parameters for discharge, time resolution, prespark, integration and selection of analytical reference lines for the individual base. Reference materials for calibration are not easily obtainable. The effect of cross-contamination in the spark chamber when moving from one base material to another will be investigated.

The analysis of precious metals using SAFT / Time Resolved OES has been found to be extremely reliable and successful. It has been installed in three refineries in South Africa, namely Rand Refinery, Impala Platinum and Lonplats, in Europe at Degusa and in Russia. The limit of detection for most elements lies between 0.1 and 10 μg/g. The technique has provided producers of precious metals with a quick turnaround time and an accurate method for production control and certification of their final products.

The certification of purity has given rise to some discussion. In the gold industry it has been the practice to add up all the limits of detection (LOD) for all the accepted impurities and to presume this value to be the total amount of impurities. The purity value of the gold is determined by the difference. This often results in the sum of the impurities being higher than the actual impurity quantity present, and the purity thus being underestimated. In the pgm (Platinum Group Metals) industry, (using spectrographic techniques) producers accept half the LODs as the possible quantity present and sum these up to determine the impurities. This improves the certified

purity of the metal, but it remains debatable how many and which elements should be taken into account. Standard levels of trace elements in the different materials are specified by the ASTM (American Society for Testing Materials) methods according to their grade produced [6]. The method of analysis is a matter of agreement between the manufacturer and the purchaser. The elements which definitely contribute to the impurities present and the materials used in the process should be included in the calculation to determine the purity of the metal. It is therefore important that the spectrometer should be programmed to identify all possible impurities.

The high speed simultaneously measuring Time Resolved Optical Emission Spectroscopy (SAFT) (Spark Analysis for Traces) technique thus fulfils, to a great extent, the analytical requirements of both the producers and consumers of precious metals.

## *1.2 References*

[1] W.C. Lenahan, R. de L. Murray-Smith, **Assay and Analytical Practice in the South African Mining Industry.** Johannesburg: **CTP Book Printers** (1986) 41

[2] C. Casparrini, **The Fire Assay Technique for the Analysis of the precious metals, its potential and its Limitations.** Ontario, Canada: Minmet Scientific Limited (1989) 581-589

[3] W.Gerlach, E. Schweizer, **Chemical Analysis by Emission Spectroscopy. Part 1, Principles and Methods.** Leipzig:**Leopold Voss.** (1930) 42

[4] K. Slickers, **Automatic-Atomic-Emission Spectroscopy.** Germany: **Brühlsche Universität Druckerei.** (1993) 181-191

[5] K. Slickers, **Automatic-Atomic-Emission Spectroscopy.** Germany: **Brühlsche Universität Druckerei** (1993) 358-370

[6] **American Society For Testing Material, ANSI/ASTM B 561-73** (1979) 653

# Chapter 2

## Chemistry and Refining of the Platinum Group Metals

### *2.1 Introduction*

Six elements of group VIII (in the periodic table) have been collectively designated the "platinum group metals" (pgm). Included in this group are platinum (Pt), palladium (Pd), rhodium (Rh), ruthenium (Ru), Iridium (Ir), and Osmium (Os). Sometimes called "noble metals", (when gold and silver are included) because of their resistance to oxidation, these precious metals are present in very low concentrations in the earth's crust. In spite of their limited availability, these metals (and chemical compounds containing them) are extremely useful as catalysts in the chemical and petroleum industries, as conductors in the electrical industry, in extrusion devices, in dental and medical prostheses, and in jewellery [1]. In their traditional applications, the platinum-group metals have been considered relatively innocuous, with respect to direct environmental impact. However, some new and more extensive uses of these materials have both a direct and an indirect impact on human health. Some of the complexes produce allergic reactions (e.g. platinosis) in humans [2]. Other complexes are used as anti-tumour agents in cancer chemotherapy [2].

In order to obtain these precious metals in pure form, two principal stages are involved: firstly, the extraction of concentrate from the ore body and, secondly, the refining of individual metals. This involves the separation of the pgm's from each other for their purification. Refining also applies to scrap and other recycled metal.

### *2.2 Occurrence*

Mineral species of the platinum metals are sperrylite, $PtAs_2$; cooperite, (Pt,Pd,Ni)S; potarite, PdHg or $Pd_3Hg_2$; stibiopalladinite, $Pd_3Sb$; and laurite, $(Ru,Os)S_2$ [1] .
The economically significant sources of platinum metals are situated in South Africa, Canada, and the U.S.S.R [3]. They are primary deposits usually associated with ultra

basic rock formations and copper and nickel sulphide deposits. The abundance of the six platinum metals in the earth's crust appears to be very low. The South African sources are the most concentrated at values between 4-10 ppm. These sources are in the Bushveld Igneous Complex and constitute at least 80 % of known world reserves [4]. The best-known source is the Merensky reef, discovered in 1925.

In Canada the platinum metals occur mainly in copper and nickel sulphide ores in the Sudbury area of Ontario and in the Thompson-Wabowden area of Manitoba. In the U.S.S.R., the richest sources are in the Noril'sk region of Siberia. Almost 90 % of the platinum metal consists of platinum and palladium. The Johns-Manville Corporation found a large deposit of platinum and palladium in the Stillwater Complex area in Montana, U.S.A. [2].

The first platinum to be identified came from South America and was taken to Europe from the New World in the seventeenth century (1735) by a Spanish astronomer Ulloa, as an almost undesirable adjunct of gold [5]. The name "platina" first applied to this material by the Spaniards means "little silver" – a debased form, perhaps, of silver. Watson gave the first scientific description of platinum. William Wollaston, who also discovered palladium and rhodium, obtained pure platinum for the first time in 1803 [6]. Palladium was named after the asteroid Pallas and rhodium (from the Greek rhodon, rose), after the rose red colour of its salt [5]. In 1804 Tennant isolated iridium and osmium from a black residue left after the dissolution of native platinum in aqua regia. The various colours of iridium salts were behind the naming of the metal (from the Greek iris, or rainbow). Osmium, or "odorous", derived its name from its strong odour. Professor Karl Karlovih Klaus of Kazan University, discovered ruthenium in 1844, and named it in honour of Russia [5]. In the nineteenth century, extensive placer deposits in the Ural Mountains of Russia constituted the main source of platinum metals [2].

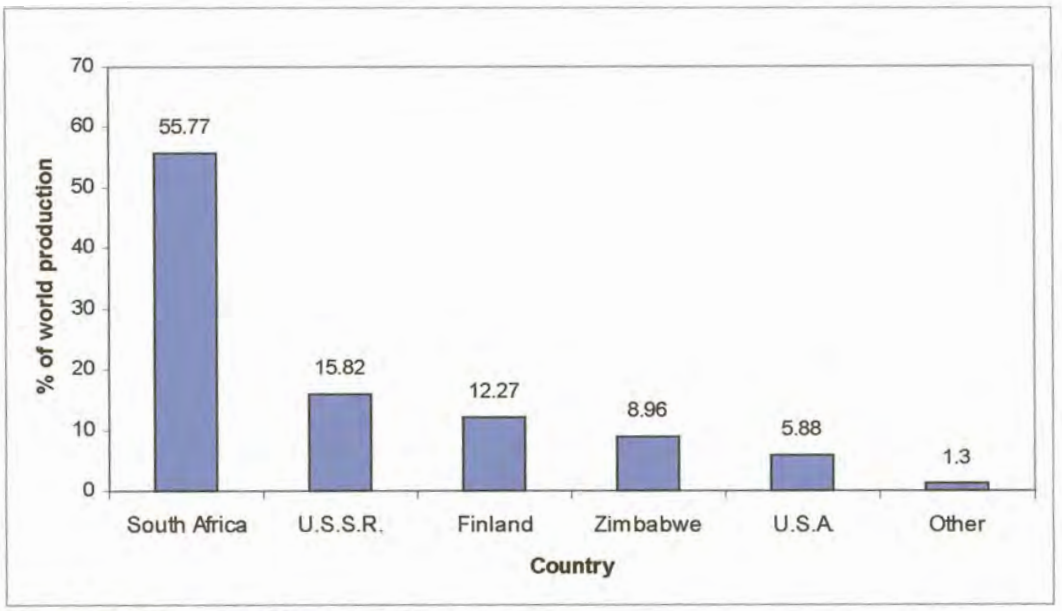


**Fig. 2.1 Distribution of Precious Group Metal resources [7].**

## *2.3 Uses*

The industrial applications of platinum metals are based on their high resistance to corrosion and catalytic activity, specific surface properties, stable electrical and thermo-electrical characteristics, wear resistance and mechanical properties at elevated temperatures.

Precious metals and the chemical compounds containing them are extremely useful in industry. The biggest demand for platinum is as catalyst in the chemical and petroleum industry. Platinum alloys are used in the electrical industry as conductors, in extrusion devices, in dental and medical prostheses, and in jewellery. Some of the complexes are used as anti-tumour agents in cancer chemotherapy [8]. Platinum has a high resistance to fluorine compounds, including hydrofluoric acid at high temperatures [9].

Palladium is used mainly as a catalyst in the chemical industry [10], but also as constructional material for protective sheaths and linings. Palladium is often used as

a substitute for the more expensive platinum, for contacts in electrical relays and in dental alloys [5].

Rhodium's main application is as an electrode coating, because of the hardness and high reflectivity of the deposit. Electrical contacts in components of radio-frequency circuits also make use of rhodium [9].

Iridium is used as an additive to harden platinum and palladium and for making extrusion dies for high melting glasses [9]. Iridium is highly resistant to attack from a wide range of molten metals, molten salts and oxides [9].

Ruthenium is used mainly to harden palladium and platinum alloys and as an additive for osmium alloys. It is also used as a catalyst for specific reactions [9].

Osmium alloys are used where extreme hardness is required. Instrument pivots are an example of such an application [9].

Supply and demand of some of the Platinum Group Metals

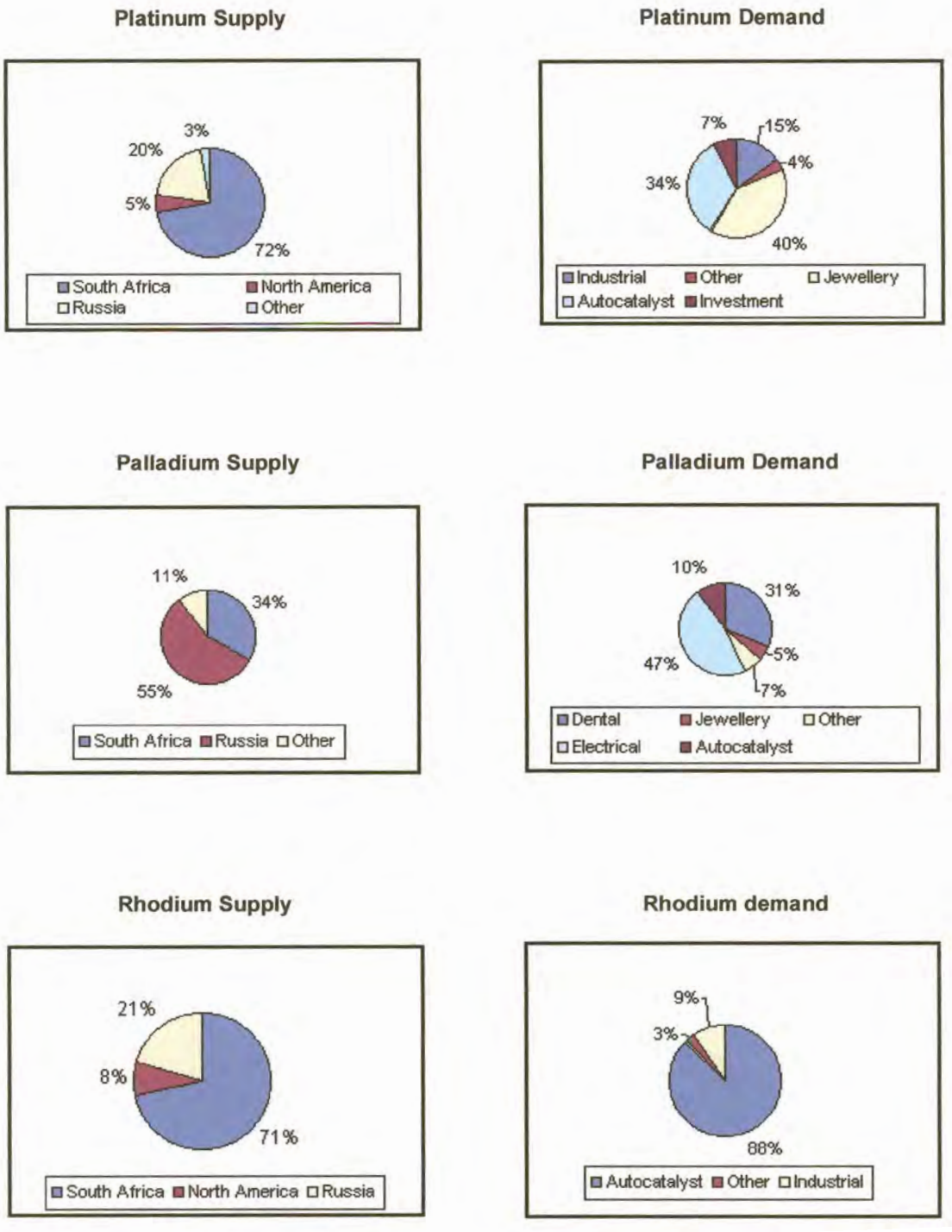


**Fig. 2.2 Supply and demand of some of the platinum group metals [3].**

### *2.3.1 Catalytic uses*

*Naphtha reforming:* Platinum is dispersed on small pellets of alumina or silica-alumina which, being porous, expose a large specific surface area of the metal. The petroleum fractions fed to the reactors comprise hydrocarbons, which boil between 100-200 °C and generate hydrogen during the process. The reactions increase the octane rating of the gasoline fraction and produce a large amount of aromatic hydrocarbons that may be separated from the product and used for purposes other than fuel [2].

*Exhaust gas control:* Ceramic honeycomb materials impregnated with platinum or other platinum metals have been produced and used for exhaust-gas purification [2]. These materials can oxidise a wide array of noxious substances that may be emitted from industrial plants or vehicles.

*Ammonia-oxidation:* The Ostwald process, used for manufacturing of nitric acid, entails oxidation of ammonia with air to form nitric oxide. This is accomplished by passing synthesis gases through gauze beds of an alloy of platinum and 10 % rhodium at pressures of about 8 atm [11].

*Sulphur-dioxide oxidation:* The burning of fuels containing sulphur, followed by the passing of the combustion products over a platinum catalyst, is one way of producing sulphuric acid. The use of platinum as a catalyst for this reaction resulted in the first patent ever issued in the field of catalysis [12].

*Hydrogen-cyanide manufacture:* By passing a mixture of air, ammonia and methane through gauze of 10 % rhodium platinum alloy, hydrogen cyanide is formed. This reaction is known as the Andrussow process [13]. Higher conversion efficiency is achieved in the newer process, which uses only methane and ammonia. This exothermic reaction is carried out in alumina reactor tubes coated inside with platinum catalyst [13].

*Hydrogenation:* Palladium, as a powdered monoxide, reduced in situ by hydrogen, produces the metal in a finely divided form [14]. Calcium carbonate, magnesium oxide, activated carbon and silica gel can be impregnated with soluble palladium compounds and can be used in an alternative production process [14]. These compounds are dried and reduced and then used as support catalysts.

*Dehydrogenation:* Platinum metal catalysts have been used for a wide range of oxidation and dehydrogenation reactions in organic chemistry [2]. Higher temperatures than for hydrogenation are required, which shifts the equilibrium towards the formation of the desired product. Palladium is mostly used for this application and is commonly supported on carbon black at 5-30 wt % metal [2].

*Co-ordination complexes of the Platinum-Group Metals as catalyst:* Rhodium halide complex with an iodide promoter is used as a catalyst for the conversion of methanol to acetic acid. This is performed with 99 % selectivity through insertion of carbon monoxide at a pressure of 1 atm. [2].

*Other industrial or commercial catalytic applications:*

- The synthesis of hydrogen peroxide based on the auto-oxidation of 2-ethylanthraquinol; the quinol is converted to the corresponding quinone and hydrogen peroxide [2].
- The oxidation of ethylene to acetaldehyde with the aid of palladium chloride, $PdCl_2$, catalyst. This process is also known as the Wacker process [2].
- Osmium and ruthenium tetroxides have been used as oxidative catalysts in organic chemistry [2].
- The synthesis of high-molecular-weight polymethylenes from carbon monoxide and hydrogen makes use of ruthenium as catalyst. This takes place under pressure [2].

*Low-temperature catalytic heaters:* Portable heaters, which burn hydrocarbons, and cigarette lighters, make use of the process. Hydrocarbons and light alcohols are mixed with air and passed as vapour over a platinum surface [15]. This enhances the emission of the heat of combustion.

### 2.3.2 Electrical uses

*Contact for relays and switchgear:* Palladium is used in industry for the production of electrical contacts. Palladium, either gold coated or alloyed with copper or silver, has been used for telephone switchgear [9].

*Resistors and capacitors:* Windings in wire-wound potentiometers and precision resistors make use of Pd and 40 % Ag because of the low temperature coefficient of resistance of the compound [9].

*Electrochemical electrodes:* Anodes made from platinum and platinum-clad electrodes are often used, since this material resists oxidation and there is a high overpotential for the formation of oxygen [9].

*Spark electrodes:* Aircraft engines make use of platinum for the electrodes in spark plugs. These operate at high temperatures under extremely corrosive conditions. The lead deposits from the fuel can cause disintegration of the electrodes if these are not made of pgm's. Alloys with ruthenium, palladium and tungsten have been successfully used for this purpose.

### 2.3.3 High-temperature uses

*Platinum-resistance thermometers:* Part of the range of the International Temperature Scale is defined in terms of the platinum-resistance thermometer [9]. This lies between the boiling point of oxygen (-182.97 °C) and the melting point of antimony (650.5 °C). For this purpose, extremely pure platinum is required with the ratio of its resistance at 100 °C and 0 °C to be not less than 1.3910:1 [2].

*Thermocouples:* For high temperature measurement, platinum and platinum-rhodium elements are used. Thermocouples from base metals cannot tolerate temperatures higher than 1000 °C. Higher temperature thermocouples make use of platinum alloys

and iridium and these alloys have been the most promising basis for developing high-temperature thermocouples above 2000 °C [16].

*Laboratory ware*: Platinum and platinum alloys are used for high temperature laboratory equipment such as crucibles, tips of tongs and combustion boats [9].

### *2.3.4 Medical and dental uses*

Cancer chemotherapy is the primary medical use in humans of the platinum-group metals, although palladium chloride and palladium hydroxide have been used to treat tuberculosis and obesity [17]. Colloidal palladium hydroxide injections (5-7 mg/day) reportedly caused a 19 kg weight loss in a 3-month period, with necrosis at the injection site. Palladium alloys are used in the crowning of teeth and also as a bonding agent during the capping of teeth with porcelain [16].

Ultra pure and precisely engineered micro gold seeds are irradiated in a nuclear reactor. The irradiated seeds become useful radioactive isotopes clinically suitable for permanent implants to eradicate tumours in cancer patients [18]. Precious metals and their alloys find applications in medical devices such as pacemaker electrodes, brachytherapy implants and catheter guidewires. This is because of their biological inertness and radio-opaque properties [17].

### *2.3.5 Jewellery*

Platinum and palladium have been used in the jewellery industry. Palladium alloys containing 4 % ruthenium and 1 % rhodium are used most, while "white gold" is an Au-Pd alloy [5].

## *2.4 Physical and chemical properties*

Six elements of group VIII (in the periodic table) have been collectively designated the "platinum-group metals." Included in this group are platinum (Pt), palladium (Pd), rhodium (Rh), ruthenium (Ru), iridium (Ir) and Osmium (Os). The pgm's are also

referred to as "noble metals" because of their resistance to oxidation and a combination of high sublimation energy and high ionisation potential [19].

Platinum and palladium are similar in appearance: grey-white metals that are malleable and ductile [20]. They have high melting points and show considerable resistance to corrosion. The platinum group metals have relatively low conductivity and platinum has the lowest coefficient of expansion of any of the metals. Platinum is unaffected by any single mineral acid, but is readily dissolved by aqua regia. It reacts with chlorine and, at high temperatures, with fused caustic alkalis, nitrates and peroxides. Platinum readily forms alloys with many of the less active metals, therefore easily reducible oxides should not be heated in platinum vessels [19]. Platinum exhibits the following oxidation states: +1, +2, +3, +4, and +6. Of these, the +2 and +4 are most abundant.

Unlike platinum, palladium dissolves in concentrated acids, particularly nitric acid. The metal forms a series of complex compounds and assumes the +2 and +4 oxidation states. Palladium has the lowest melting point and the highest volatility of the platinum group metals [19].

Ruthenium, also a greyish white metal, is harder and more brittle than platinum. Ruthenium forms compounds in which it exhibits the oxidation states +2, +3, +4, +6, +7 and +8 (as in the volatile tetroxide, $RuO_4$) [20].

Rhodium is a ductile, malleable metal. Like the other metals in this group, rhodium has a number of different oxidation states: +1, +2, +3, +4, and +6, of which the +3 and +4 are most abundant [20]. Rhodium is readily attacked by chlorine when heated and the reaction is accelerated under pressure. It is highly resistant to acids and aqua regia.

Osmium is a brittle metal and hard enough to scratch glass. Osmium unites readily with oxygen to form $OsO_4$. Although not an acid, it has been called osmic acid due to its corrosive properties, which result from the high oxidising power of the +8 oxidation state. Oxidation states of +2, +3, +4 and +6 also exist.

Iridium is a hard and brittle metal, which has the greatest density of any known substance [20]. Chlorine attacks the metal as in rhodium and it resists the action of aqua regia. The most important oxidation states of iridium are +3 and +4.

It should be noted that the chemical activities of compacted metal platinoids differ substantially from those of a powder and sponge refined material [6]. Traces of impurities, including other platinum metals, cause marked changes in some properties, such as hardness, tensile strength and electrical resistance. Beamish, McBryde and Barefoot pointed out that the failure to achieve a high state of purity has led to lack of agreement on the values of the various physical properties as determined by different investigators [21]. The platinum metals have the tendency to absorb gases such as hydrogen and oxygen, which has a significant influence on the physical properties of the metals [2]. There is an unexpected, and as yet unexplained, feature of alloy formation in platinum and palladium: the occurrence of extensive miscibility gaps in some alloy systems prepared at lower temperatures, whereas the same system prepared at higher temperatures exhibits complete miscibility.

### *2.5 Effect of Platinum Group Metals on human health*

In their traditional applications, the platinum-group metals have been considered relatively innocuous with respect to direct environmental impact. However, some new and more extensive uses of these materials may have both a direct and an indirect impact on human health. Physiologic activity is associated with some platinum-group metal compounds [2,17]. Among the platinum-group elements, the allergic reaction is evidently peculiar to platinum. Some of the complex salts produce allergic reactions such as platinosis in humans, and a few of the volatile oxides are very toxic.

"Platinosis" has been defined as "the effects of soluble platinum salts on people exposed to them occupationally" [17] .The condition is characterised by pronounced irritation of the nose and upper respiratory tract, with sneezing and coughing. In

some cases, radiographic examination of the lungs has indicated a low-grade pulmonary fibrosis. Later, the "asthmatic syndrome" develops, with coughing, tightness of the chest, wheezing, and shortness of breath, becoming progressively worse with extended exposure. People with light complexion, light hair, blue eyes, and delicate textured skin appear to be more susceptible than darker-skinned people [22]. Skin tests are done on laboratory and refinery workers to check for allergy sensitivity for platinum salts. The skin testing procedures for Type I (immediate) allergies are the prick test, the scratch test and the intracutaneous test. The prick test is the most acceptable, being the simplest, the safest and the most precise. It is performed by pricking, with a gentle lifting motion, through a drop of test solution into the superficial epidermal layer, with a separate fine needle for each preparation. When this is carefully done, and preferably on the flexural surface of the forearm, no blood is drawn and no reaction is elicited at control or negative sites [22,2]. The sensitivity of the test is shown by positive reaction to the prick test. The reaction is indicated by a weal, an erythematous flare and often accompanied by itching. There are many other tests, such as Type II (autoallergic), Type III (immune-complex, complement-dependant), patch test Type IV (contact dermatitis), and nasal and bronchial tests, but they are beyond the scope of this dissertation [22].

## 2.6 *Toxicology – environment*

The toxicology of the platinum-group metals includes the study not only of the six metals themselves, but also of their compounds. The catalytic converters using platinum, palladium and rhodium to control motor vehicle exhaust emissions cause quantities of the metals and their compounds to enter the environment. Radio ruthenium enters the environment through the waste effluent from nuclear-fuel reprocessing plants [23]. The human population may ultimately be exposed to these metals through the skin, by inhalation and orally. The toxic and potentially toxic effects of platinum on humans are caused by the water-soluble salts (potassium hexachloroplatinate, potassium tetrachloroplatinate, sodium chloroplatinate and ammonium chloroplatinate), and not by platinum itself [23]. It has been reported that dermatitis has resulted from contact with platinum oxides and chlorides.

## 2.7 *Refining of Platinum Group Metals*

There are two stages in the isolation of reasonably pure platinum metals from raw materials. One is the extraction of a concentrate of precious metals from an ore body, and the other the refining of the precious metals, which involves their separation from the concentrate and from each other and ultimately their purification. Refining applies not only to native sources of raw and new material but also to scrap and used material. Due to the high intrinsic value of the metals, their chemical inertness and physical durability, the metal is recycled. A specialised technology is involved in separation and purification, for which a fee or toll is charged; hence "toll refining".

A typical treatment route of the precious metals is as follows:

FEED → CONCENTRATE → MATTE → REFINERY FEED → FINISHED METALS.

The initial stage of the recovery process is a metallurgical flotation process. The ore from the mining process is ground to a fine powder and, in the form of a pulp, treated with various chemical reagents. The pulp is pumped into large agitation tanks and a large volume of air is introduced from the bottom. The sulphide minerals float to the top of the tank on the resulting air bubbles, where they overflow. This contains the concentrate of minerals of interest, which has a pgm content one or two orders of magnitude higher than the ore and a small quantity of silicates. The unwanted silicate gangue minerals sink to the bottom of the tank and are removed. The concentrate is then melted in an electrical furnace at temperatures in excess of 1200 °C. When the concentrate is molten, the high density of the sulphides allows them to sink to the bottom of the furnace, while the silicates form a separate upper layer. The two layers are separated by removing them from the furnace through separate tapping holes at appropriate heights. The precious group metals are now contained as what is known as a matte. In South Africa this is essentially a copper nickel sulphide compound, containing low levels of iron and cobalt, and still smaller amounts of pgm's. The base metals are removed and separated by hydrometallurgical processes and a precious group metal concentrate is produced.

This pgm concentrate contains significant amounts of base metals and is dissolved in an oxidising acid. The pgm's are then separated from each other and from the remaining base metals by hydrometallurgical processes to produce finished metals with purities normally in excess of 99.9 % [3].

The metallurgical operation of the International Nickel Company in Sudbury, Ontario can be summarised as follows: the platinum-group metals are separated from the bulk of the copper and nickel during slow cooling of a Bessemer matte [24]. During the cooling process, the oxidation of sulphur is regulated to produce small amounts of metallic nickel and copper. The latter serve as collectors of the precious metal from the original ore, and the separation of the metallic phase is facilitated, as this phase is magnetic. The separated material is further pre-concentrated by electrolytic refining, yielding concentrates in the anodic slimes. The osmium is recovered by means of acid treatment and roasting of the sludges. The remainder is sent for refining.

In South Africa two thirds of platinum metal is recovered by means of gravity concentration alone [24,25]. The remainder can be obtained after smelting of the tailings, which contain appreciable amounts of copper and nickel.

The electrolytic anodic slimes and other rich concentrates are subjected to roasting and then acid leaching to extract copper, nickel, or other base metals. Under these conditions the osmium may form a volatile tetroxide and may be totally or partially lost.

If the osmium needs to be recovered, dried anodic sludges are treated with sulphuric acid but the temperatures are limited and not allowed to exceed 200 °C [24,25]. This renders copper and nickel soluble, but leaves the platinum metals insoluble (less than 5 % of the osmium will volatilise). The insoluble residue is dried and ignited at 800-900 °C. This volatilises about 85 % of the osmium as the tetroxide $OsO_4$. The tetroxide is absorbed in an alkaline scrubbing solution and retained for further purification [26]. The ignited acid-soluble residue is freed of sulphur, selenium and

arsenic by this treatment. This residue is then treated with aqua regia, which dissolves most of the platinum, palladium and gold. The gold is precipitated by addition of a ferrous salt. After separation of the gold, ammonium chloride is added to precipitate the yellow salt, ammonium hexachloroplatinate $(NH_4)_2PtCl_6$, which is separated and ignited to yield the metal. For further purification, the platinum is redissolved in aqua regia and the solution is evaporated gently with sodium chloride and hydrochloric acid to destroy oxides of nitrogen and nitrosyl compounds [24,25]. The solution of sodium hexachloroplatinate (IV), $Na_2PtCl_6$, is then treated with sodium bromate and its pH carefully raised to cause precipitation of the hydrous oxides of any rhodium, iridium or palladium that has been carried down in the initial precipitation of platinum. After removal of solids by filtration, the solution is boiled with hydrochloric acid to destroy bromate, and then treated with ammonium chloride for a second precipitation of platinum as ammonium hexachloroplatinate (IV). This precipitate is filtered off, dried and slowly ignited to 1000 °C. The product obtained is a grey platinum sponge with purity in excess of 99.9 %.

The remaining filtrate contains palladium as chloropalladous acid, $H_2PdCl_4$. Aqueous ammonia is added to precipitate diammine dichloride, $Pd(NH_3)_2Cl_6$ (yellow complex), which is redissolved in an excess of ammonia due to the formation of the complex ion, $Pd(NH_3)_4^{2+}$ [24,25]. The insoluble diammine dichloride is reprecipitated by the addition of hydrochloric acid. Successive precipitation and redissolution of this compound further purify palladium in the same way. The purified compound is then ignited and a grey palladium sponge is produced. The ignited sponge is usually cooled in a hydrogen atmosphere to avoid superficial oxidation.

The undissolved residue is treated further to recover silver, rhodium, iridium, ruthenium and osmium. Treatment of these products varies at different refineries and details are not always disclosed nor are they uniform. These techniques have always been a sensitive issue in the platinum industry and are kept confidential. However, in one instance, [24] the insoluble residue is treated with a combination of fluxes to produce a lead alloy containing the precious metals. Nitric acid is used to dissolve the lead and silver. The insoluble residue is then fused with sodium bisulphate, which selectively converts rhodium to water-soluble sulphate. Rhodium hydroxide,

$Rh(OH)_3$, is precipitated when the solution is made alkaline. The precipitate is separated and dissolved in hydrochloric acid. Impurities carried through this stage are later separated by hydrolytic precipitation in the presence of nitrite. The rhodium is later precipitated as ammonium hexanitrorhodate (III), $(NH_4)_3Rh(NO_2)_6$. Hydrochloric acid is added to this compound and chlororhodite forms. This solution is passed through an ion-exchange column to remove traces of base metals. Rhodium is finally precipitated from this purified solution with formic acid, dried, and ignited under hydrogen to a residue or very pure metallic sponge. The remaining metallic material is heated with sodium peroxide at 500 °C to convert ruthenium and osmium (if not previously recovered) to water-soluble salts sodium ruthenate, $Na_2RuO_4$, and sodium osmate, $Na_2OsO_4$. The volatile tetroxides are distilled off. The osmium and ruthenium are separated at this stage since the osmium can be distilled from nitric acid solutions while the ruthenium is retained in the pot as nitrosyl complexes.

Distilled osmium tetroxide is collected in a solution of sodium hydroxide, usually containing alcohol. The absorbate is then digested with ammonium chloride, during which process osmyltetrammine chloride, $OsO_2(NH_3)_4Cl_2$, precipitates. This compound is then dried and ignited in hydrogen to form osmium metal sponge. The ruthenium is precipitated by the addition of ammonium chloride as hexachlororuthenate (III), $(NH_4)RuCl_6$. This may be heated in an inert atmosphere to yield the metal.

If larger amounts of osmium are present, the amount of nitric acid required for their removal as trioxide may result in an alternative precipitation form for ruthenium, namely, pentachloronitrosylruthenic acid (III), $H_2RuCl_5NO$ [24].

The previously mentioned fusion with sodium peroxide converts iridium to its dioxide, which is insoluble in water. This may be brought into solution by treatment with aqua regia. Ammonium hexachloroiridate salt, $(NH_4)_2IrCl_6$, is precipitated by the addition to this solution of ammonium chloride and nitric acid. Dissolving this salt in an ammonium sulphide solution, in which iridium remains soluble, may further purify this salt, while impurities are precipitated as before. The salt is ignited in an atmosphere of hydrogen to yield a pure sponge of the metal. More recently, solvent extraction

and ion-exchange techniques for the recovery of the platinum group metals have been used [25].

## *2.8 References*

[1] Kallmann Slive, **The survey of the determination of the platinum group elements,** Talanta Vol 34, No 8, (1987) 677-698

[2] The National Research Council, **Platinum Group Metals, Sub Committee on Platinum Group Metals, Committee on Medical and Biological effects of environmental pollutants,** (1976) 14-65

[3] N.J. Randolph, J.C.I. Min. Proc. Res. Labs. Knights, **Pure and Applied Chemistry, Vol 12,** (1993) 2411-2416

[4] W.C. Lenahan, & R. de L. Murray-Smith, **Assay and Analytical Practice in the South African Industry, J**ohannesburg: **CTP Book Printers,** (1986) 507

[5] C.F. Vermaak, **The Platinum-Group Metals: A global perspective,** Mintek, (1995) 1-83, 133-181

[6] E. Savitsky, V. Polyakova, N. Gorina, & N.Roshan, **Physical Metallurgy of Platinum Metals,** Moscow: MIR Publishers, (1978) 331-355

[7] S.M. Linski, **Trace enrichment and determination of platinum using a FIA-ICP system,** Master Scientiae, University of Pretoria, (1997) 10

[8] N.N.Greenwood, A.Earnshaw, **Chemistry of the Elements,** Oxford: Pergamon Press, (1990) 1064-1066, 1242-1355

[9] J.C. Bailar, H.J. Emeléus, Sir Ronald Nyholm, A.F. Trotman-Dickenson, **Comprehensive Inorganic Chemistry,** Volume 3, Oxford Pergamon Press, (1973) 1181-1185

[10] A. J. B. Robertson, **The early review of catalysis, Platinum Metals Review,** (1975) 19:64-69

[11] B.H.J. Bell, **Platinum Catalyst in ammonia oxidation: Platinum Metal Review,** (1960) 4:122-126

[12] A.J.B. Robertson, **The early history of catalysis: Platinum Metal Review,** (1975) 19:64-69

[13] J.M. Pirie, **The manufacture of hydrocyanic acid by the Andrussow process, Platinum Metal Review,** (1958) 2:7-11

[14] P.N. Rylander, **Palladium Catalyst in organic Chemistry, Properties and uses, New York: Academic Press,** (1968) 159-181

[15] J.D. Mac Connell, **Low temperature catalytic heaters: The cataheat range of flameless combustion systems. Platinum Metal Review,** (1972) 16: 16-21

[16] F.R.Hartley, **Chemistry of the platinum Group Metals: Recent developments, Amsterdam** : Elsevier , (1991) 9-31

[17] M.J.Abrams, **The use of Precious metals in medicine,** Johnson Matthey, West Chester, Proc. International Precious metals Institute, (1992) 165

[19] J.Ching, **Gold system for the treatment of cancer,** Engelhard West, Anaheim, Proc. International Precious metals Institute, (1992) 129

[19] F.R. Hartley, **The Chemistry of Platinum and Palladium,** London: Applied Science Publishers LTD, (1973) 1-5

[20] H.H. Sisler, C.A. VanderWerf, & A.W. Davidson, **College Chemistry,** Third edition, New York, The Macmillan Company, (1967) 800-805

**[21]** F.E. Beamish, A.E. McBryde, R.R. Barefoot, **The Platinum Metals, in Rare metals Handbook,** Second edition, London: Reihold , (1961) 304

**[22]** A.E. Roberts, Platinosis: **A 5-year study of the effects of soluble platinum salts on employees in the platinum laboratory and refinery,** A.M.A. Arch.Ind.Hyg. Ocup. Med., (1951) 4:549-559

**[23]** S.O. Freedman, J. Krupey, **Respiratory allergy caused by platinum salts,** (1968) 42: 233-237

**[24]** F.S.Clements, **Twenty-five years progress in platinum metals refining, Ind. Chemist,** (1962) 38:345-354

**[25]** R.I. Edwards, **The refining of the Platinum Group Metals. TMS Paper Selection No A57-59, New York: The Metallurgical Society of AIME**, (1964) 1075.21

**[26]** C. A. Hampel, Ed. **Rare Metals Handbook.** Second Edition, New York: Reinhold Publishing Corporation, (1961) 304-335

# Chapter 3

## Methods of analysis of Platinum Group Metals

In discussing "analysis of platinum group metals" three general modes of analysis come to mind.
(1) The determination of the individual pgm's as minor or trace concentrations in a particular matrix.
(2) The determination of precious metals in the range from mg/g to the high percentage region.
(3) The determination of trace impurities in pure refined platinum metals.

The context of this dissertation is the analysis of trace impurities in refined Ruthenium. This technique requires the concentration of all trace metal impurities to be determined and the calculation of the purity by difference. The impurities required for analysis are dictated by the American Standard of Testing Materials standard (ASTM standard) methods. For fine gold it is ASTM B562, for platinum ASTM B561, and for palladium ASTM B589, etc. [1].

The analysis of refined platinum may give rise to several problems. Refined pgm's are usually very pure, but contain many impurity elements at very low concentration levels [1]. Refined platinum metals are usually produced as powders called sponges. The distribution of impurities in these powders may be heterogeneous. Melting will homogenise the sample, but could drive off the volatile elements. Errors relating to trace element analysis occur at various steps from sampling to determination. The magnitude of error varies from sampling > sample preparation > determination.

Physical grinding and sieving can cause contamination if metal equipment is used. Losses of trace metals may result if a fraction of the sample is rejected. Chemical sample preparation is crucially important and no unanimity of opinion exists on the proper treatment for each sample type. Great care needs to be taken in calibration and preparation of calibration standards. Initially, problems were encountered when

dissolving platinum and determining trace elements by wet chemical methods. This probably encouraged the early use of spectrochemistry. In 1928, Gerlach and Scheitzer worked on the spectrographic analysis of the platinum metals [2,3]. Spectrographic analysis is still used today. Various other techniques are also used and will be discussed below.

### *3.1 Globular Arc*

For many years, the analysis of precious metal bearing material has utilised globular arc optical emission spectrometry [4]. The technique is highly sensitive but suffers from the fact that the arc burns either in air or with a sheath gas of argon and oxygen. Strong absorption of either radiation by oxygen or air at a wavelength of less than 210 nm is unavoidable. This prevents elements, which have their most sensitive analytical lines in the UV region, below 210 nm, from being measured. In globular arc analysis, an arc is created by striking a direct current arc between a carbon or graphite counter electrode and another electrode with a small cavity. The discharge is initiated either by momentarily bringing the two electrodes into contact or by creating a high voltage across them. A known quantity of the precious metals is placed in this cavity. Under the effect of the arc, the sample melts and forms a metal globule. Electrical heating of the tips of the electrodes causes the material to be vaporised and ionised. As the electrodes are drawn apart, the number of these ions multiplies and becomes capable of sustaining an electrical discharge across the gap. Thermal energy created by the electrical resistance to movement of electrons and ions within the gap is sufficient to vaporise material continuously from the tip of the sample electrode. The material is broken down into atoms and ions within the electrical plasma discharge where species can become excited to higher electronic orbital states. When atoms are in this excited state they fall back to their ground state and line spectra are emitted at characteristic wavelengths and subsequently detected by the spectrometer.

### 3.1.1 Disadvantages of Globular Arc analysis

Globular arc is a method, which requires special expertise. It is also tedious and time-consuming. The technique makes use of photographic plates recording the spectra. Data interpretation from photographic systems is time-consuming and relies on the evaluation of a skilled individual [5].

### 3.1.2 Matrix effects

Fractional distillation causes elements to evaporate at different rates and the excitation of the various elements is interdependent. This means that the results may change with the composition of the matrix. This can, however, be overcome with closely matched standard reference materials.

### 3.1.3 Poor limits of detection

The system operates in air or in an argon/oxygen atmosphere. This has a limitation in that the most sensitive wavelengths, which are in the ultra violet region, cannot be used.

### 3.1.4 Poor precision

Due to arc wandering the source is not consistent, which has an influence on the precision. The dc discharge follows the line of least resistance, usually from some high point on the surface of the sample electrode. This high point (an individual mineral grain) heats up, becomes vaporised and is rapidly eroded. The dc arc then wanders to an adjacent grain that now offers the line of least resistance. In practice, the discharge wanders quite rapidly across the surface of the sample electrode, causing large fluctuations in the corresponding optical emission signal. Even at concentrations above the detection limit the precision is poor unless long exposure times are used.

### 3.1.5 *Low analytical throughput*

The procedure requires samples to be weighed and cut into small pieces to load into electrodes. This is time-consuming and labour intensive. The developing of photographic plates and reading also takes a long time. When direct reading techniques are used, great care must be taken to observe the arc and maintain the correct gap. Burn times are relatively long.

### 3.1.6 *Skilled labour*

Operators must be well trained, as data evaluation from photographic plates requires skill and experience.

### 3.1.7 *Cost*

Running cost is high because of the high cost of electrodes and photographic plates or film. The photographic plates are not readily available and are produced only on demand.

Since the application of solid-state detectors, direct current arc spectrometry has once again become important. The reason is the possibility of simultaneous background correction offered by the application of a solid-state detector [6]. Using background correction, the instability of the dc arc discharge can be corrected for. The simultaneous measurement of the background with the solid-state detector is taken 0.02 and 0.1 nm away from the peak position [5]. This reduces the baseline noise significantly, giving better detection limits. The other advantage of the solid-state detector system is the ability to analyse many different matrices by the same excitation technique. The detection limits are lower for all trace elements than for the detection limits using spark excitation.

The great disadvantage of the technique, especially for the precious metal industry, is the rather high sample consumption of approximately 400 mg of material per run. Another distinct disadvantage is the difficulty the system has in the analysis of

elements absorbing energy in the UV region. Very long integration times are necessary if trace values in this range are to be determined.

### *3.2 Glow Discharge technique*

The glow discharge technique [7] has been used for the analysis of precious metals and gives extremely high precision of measurement because all parameters such as current, voltage and gas pressure may be controlled accurately [8]. The Precious Metal Refinery at Degussa uses optical emission spectroscopy with glow-discharge excitation as a complementary technique to other spectroscopic methods [8]. The operating principle of the glow-discharge lamp is as follows. The body of the lamp, which is at earth potential, is the anode. The sample, which must be electrical conducting, vacuum tight, flat and smooth, is pressed onto the packing ring of the disc-shaped cathode. The smallest sample diameter permitted measures 20 mm. In order to avoid an electrical discharge between the sample surface and the front end of the anodic tube, which has a critical spacing of 0.15 to 0.20 mm, the space between the anode and cathode is evacuated separately. The cathode disc and the sample are water-cooled. In later generations the anode is also water-cooled. Argon gas pressure of 5-5 mbar, a voltage of 500-500 volt, is applied and a current of 50-200 mA. These parameters vary according to the analytical range required.

The glow-discharge analysis entails the erosion of the sample surface by cathode sputtering and the excitation of the atoms by electron collisions in the glow discharge layer. The sputtered sample material is deposited partly at the edge of the burning spot and partly in the anodic tube. The generated light, showing additional lines of the discharged gas, enters the spectrometer through a quartz window.

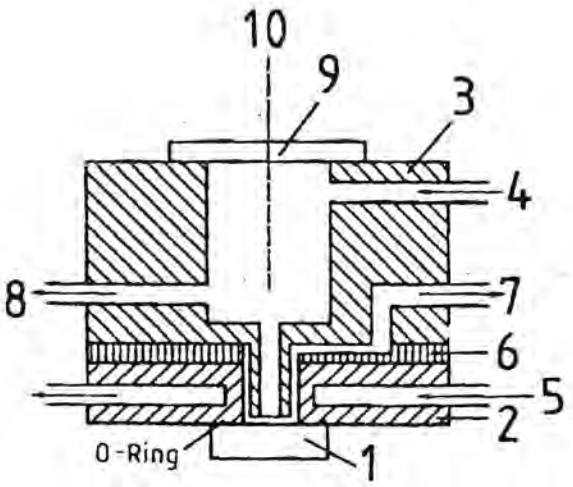


**Fig. 3.1 Glow Discharge lamp schematic diagram [9].**

**1= sample, 2=Cathode, 3= Anode, 4=Gas, 5=Cooling, 6=insulation, 7= Volume1, 8= Volume 2, 9= Window, 10=Radiation off take**

Lüschow [10] claims that uniform sputtering of the sample material results in good reproducibility. However, cathodic sputtering is highly dependent on the metallurgical history (crystalline structures) and also on the level and nature of the impurities in the metal. The sensitivity of this technique is also generally insufficient for the determination of several impurities. However, at Degussa they have found that the technique meets their requirements in determining the most important impurities directly in the metallic samples. Memory effects, theoretically, should not be a problem, even if the anode has not been cleaned. The argon ions are accelerated in the direction of the cathode, so it is impossible for atoms of the anode to be sputtered. The plasma temperature is not high enough for the anode material to evaporate. In practice, some memory effects did occur with the analysis of the precious metals. The possible cause for this could have been fine particles of the material adhering loosely to the inner walls of the anode and being carried into the discharge by the argon stream. Some internal design changes were made to reduce memory effects [8]. The anodes were designed with interchangeable tubes for each matrix, which could be unscrewed without moving the cathode disc.

Samples in the form of sponges and powders are best analysed as pressings. The ease of pressing the pgm decreases as the melting point increases [11]. Pd and Pt can be pressed at 30 bar. Rh and Ir do not become vacuum tight at that pressure. It is important that PGM-sponges and powders containing oxides be reduced under hydrogen in order to get a stable discharge. Potassium, as well as most of the volatile elements, are nearly completely lost by the hydrogen reduction and have to be determined by an alternative method.

Glow discharge occurs at low pressure (10-12 Torr). Narrow line widths are associated with a low-pressure discharge, resulting in better resolution [12]. Self-reversal of emission lines is absent due to the fact that there are no cold zones in the excitation regions. This ensures calibration curves with a wide linear range. Self-reversal occurs when identical atoms are present between the radiation source and the detector. The radiation is partly absorbed by these atoms because absorption and emission profiles show the same curve. Because of reduced intensity of the central wavelength the line profile changes and line broadening appears. As the element concentration in the sample increases, the number of vapourised and unexcited atoms also increases, as well as the number of excited atoms emerging from plasma, and the probability of absorption increases. The glow discharge lamp and the inductively coupled plasmas have "optical thin" plasma in comparison to the dc arc, which has an "optical dense" plasma in relation to the analyte [13].

Professor Marcus and others [14,15] experimented, not with the original direct current glow discharge (DC GD) lamp, but with a radio frequency (RF) powered GD source. The high amount of sputter material presented no difficulties in the case of fine gold (99.99 %) (18 mg/min at a power of 120 W and a focal spot diameter of 8 mm), if the milling process for the cleaning of the anode cylinder was programmed appropriately [14]. The data from Marcus and co-workers using the RF powered GD produces significantly lower detection limits than the DC-GD. The comparatively low detection limits result, using the ratio of the analyte signal intensity to that of the spectral background adjacent to within 0.1 nm of the analytical wavelength [15]. Lüschow indicated his concern as to whether these are genuine background measurements [5].

### *3.3 Inductively Coupled Plasma (ICP)*

ICP is a multi-element technique, which was established as a powerful spectroscopic source during the mid-sixties, and many analytical applications of this technique were developed. Work was initiated by Greenfield [16] in 1964 and Wendt [17] and Fassel in 1965.

Inductively coupled plasma is formed when energy is transferred to a gas by means of an induction coil [18]. The torch consists of three concentric coaxial tubes made from quartz. These are for the auxiliary gas, coolant and nebuliser gas. The plasma forms above the inner tube. The induction coil normally Cu, surround the top end of the torch and is part of the radio frequency generator or oscillator circuit. Argon gas at atmospheric pressure flows upwards through the tube. The induction coil is connected to the generator, which operates in the region between 12 kW –14 kW. When RF power is applied to the coil an alternating current moves back and forth within the coil, or oscillates, at a rate corresponding to the frequency of the generator. The frequency is generally 27 or 40 megahertz (MHz).

A spark is applied to the gas causing some electrons to be stripped from their argon atoms. These atoms are then caught up in the magnetic field and accelerated. These high-energy electrons collide with other argon atoms and continue in a chain reaction, breaking the gas down into plasma consisting of argon atoms, electrons and argon ions, forming the inductively coupled plasma (ICP) discharge. The ICP discharge is then sustained within the torch and load coil as RF energy is continually transferred to it through the inductive coupling process [19].

**Fig. 3.2 Inductively Coupled Plasma [19].**

The liquid sample is nebulised into an aerosol, a fine mist of sample droplets, in order to be introduced into the ICP. The aerosol is carried through the centre of the plasma by the inner tube of the torch. Due to the high temperature achieved in the plasma (10 000 K) the aerosol is desolvated, vaporised and dissociated into atoms and ionisation and excitation takes place.

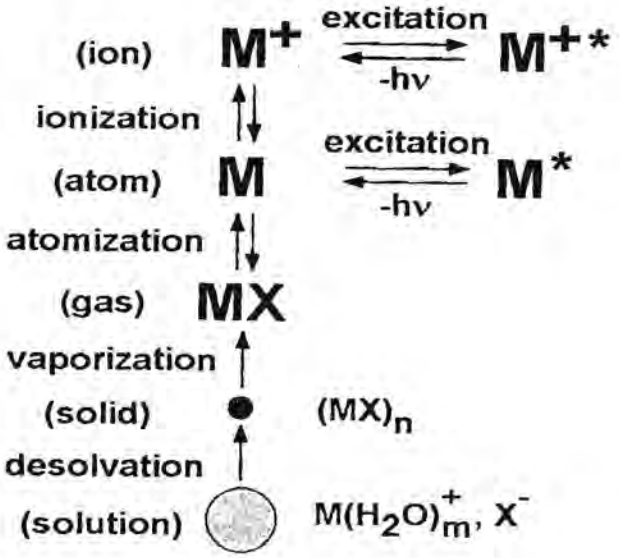


**Fig. 3.3 Process that takes place when a sample droplet is introduced into an ICP discharge [20].**

The excitation and ionisation process takes place in the initial radiation zone (IRZ) and in the normal analytical zone region (NAZ) of the plasma, from which the analyte emission is typically measured.

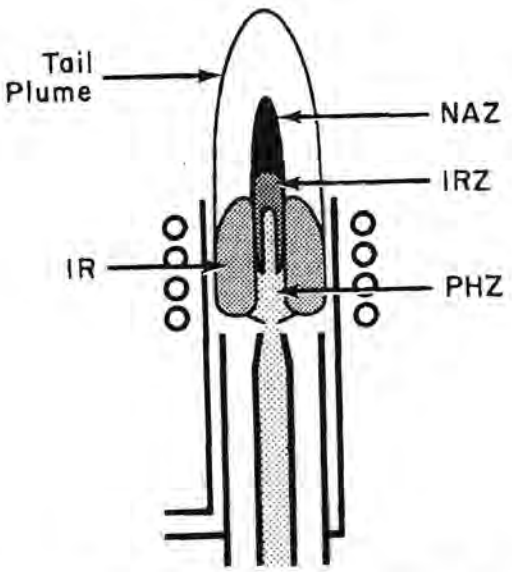


**Fig. 3.4 Zones of the plasma: IR – Induction region, PHZ – Pre-heating zone, IRZ – Initial radiation zone, NAZ – Normal analytical zone [19].**

Because the excited species in the plasma emit light at several wavelengths, the emission from the plasma is polychromatic. This polychromatic radiation must be separated into individual wavelengths so that the emission from each excited species can be identified and its intensity measured without interference at other wavelengths. The emitted light enters through an entrance slit of typically 10-25 μm and is focused on a diffraction grating to disperse the light into its various wavelengths. The separation of light according to wavelength is generally achieved using a monochromator for a single element at a time or a polychromator for multi-element determination. The actual separated light is detected by using a photosensitive detector such as a photomultiplier or a charge-coupled device.

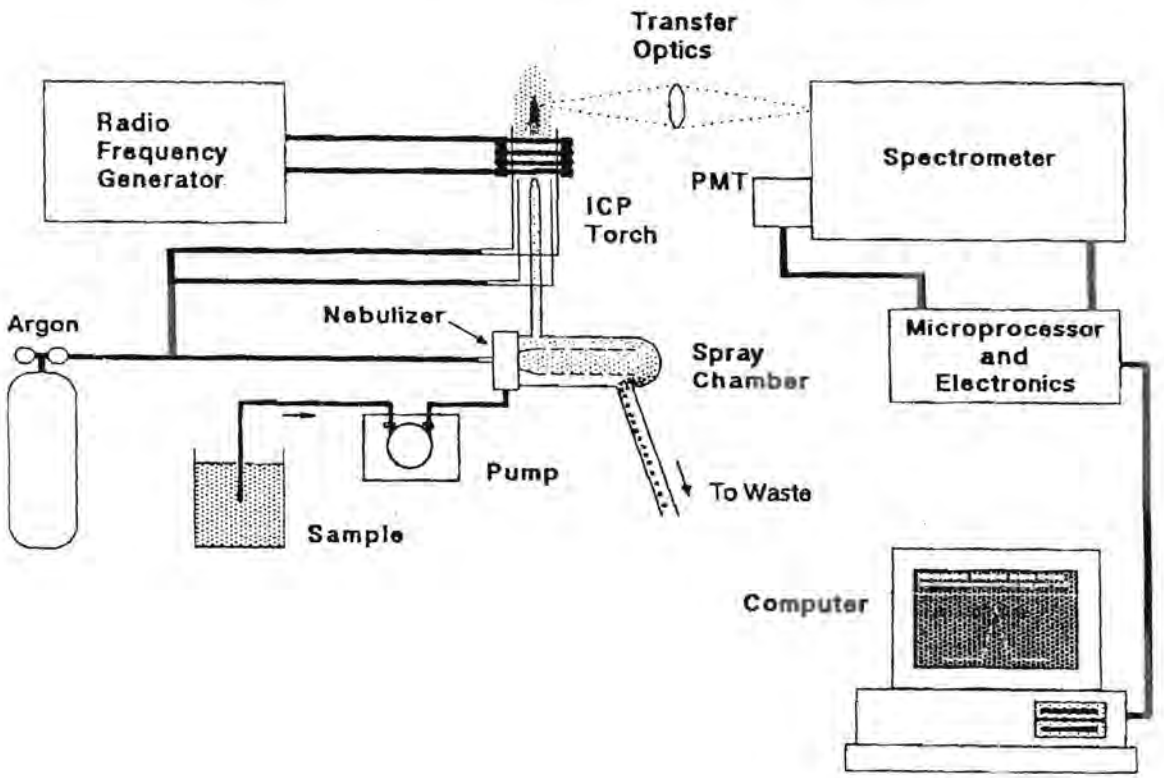


**Fig. 3.5 Layout of a typical Inductively Coupled Spectrometer [19].**

ICP has become a widely used technique and has replaced AAS (Atomic Absorption Spectrometry) in many laboratories for the determination of impurities in precious metals. This is due to the superior precision of ICP, and its simultaneous detection capabilities. Each element can be analysed at multiple wavelengths, minimising the

risk of unobserved bias due to unknown spectral interferences. The dissolution of precious metals leads to problems with dilution, contamination and the fact that some pgm's do not dissolve easily. Dissolution time is also a very serious factor in production.

Work done by Myers and Tracy [21] stipulated that by using internal reference standards the "noise", defined as the relative standard deviation (RSD) of the emission signal, could be reduced to less than 0.1 %. Internal standardisation eliminates the effect of density fluctuations arising from corresponding fluctuations of the sample density. Instrument drift is reduced and nebulisation improved since it is less sensitive to variations in liquid sample uptake rate. Internal standard addition is done by exact weighing.

ICP is used extensively for the analysis of pgm's at the analytical laboratory of Union Miniére Hoboken in Belgium [22]. ICP is a comparative technique and accuracy is therefore related to the quality of the standards. With all statistical tools (significance tests, outlier tests and control charts) for quality assurance in place, the accuracy for routine ICP measurement can be in excess of >99 %. Due to drift caused by unstable plasma and nebulisation conditions this is not always obtained. To obtain accurate and precise results for precious metals by ICP, measuring conditions must be optimised [22].

### *3.4 Inductively Coupled Plasma - Mass Spectrometry (ICP-MS)*

ICP is not only a powerful emission source, but it also ionises strongly. Its combination with mass spectrometric methods has generated another powerful technique with even lower detection limits. The same limiting factors with regard to the dissolution prevail although ICP-MS is more sensitive than inductively coupled plasma-optical emission spectroscopy (ICP-OES).

The instrument comprises an inductively coupled plasma source for ion production and a quadrupole mass spectrometer for ion detection and quantification. An interface links them together. For solution analysis the liquid sample is nebulised into

an inductively coupled plasma. The aerosol produced is sprayed into the spray chamber that removes large droplets (typically larger than15 μm in diameter). Within the plasma the aerosol is evaporated until a desolvated particle remains. Molecular species are decomposed into their constituent atoms, and a large percentage of the atoms are ionised by the energetic plasma environment. A fraction of these ions, (with an appropriate mass) then enters an interface region held at a pressure of 1 torr and then passes through a series of ion optic where it is focused at the entrance of the mass spectrometer. The mass spectrometer, held at a much lower pressure, serves as a mass filter and selectively transmits ions according to the ratio of their mass to their charge. The ions are detected by an electron multiplier and are quantified [23].

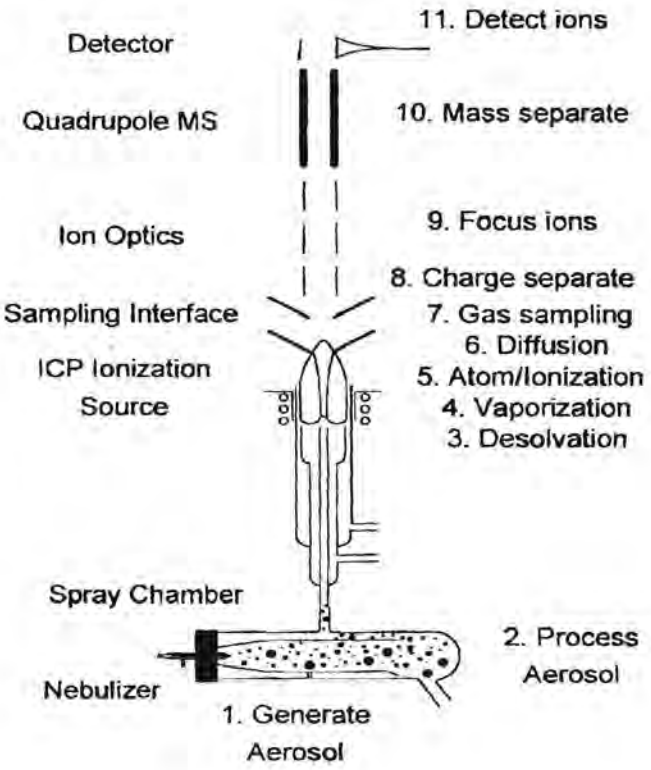


**Fig. 3.6 Schematic diagram of ICP-MS and reference- quadrople [23].**

Graham and Robért from Mintek [24] have established methods for the determination of trace level impurities in high purity noble metals and their salts. Spectral interferences are caused by the high concentration of the precious metals matrix and the acids used for sample preparation. With the exception of indium and caesium in the presence of ruthenium and bismuth in an iridium matrix, most of the precious metal oxides, which form alternative isotopes, can be selected for measurement. The presence of chlorides results in molecular ion interferences. The determination of $^{51}V$ $^{52}Cr$, $^{53}Cr$, $^{54}Cr$ isotopes is precluded due to be overlap of $ClO^+$ and $ClOH^+$ molecular ion formation. In a chloride solution, the analysis of $^{75}As$ and $^{77}Se$ isotopes has interference from the ArCl overlap. By introducing nitrogen gas (5 % v/v) with the argon carrier gas in the nebuliser the formation of $ArCl^+$ is minimised by the preferential formation of $NCl^+$ [24]. Due to the high matrix, the signal was suppressed between 5–30 % for the analyte elements. Internal standards, scandium, indium, and rhenium (100ng/ml) were found to compensate for the suppression. Na, Si, Ca, K and Fe cannot easily be measured by ICP-MS due to spectral interferences from background molecular ions.

The precision of measurement varies according to the concentration levels present and ranges between 0.72 and 49 % relative standard deviation for concentrations of 15 and 0.3 µg/g respectively [24]. Gray [25] commented that most of the limitations of the technique are now accepted as inherent and are accommodated by sample treatment and introduction methods as well as by the proper choice of plasma parameters. These instruments are, however, very sensitive and cross contamination by memory effects from other precious metals (usually the major impurities) is problematic. Wash out times and cleaning of the introduction systems, sampler and skimmer cones is fairly time-consuming, not favouring the technique for routine analysis in precious metal plants.

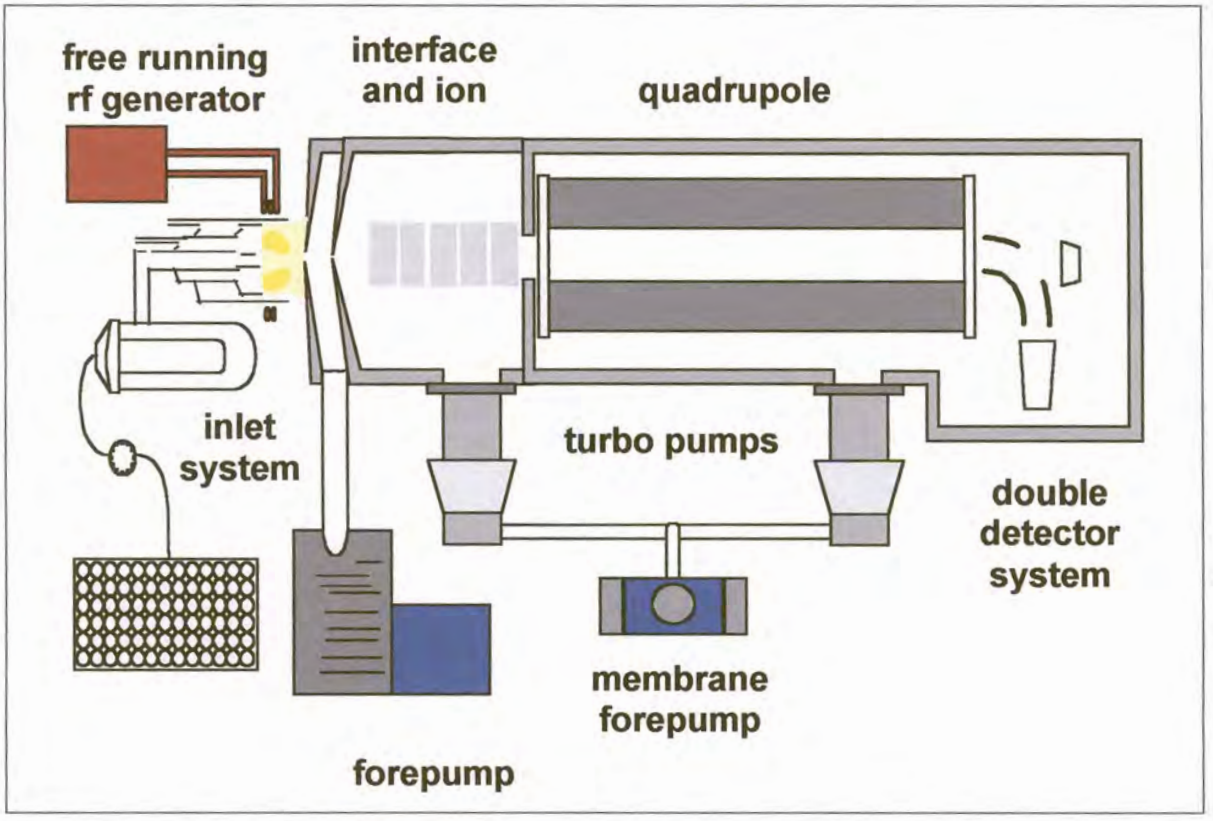


**Fig. 3.7 Schematic layout of Inductively Coupled Plasma Mass Spectrometer [20].**

### *3.5 Spark Ablation –Inductively Coupled Plasma*

The technique offers the possibility of direct impurity analysis in which sample ablation is produced by high voltage sparks and the resulting aerosol is transported into the ICP by an argon carrier gas stream without a nebuliser chamber, directly into the aerosol tube. In the spark a dense plasma (with self-absorption) is produced as the burning time is 0.1 msec (100 Hz spark sequence). The aerosol has fine particles (1 μm) and it reaches a constant density within a few seconds and after about 10 seconds a constant signal at the ICP. The plasma is optically thin without self-absorption, delivering linear calibration graphs over more than four orders of magnitude. Good limits of detection (LODs) have been achieved [26] but sensitivity, precision and contamination have made the method less attractive than others. From experience at the Degussa Laboratory in Hanau-Wolfgang (Dr. Lüschow), the

detection limits for Spark Ablation ICP/OES are less favourable than for spark spectrometry [8].

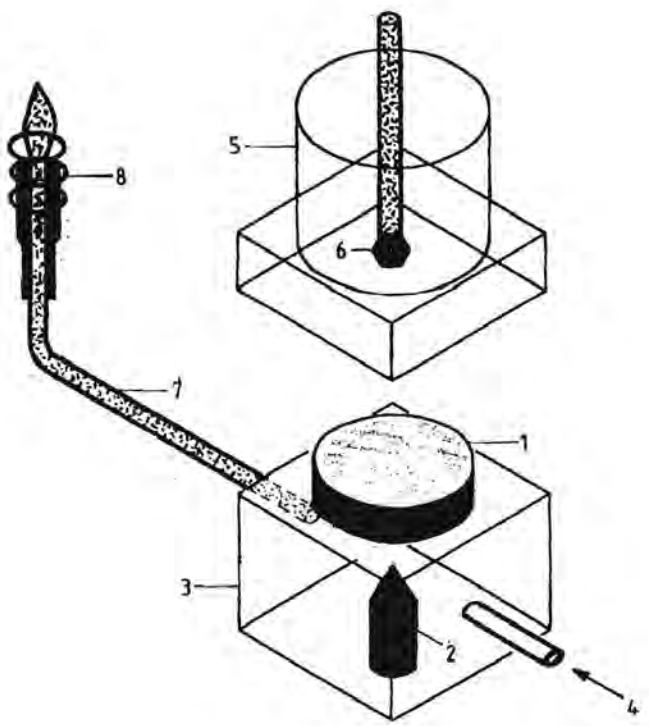


**Fig. 3.8 Principle of Spark Ablation Inductively Coupled Plasma [9]. 1=sample, 2=Tungsten counter electrode, 3=stand, 4=Argon, carrier gas, 5=cap, 6=Mini sample, 7=Aerosol, 8=ICP**

### *3.6 Laser Ablation Inductively Coupled Plasma – Mass Spectrometry*

Laser ablation ICP-MS can be used for quantitative determination of trace impurities in high purity gold with detection limits of less than 0.18 μg/g, as shown by Kogan and M. Hinds [27]. Ablation is initiated by a short pulse of focused photon energy, which strikes the sample and forms a small plasma above the sample surface. Intense heat radiated from the plasma vaporises a small portion of the sample. The material is slightly thermally ionised. It absorbs incoming laser radiation and generates expanding plasma of ionised argon, sample atoms and ions, and free electrons above the sample surface, leading to the ablation of the material.

Formation and expansion of laser-induced plasma spreads the heating effect over a much wider area than the diameter of a laser beam. The aerosol is transported to the plasma where ionisation occurs due to the high temperature. Many authors claim that matrix effects suppress the intensity of the analyte signals [28]. The degree of these influences depends on the mode of laser operation and physical properties of the sample. These suppression effects are mainly due to the ablation process. Kogan, Hinds and Ramendik [28] have managed to produce reliable results, which were relatively free of matrix influences, using only one set of reference materials. However, matrix effects were observed for the determination of Ni, Cu, Zn, Pd, Pt, Pb and Bi in gold and silver material. The system is used for semi-quantitative survey analysis of unknown samples by a scanning procedure.

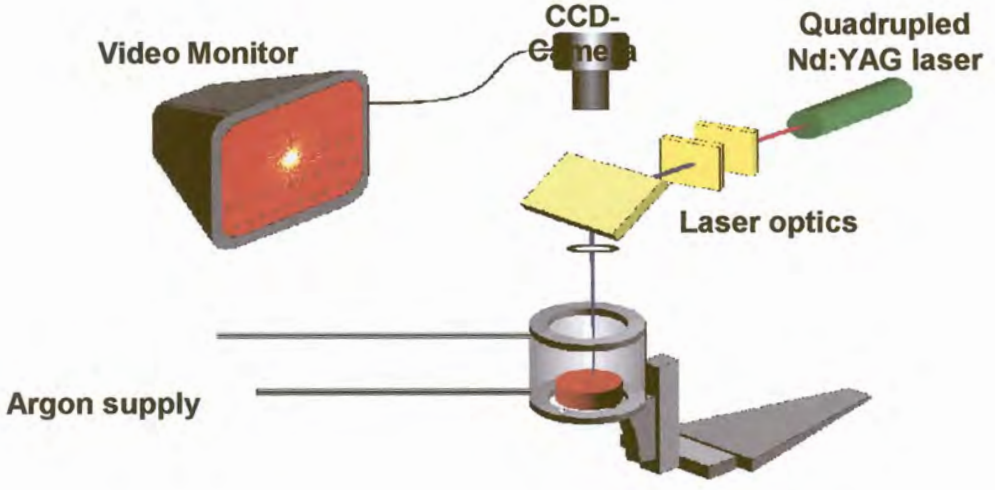


**Fig. 3.9 Schematic layout of Laser Ablation Inductively Coupled Plasma – Mass Spectrometry [29].**

Greenhill (Research Centre, Comalco, Australia) [29] confirmed that the most important parameter of the technique is the elimination of any dependence of the

amount of material ablated on the sample morphology, commonly called "ablation efficiency".
To overcome ablation efficiency effects, calibrations are based on determinations in which the signal from the element of interest is ratioed to the signal from the major element in the sample and then multiplied by the actual concentration of the major element.

Unrefined gold of different origin can be characterised by its trace element composition. This technique, as shown by Watling [30], enables the identification of element assemblages and isotopic abundance changes at analyte concentrations in the μg/kg region. The term "fingerprinting" of the material is used to identify and confirm differences in gold samples from different continents and even closely associated mines, facilitating the identification of stolen gold. The forensic laboratory and Anglo American Research Laboratory use fingerprinting for the identification of gold in South Africa.

### *3.7 XRF*

X-Ray fluorescence spectrometry (XRFS) is one of the most widely used instrumental analytical techniques. The method is non-destructive and can be applied to solids, powders or liquids. XRFS can be applied over a wide range of concentrations, from 1 ppm to 100 % and elemental coverage from atomic number 11 to 92, Na to U. Although matrix effects are always present, these factors are normally predictable and can be corrected for [31]. The instruments usually consist of a high voltage (60-100 kV) generator providing power to an X-Ray tube. X-rays from the tube irradiate the analyte sample, generating secondary (fluorescence) X-rays, which are characteristic of each element in the sample. These characteristic X-rays (each element emitting X-rays of a different wavelength or energy) are separated into individual wavelengths by a spectrometer and measured by an X-ray detector. Intensities from analyte samples are compared with those from standards, corrections made for inter-element effects, to provide accurate quantitative data [32]. There are two types of XRF Spectrometers, energy dispersive and wavelength dispersive.

In wavelength dispersive spectrometers (WDS), the analysing crystal disperses or splits up the secondary spectrum from the sample in such a way that each wavelength may be measured individually. There are two types of spectrometers, flat crystal reflection spectrometers and curved crystal spectrometers. Wavelength dispersive XRF spectrometry is based on the Bragg Law [33]:

$$n\lambda = 2d\sin\theta$$

n = order of the diffracted beam and is numerically equal to the path difference, in wavelength, for successive planes.

d = interplanar spacing of diffracting planes.

$\theta$ = Bragg angle, the angle between the incident x-rays and the diffracting planes.

XRFS usually measures the angles in degrees $2\theta$, i.e. the angles through which the detector moves.

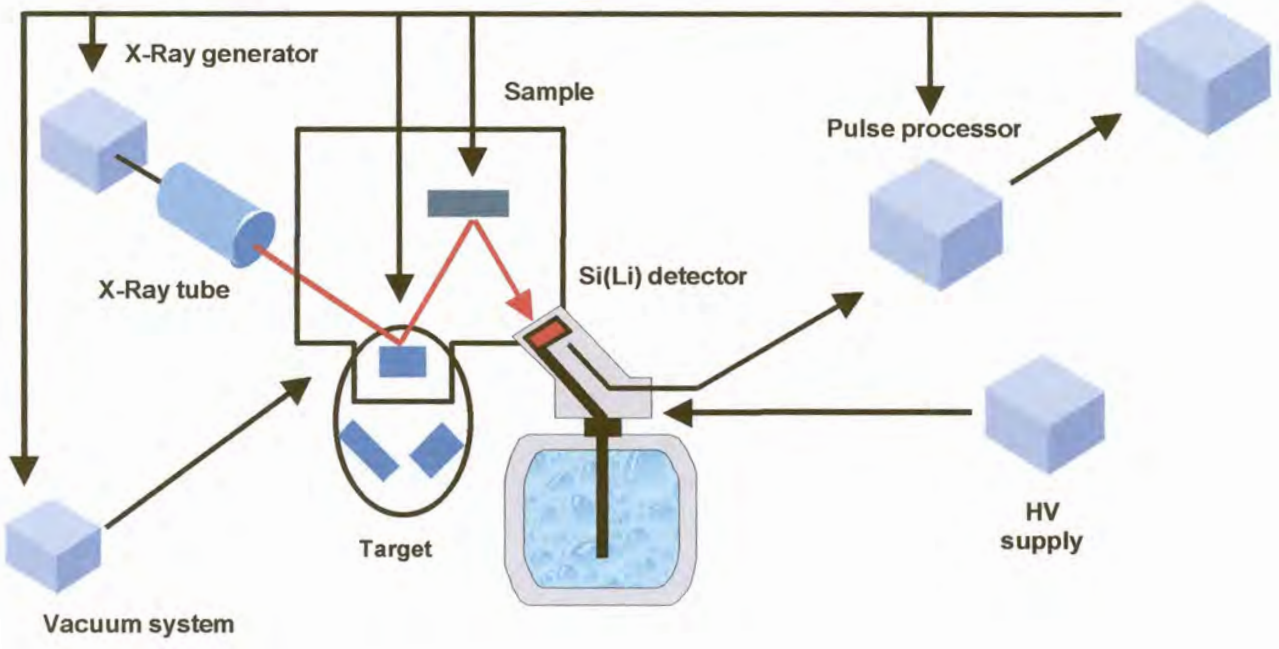


**Fig. 3.10 Schematic layout of an Energy Dispersive X-ray system [34].**

A portion of the x-rays arriving at each crystal plane is scattered in all directions. In most directions the scattered rays are out of phase and undergo destructive

interference. In certain directions they may be in phase and mutually reinforce one another. This phenomenon is known as diffraction, and a group of such reinforced rays in one direction is a diffracted x-ray beam [31].

Energy Dispersive X-rays generally use cryogenic lithium drifted silicon detector systems [35]. The two best-known spectrometers' configuration differs in their excitation systems: using a direct X-ray tube for polychromatic bremsstrahlung excitations versus a secondary target system for monochromatic incident radiation.

XRF can be used for analysis of refined gold [36,37] containing 99.5 to 99.9 % Au through measuring all relevant impurities and determining the percentage of gold by difference. Using solutions may offer many advantages compared with the direct measurement of solid samples. Advantages include complete sample homogeneity, the possible introduction of an internal standard, and separation of interfering elements during preparation by using wet chemical or fire assay procedures. This is one of the techniques used at the Degussa Laboratory in Hanau-Wolfgang (H.M. Lüschow) for all precious metals except silver. An accuracy of 0.1 to 0.2 % relative standard deviation can be achieved for the analysis of the main constituents [36,37].

### *3.8 Neutron Activation*

Von Hevesey and Levi first introduced neutron activation analysis as an analytical technique in 1936. However, it is only since Gordon (1968) and Gijbels (1971) that successful application of the technique has been introduced. They had to await the commercial development of high-resolution germanium detectors during the sixties (1960) to allow satisfactory analysis of the complex gamma spectra obtained from irradiate material. Samples are "activated" by irradiation with neutrons, in a nuclear reactor. Specific isotopes become radioactive by a neutron capture-type nuclear reaction. Once samples are removed from the reactor, they are allowed to decay to get rid of any unwanted short-lived activity such as $^{24}Na$. The activated samples' gamma-ray spectra are measured using solid-state germanium gamma-ray detectors. Isotopes are identified by their gamma rays of characteristic energy. Quantitative determinations are made by comparing the areas of a sample's photo peaks with those of a standard sample spectrum, irradiated and counted under

identical conditions. The two procedures used are (i) instrumental neutron activation analysis (INAA), where the sample is irradiated and undergoes no chemical treatment (non-destructive technique) and (ii) radiochemical neutron activation analysis (RNAA), where the irradiated samples are brought into solution and the trace elements are isolated from the more active matrix by means of a chemical separation procedure. The latter procedure lowers the detection limits by one or two orders of magnitude. The technique is very sensitive, more so for rare earth elements than for the platinum group elements, and claims [38] to be virtually free of matrix interference effects (except overlap interference in complex gamma spectra). A disadvantage is that the technique requires specialised irradiation facilities and is therefore confined to an establishment adjacent to nuclear reactors.

In private communication between Beamish and Gijbels [39], Gijbels discussed some of the limitations of the method. Nuclear interferences exist when platinum group elements must be determined in other platinum elements (interference from uranium fission products when determining Pd and Ru). Samples need to be processed within one day of radiation, since the process produces very short-lived radionuclides. Decomposition of samples and containers takes place under irradiated conditions. The sample size required for activation is small and this causes a problem when securing a representative sample. Few satisfactory comparisons of results obtained by activation methods and by other established methods have so far appeared, and until they do, the activation method must remain suspect when applied to sampling problems [39].

The sensitivity of the method is defined as "the weight of an element that would produce a measurable amount of radioactivity after it had been irradiated by a given flux of neutrons for a given time period" [39]. The sensitivity may increase in longer periods of irradiation. The accuracy of the method depends on the availability of a standard that has a composition known to have accuracy greater than the maximum accuracy of the trace determination. The behaviour of the standard in activation must be exactly the same as that of the trace element to be determined. This method is less sensitive than spectrophotometric or even spectrographic methods.

## 3.9 *Spark Analysis*

The spark is a more precise emission source than the arc for conductive material, but has been considered to be too insensitive for trace element determinations. This is mainly due to the intense background radiation in spark excitation, which adversely affects the signal to background ratio and, in turn, the limit of detection.

### 3.9.1 *Advantages of Spark Analysis*

*Sample preparation*

Sample preparation is relatively simple. A clean, flat surface is required, which can be achieved using a milling machine or lathe. Acetone can be used to clean the analytical surface.

*Analytical standards*

Analytical standards are difficult and expensive to obtain. Very little of the sample is consumed during analysis (which is important due to the high cost of precious metals) when compared with the arc method.

*Simple and rapid*

Results are available after completion of the spark (within approximately 1 minute). Operator skill requirements are much less stringent.

*Memory effects*

Changeover from one matrix to another can be done within minutes. Tests have shown that memory effects are negligible.

*Matrix effects*

The excitation temperature of the spark is much higher than the arc so that fractional distillation effects are much less than in the DC arc method.

### *3.9.2 Time Resolved Spectroscopy*

The lack of sensitivity of spark excitation compared to the DC arc, resulting from the high background radiation, has been overcome by time resolution of individual sparks. Time resolved spectroscopy is not a new concept. The technique was not used in the past because of the unavailability of high-speed computer technology and electronic techniques. The excitation characteristics of individual sparks were studied, relating the emission of spectral lines to time. It was noticed that the background radiation, due to electron effects, followed the electrical discharge closely. The time switching technique called SAFT (Spark Analysis For Traces) or Time Resolved Spectroscopy uses the different emission characteristics of ionic lines [40,41].

Ionic lines cause severe background whereas the radiation of atom lines continues after the electrical discharge decays. The photomultiplier is switched on for a period during the after-glow, thus showing the radiation from the after-glow only and not the background and thus the line to background ratio is enhanced. These phenomena take place in micro-seconds and sophisticated electronic techniques are necessary to observe them. SAFT involves using fast read-out electronics to allow time resolution of each individual spark discharge to be detected. The SAFT method for trace element detection in pure metals is as sensitive as the globular arc, but has greater precision [40].

The spark takes place in a pure argon atmosphere and elements with their most sensitive lines in the vacuum UV region can be determined. Using this approach, the background can be vastly reduced and certain spectral line overlaps eliminated, yielding significant improvements in sensitivity, precision and accuracy. In general, one exposure can cover at least four orders of magnitude of concentration. SAFT is only used for trace elements up to approximately 100 μg/g. Higher concentrations are measured without time resolution of the spark.

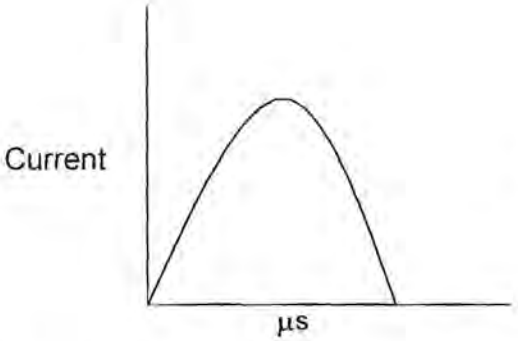


**Figure (a)** Electrical Discharge

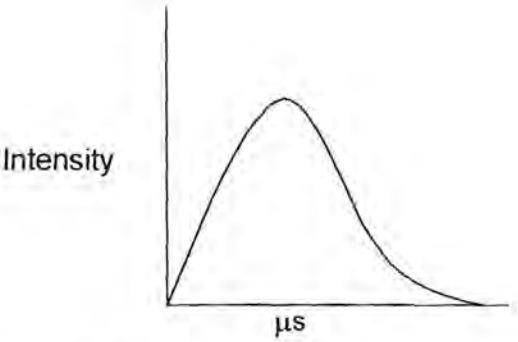


**Figure (b)** Total light radiation

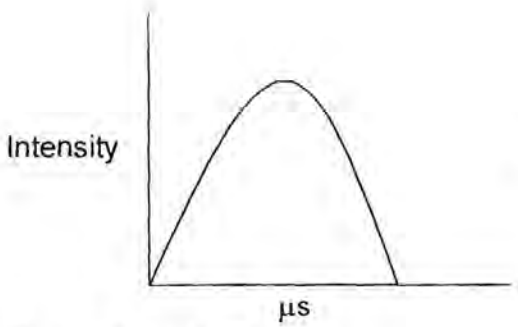


**Figure (c)** Background

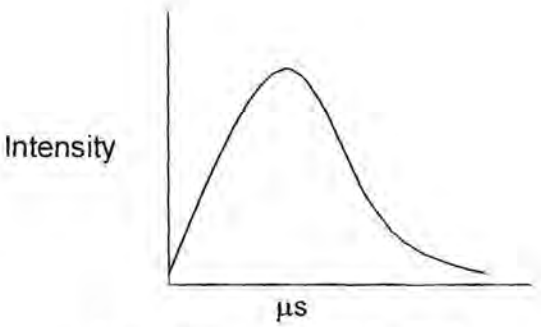


**Figure (d)** Atomic spectra

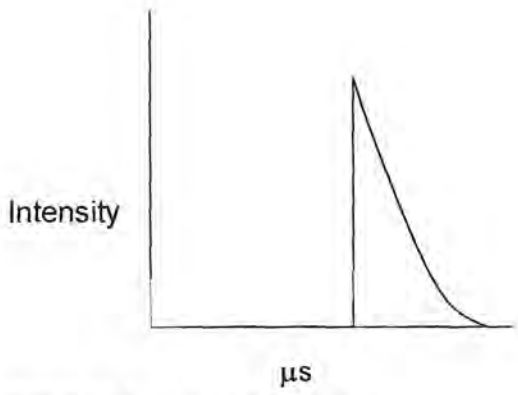


**Figure (e)** SAFT Radiation

**Fig. 3.11 Properties of Time Resolved Spark Analysis For Traces (SAFT) [42].**

Fig. 3.11(a), 49 show the current of a single discharge. Fig. 3.11(b), 49 show the total light radiation. Fig. 3.11(c), 49 show radiation due mainly to electronic, ionic and electron-ion recombination. It was noticed that the background radiation closely follows the electrical discharge. Radiation from ionic lines causes a severe background. Fig. 3.11(d), 49 shows the radiation from atom lines continued after the electric discharge has decayed. This is termed the "after-glow". Fig. 3.11(e), 49 show the contribution to the radiation by the atomic after-glow.

Spectral analysis with time resolved spectra is worthwhile if the following features, singly or in combination, can be achieved [43].

- Improving the power of detection when determining trace elements.
- Improvement of analytical accuracy.
- Removal of interferences in the spectrum (interfering lines, interfering backgrounds).
- Reducing or removing the effect of interference on the determination of certain elements.
- Achieving optimal excitation conditions for the removal of material from the electrode.
- Increasing the application areas of spectral analysis.

The most important aspect of power of detection when studying the application of time resolved spectra analysis is its achievable limits of detection.

#### *3.9.2.1 Research arrangement*

A rotary disc system was used. The advantage of a rotary disc is the ease of mounting and adjustment on the optical bar in the radiation path of a photographic or photoelectric spectral apparatus. The rotary disc was used in such a manner that, with a wide slit, a time interval of approximately 50 μs was realised as well as a particular time sequence (referred to as "fade out time") and the complete excitation was allowed to continue to the end of the "appearance of light" Using the damped condenser excitation, essentially only the first microsecond needs to be recorded.

Synchronisation of the disc and the spark was better than 0.3 µs and the setting of the "fade out time" could be done with a precision of 0.5 µs.

Time resolved spectroscopy could be used to improve the power of detection. By increasing the resolution of the spectral apparatus the line to background ratios and consequently the power of detection can be improved to a point where the line width of the source is reached [43]. In this manner, going from medium resolution spectrographs to very high-resolution instruments, the limits of detection can be improved up to a factor of 10. In the majority of cases, the most sensitive lines are the easily excited atom lines, the so-called "ground state" lines. These lines prove to be the most sensitive in an arc excitation. In favourable cases, these levels can be achieved with time resolved spectra, which in most cases give a weak spark excitation. Because of the very weak intensities of the "after-glow" (at the maximum achievable sensitivity), the speed of the spectral apparatus plays a deciding role. The faster the instrument, the later the measurable "after-glow" and the better the power of detection will be.

The question of whether the conventional damped oscillating or non-oscillating spark excitation is the best light source for use with time resolved spectroscopy remains unanswered. The carrier gas influences the particular excitation in a decisive way. The medium and high voltage sparks techniques are very similar in effect to the time-resolved spectroscopy. Further improvements will probably be realised by using favourable counter electrodes of different materials.

In general it can be said that the analytical accuracy is determined by three broad criteria [43].

- Systematic and statistical inhomogeneity of the sample.
- Systematic and statistical errors in the light source, such as evaporation, excitation and variable background.
- Systematic and statistical errors of the detector.

Theoretically, systematic errors can be removed by calibration. These errors may be different for time resolved spectroscopy and non-time resolved spectroscopy.

Increasing the number of single sparks in an analysis improves the information concerning the effect of inhomogeneity of the sample. If the error of the light source predominates, time resolved spectra allow a "harder" excitation to be used and interferences by lines or background to be removed. If the statistical error of the detector predominates in the application, time resolved spectra results in a reduction of the errors.

The photoelectric standard deviation is given by [43]:

$$\frac{\sigma_1}{I_x} = \frac{1}{\sqrt{n_x}} \sqrt{\left(1 + \frac{2n_u}{n_x}\right)}$$

Where: $I_x$ = Net measured intensity of the analytical line

$n_x$ = Gross Intensity of the analytical line

$n_u$ = intensity of the background

The following is suggested for traces and alloy elements;

- Weak sparks - imprecise for alloy elements (due to errors in the light source).
- Hard sparks - too insensitive for traces.
- Hard sparks - partly faded out and exposure time lengthened.

Alloy elements are analysed more effectively using hard sparks and traces using weak sparks.

#### 3.9.2.2 *Advantages of the Time Resolved method*

*Sensitivity*

At least as sensitive as the globular arc method, but has greater precision, thus giving much-improved limits of detection.

*Wavelength range*

The spark takes place in a pure argon atmosphere and elements with their most sensitive lines in the UV region (120-200 nm) can be measured.

*Wide concentration range*

One exposure can cover at least four orders of magnitude of concentration. Time resolved spectrometry is used for trace element determinations. The higher concentrations are measured using spark parameters simultaneously.

*High Energy Pre-Spark (HEPS)*

A spark discharge creates plasma, which contains elements representative of the whole sample. The sample surface is micro-melted in an argon atmosphere during the high-energy pre-spark, before the photomultiplier tubes start measuring radiation. Cooling and recrystallisation occurs rapidly and the surface is uniformly reformed. Thus any crystalline effect caused by metallurgical history is partially overcome.

### *3.10 Standards*

Standards for solution techniques are readily available, but not for solid platinum metals. Direct solid analysis avoids time-consuming sample dissolution, minimises the risk of contamination, and does not dilute already low analyte concentrations below levels of detection. The most serious problem in platinum metal spectrochemistry is the lack of commercially available standard samples for low concentrations of impurity [44].

Standards have been prepared by dissolving the metal and adding aliquots of the impurities, co-precipitating the platinum metal and the impurities, and reducing the precipitate to metal powder. The metal powder is then ground to produce a homogeneous mixture. However, due to the very low concentrations of impurities, non-homogeneous precipitation and crystallisation occurs which prevents satisfactory homogeneous mixtures, even with extensive grinding after reduction. This renders the method unsatisfactory [44].

Alternative methods, as developed by Lincoln and Kohler in 1962 [45], are used for DC arc analysis. Stock solutions of the impurity elements are added to high-purity ammonium chloride, the mixture is dried, blended mechanically by shaking the mixture in a mixer-mill and then ground in a rotary mill for up to 72 hours. Reduction

takes place by heating the material in a hydrogen or nitrogen / hydrogen atmosphere to a platinum sponge.

The Royal Canadian Mint has successfully prepared a set of solid calibration standards for calibrating an ICP spark ablation spectrometer and laser ablation ICP-MS [46]. These standards were prepared in a vacuum induction furnace under an argon atmosphere, using a graphite crucible. Volatile elements such as Zn, Pb and Bi were wrapped in gold foil and dropped in at the end of a melt. The melt was cast in an oxygen free, high conductive, water-cooled copper mould, to minimise any segregation that usually occurs during the solidification process. The ingots were homogenised at 750 °C for one hour in a nitrogen atmosphere and then annealed at 400 °C for one hour, also under nitrogen. This was to ensure a uniform and fine grain structure, since some elements preferentially segregate at the grain boundaries. Homogeneity tests were performed by analyses in 30 different positions on the sample using laser ablation ICP-AES.

Analysis of the impurities was achieved using shavings of the material and analysing these on ICP-AES, ICP-MS, flame and graphite furnace atomic absorption spectrometry. These were analysed against matrix-matched standards containing an appropriate amount of dissolved Au at 99.999 % purity. Samples were also sent to four different laboratories. Some of the elements could only be determined by two of the three methods. On average, there was agreement amongst only half the laboratories for any given element. Outliers in each set of data were eliminated by a Grubb's Test, based on standard deviation on the average result [47]. Regression coefficients were all above 0.997 except for Mn, 0.99261, and Ti, 0.9965. However, these reference standards were judged suitable for their needs.

### *3.10.1 Standard specifications for refined Precious Metals*

Standard levels of trace elements in different materials are specified by the ASTM methods according to their grade produced. The method of analysis is a matter of agreement between the manufacturer and the purchaser [48]. This study deals with

high purity pgm's therefore only the specifications for 99.95 % and higher grades will be discussed.

**Table 3.1 Chemical requirements for Palladium as per ASTM B589-77 [48].**

| Element | Composition % Grade 99.95 % |
|---|---|
| Palladium min. (by difference). | 99.95 % |
| Platinum max. | ..... |
| Rhodium max. | ..... |
| Ruthenium max. | ..... |
| Iridium max. | ..... |
| Total platinum group metals other than palladium max. | 0.03 |
| Gold max. | 0.01 |
| Silver max. | 0.005 |
| Lead max. | 0.005 |
| Tin max. | 0.005 |
| Zinc max. | 0.0025 |
| Iron max. | 0.005 |
| Copper max. | 0.005 |
| Silicon max. | 0.005 |
| Magnesium max. | 0.005 |
| Calcium max. | 0.005 |
| Aluminium max. | 0.005 |
| Nickel max. | 0.005 |
| Chromium max. | 0.001 |
| Cobalt max. | 0.001 |
| Manganese max. | 0.001 |
| Antimony max. | 0.002 |

By agreement between manufacturer and purchaser, analyses may be required and limits established for elements or compounds not specified in this table.

**Table 3.2 Chemical requirements for Platinum as per ASTM B561-73 [48].**

| Element | Composition %<br>Grade 99.95 % |
|---|---|
| Platinum min. (by difference) | 99.95 % |
| Palladium max. | ..... |
| Rhodium max. | ..... |
| Ruthenium max. | ..... |
| Iridium max. | ..... |
| Total platinum group metals other than palladium max. | 0.03 |
| Gold max. | 0.01 |
| Silver max. | 0.005 |
| Lead max. | 0.005 |
| Tin max. | 0.005 |
| Zinc max. | 0.0025 |
| Iron max. | 0.005 |
| Copper max. | 0.005 |
| Silicon max. | 0.005 |
| Magnesium max. | 0.005 |
| Calcium max. | 0.005 |
| Aluminium max. | 0.005 |
| Nickel max. | 0.005 |
| Chromium max. | 0.001 |
| Cobalt max. | 0.001 |
| Manganese max. | 0.001 |
| Antimony max. | 0.002 |

**Table 3.3** **Chemical requirements for Gold as per ASTM B562-73** (re approved 1979) [48].

| Element | Grade: 99.95 | Composition % 99.99 | 99.995 |
|---|---|---|---|
| Gold min. (by difference) | | 99.95 | 99.99 |
| Silver and Copper max. | | 0.04 | ..... |
| Silver max. | | 0.035 | 0.009 |
| Copper max. | | 0.02 | 0.005 |
| Palladium max. | | 0.02 | 0.005 |
| Iron max. | | 0.005 | 0.002 |
| Lead max. | | 0.005 | 0.002 |
| Silicon max. | | ..... | 0.005 |
| Magnesium max. | | ..... | 0.003 |
| Arsenic max. | | ..... | 0.003 |
| Bismuth max. | | ..... | 0.002 |
| Tin max. | | ..... | 0.001 |
| Chromium max. | | ..... | 0.0003 |
| Nickel max. | | ..... | 0.0003 |
| Manganese max. | | ..... | 0.0003 |

## *3.11 References*

[1] **ASTM Committee E-2 on Emission Spectroscopy, Methods for Emission Spectrochemical Analysis,** Sixth edition, (1971) 658, 692

[2] W. Gerlach, E. Scheitzer, **Chemical Analysis by Emission Spectroscopy, Part 1, Principles and Methods published by Leopold Voss,** Leipzig, (1930) 42

[3] W . Gerlach, E. Z. Schweizer, **Anorg. Chimica, 173,** (1928) 92

[4] L. H. Ahrens, S.R. Taylor, **Spectrochemical Analysis,** II edition. Addison n-Wesley Mass USA, (1961) 14-21

[5] H.M. Lüschow, **DC arc Spectrometry, GDMB Erzmetall Nr 1,** (1997) 22

[6] Jack Roberts, et al., **Thermo Jarrel Ash Corp., Application Note No. 60,** (1995)

[7] M. Hinds, V. Kogan, **Spectroscopy 10,** (1995) 23-26

[8] H.M. Lüschow, **Proc. Tenth Edition Precious Metals Conference, Lake Tahoe, USA**, (1986) 92-102

[9] Karl Slickers, **Automatic Atomic-Emission-Spectroscopy,** Second Edition, (1993) 125, 143-209

[10] H.M, Lüschow, **Experience gained with glow-discharge excitation in the emission spectrometric analysis of precious metals, Proceedings of the tenth International Precious Metals Institute Conference, Lake Tahoe, Nevada, Precious Metals,** (1986) 91-103

[11] H.M. Lüschow, **RSV-Colloquim, Herrsching,** (1981)

[12] S.B. Malkit, **Development of Spectrochemical techniques for Precious Metal Analysis - A Historical Perspective, Proc. of the twentieth international Precious Metal Conference, Newport Beach, California, USA Precious Metals** (1996) 309-317

[13] Karl Slickers, **Automatic Atomic-Emission-Spectroscopy,** Second Edition, (1993) 46

[14] T.R. Harville, R. K. Marcus, **Anal. Chem. 67,** (1995) 1271

[15] V. Kogan, et al., **Proc.17th IMPMI Conf., Newport, R.I.,** (1993) 101

[16] S. Greenfield, I. Jones, C.T. Berry, **Proceedings Soc. Anal. Chem.** (1965) 2, 111

[17] R.H. Wendt, V.A. Fassel, **Anal Chem.,** (1965) 37, 920

[18] G.L. Moore, **Introduction to Inductively Coupled Plasma, Atomic Emission Spectroscopy, Amsterdam: Elsevier,** (1989) 30-65

[19] C.B. Boss, K.J.Fredeen, **Concepts, Instrumentation, and Techniques in Inductively Coupled Plasma Optical Emission Spectrometry,** (1999) 2-4,5

[20] U. Gerb, **Inductively Coupled Plasma Mass Spectrometry, Power point presentation,** Spectro Analytical Instruments, Kleve, Germany, (1998)

[21] S.A. Myers, D.H. Tracy, **Spectochim. Acta, Vol.38 B,** (1983) 1227

[22] D. Hofmans, E. Adriaenssens, **Determination of Pgm's by ICP at Union Miniére: advantages and quality assurance, Proc. of the seventeenth international Precious Metals Conference Newport, Rhode Island**, (1993) 235-245

[23] J.W. Olesik, I.I. Stewart, **Plasma Source Mass Spectrometry, New Developments and applications,** (1998) 3-17

[24] S.M. Graham, R.V.D. Robért, **The Analysis of high purity noble metals and their salts by ICP-MS, Talanta, Vol 41, No 8,** Mintek South Africa (1994) 1369 – 1375

[25] Alan L. Gray, 4 Dene Lane, Farnham, Surrey, UK, GU10 3PW, **ICP-MS in maturity. What problems remain? Analytical Proceedings Analytical Communications, December, Vol. 33,** (1994) 371-375

[26] W. Grimm, **Spectr. Acta, 23B,** (1968) 443

[27] V.V. Kogan, M.W. Hinds, **19th IPMI Conf., Incline Village, Nevada,** (1995) 415

[28] V.V. Kogan, M.W. Hinds, G.I. Ramendik, **The direct determination of trace metals in gold and silver materials by laser ablation inductively coupled plasma mass spectrometry without matrix matched standards, Spectrochimica Acta vol. 49B, No 4,** (1994) 333-343

[29] Paul G. Greenhill, Comalco Research Centre, 15 Edgars Rd, Thomastown, Victoria 3074. Australia, **Laser Ablation for ICP solid sampling, Chemistry in Australia,** July (1990) 225-227

[30] J. Watling, et al., **Spectrochim. Acta, 49 B** (1994) 205

[31] R. Jenkins, J.L De Vries, **Practical X-ray Spectrometry, New York,** (1970) 27

[32] J. Willis, **X-Ray notes training course, Cape Town, South Africa,** (1986)

[33] R. Jenkins, **An introduction to X-Ray Spectrometry, New York: Heyden,** (1976)

[34] R. Schramm, **Fundamentals of Energy Dispersive X- Rays, Power point presentation, Spectro Analytical Instruments, Kleve, Germany,** (2001)

[35] Karl Slickers, **Automatic Atomic-Emission-Spectroscopy, Second Edition,** (1993) 491

[36] A.M. Gillespie, **I.U.P.A.C. Symposium, Pretoria,** (1985) 305

[37] A.M. Gillespie; **Bull. S.A.I.A.A.**, September, (1989) 209

[38] P.J. Potts, **A Handbook on Silicate Rock Analysis, Blackie,** (1987) 399

[39] F.E, Beamish, J.C. Van Loon, **Recent advances in the Analytical Chemistry of the noble metals, Pergamon Press,** (1972) 104-108

[40] G.J. Roberts, **Proc. 16th IPMI Conf., Scottdale, Arizona,** (1992) 9

[41] K. Laqua, W. Hagenah, **Spectrochim. Acta, 18,** (1962) 183

[42] M. Julsing, P. Butler, C. Rademeyer, **Proceedings of Analytika Stellenbosch SA, Trace element Analysis in Precious metals using Time Resolved Emission Spectroscopy,** (1998)

[43] K. Laqua, W.D. Hagenah, **Spektrochemische Analyse mit zeitaufgelösten spektren von Funkenentladungen, instutut für Spektrochemie und angewandte Spektroskopie, Dortmund, Spectrochemica Acta, Vol. 16** (1962) 183 – 199

[44] F.E. Beamish, **The Analytical Chemistry of the Noble Metals, University of Toronto,** (1966) 503-507

**[45]** A.J. Lincoln, J.C. Kohler, **Method of impurities in platinum using arc/spark Analyt. Chem.,** (1962) 34, 1247-51

**[46]** V. Kogan, M.W. Hinds, G. Ocampo, G. Valente, **Development of reference materials for assay of fine gold, Royal Canadian Mint, Canada, Proc. 17th International Precious Metals Conference, Newport, Rhode Island,** (1993) 101

**[47]** D. Hofmans, E. Adriaenssens, **Determination of PM's by ICP at Union Miniére: Advantages and Quality Assurance, Proc. 17th International Precious Metals Conference, Newport, Rhode Island,** (1993) 2350

**[48]** American Society for Testing and Materials, **Methods for emission Spectrochemical Analysis,** (1971) 653, 658, 691

# Chapter 4

## Instrumentation

### *4.1 Introduction*

A very important part of analysis is the sample preparation. Samples as well as standards are prepared by melting the sample in an induction oven or by pressing the sample in a press. Whether samples are pressed or melted depends on the material and the requirement of the technique. Material such as gold is very malleable and presses easily into a compact disc at 30-40 ton. However, the same cannot be said for Ir. This material would be better if melted in the induction furnace. The Lifumat – Met 3.3 induction furnace was used for the melting of the material in this study. Samples, which were melted, need to be milled in order to produce a flat surface for the spark process. The Breitländer Semi-Automatic Milling Machine was used for this purpose. The analysis of the samples was conducted using a Spectro Lab M8 Optical Emission Spectrometer.

### *4.2 Lifumat-Met-3.3/Vac-Gas Induction Furnace*

The Lifumat is a microprocessor-controlled High Frequency melting-system used for inductive melting [1]. The casting machine works on the principle of energy transfer of a transformer, the inductive heating process. After applying a high frequency magnetic field, a secondary current flows onto the material surface. The current is modified to heat the different material and thereby the metal is melted.

*Assembly of the system:* The HF (high frequency) generator, encased in a safe sheet steel casting, is the core of the system and corresponds to the demands of modern work protection as well as the requirements of electromagnetic compatibility. The casting arm is fitted inside the casting chamber. The arm contains the crucible and the muffle. A smooth run is provided by a counter weight, which is fitted to the arm. The power switches off automatically when the chamber cover is opened.

The induction coil, which is the heat source, surrounds the crucible. The casting arm is fixed and the coil is lifted, by means of a motor, into the casting chamber for the melting process. Before the centrifugal process of the liquid metal takes place, the coil is lowered again. The melting process can be observed through a blue glass, which is build into the cover. An Infrared spectral pyrometer measures the temperature. Electronic controls and safety devices are available to make adjustments during the process for the torque acceleration of centrifugal rotation. The centrifugal arm is evacuated and the system is purged with Argon gas to prevent any undesired chemical reactions with oxygen/air. The connected vacuum duct also serves as a gas-leading duct for the argon. It connects the interior of the tube-shaped drive cam with the vacuum chamber of the casting arm. It is therefore possible to maintain vacuum or purge with the argon during the rotation procedure.

**Fig. 4.1 Lifumat-Met-3.3/Vac-Gas Induction Furnace [2].**

The dwell time, which is the period between the melting process and the casting process, can be set by means of a potentiometer. This cooling period prevents fusion of the sample with the bottom of the mould. Ceramic crucibles and graphite inserts for the ceramic crucibles are used to melt the samples. Crucibles can be re-used but must be checked for damage, such as fractures. These ceramic crucibles can be cleaned with compressed air. A ceramic nozzle is used to connect the crucible to the mould. Copper and graphite moulds are available, but we used a combined system. The copper moulds were damaged by an amalgam forming with the melted material and the mould. The graphite worked well and was free of

contamination, but the moulds were too fragile and did not last long. The combined mould contained a copper base with graphite inserts and a base plate. The material was then in contact only with the graphite. The sample is removed with tongs from the mould and when cooled it is resurfaced to obtain a flat smooth surface for analysis.

### *4.3 Breitländer Semi-Automatic Milling Machine*

**Fig. 4.2 Breitländer Semi-Automatic Milling Machine [3].**

The milling machine is semi-automatic in that the cutting depth is set manually. Cutting speeds for different materials can be selected. This is a bench top unit, with an enclosed cutting area, which is accessible through a door with a safety glass window and an automatic cut-off switch. Samples are clamped on to a chuck. The height measurement gauge is used roughly to set up the milling head for cutting. The milling head is moved horizontally by a computer operated stepping motor. The cutting blades of the milling head are all on exactly the same level to obtain a perfect surface. These blades are set with a measuring device. The samples are mounted on a chuck. The cutting speed influences the quality of the milled surface and the lifetime of the cutting blades. Cutting speed depends on the diameter of the milling

head and its rate of rotation. The rotation is fully adjustable by changing the frequency. The manufacturers suggest a lower cutting rotation speed for harder metals. If the cutting speed is too high the samples will overheat and the surface quality will be impaired. The operating revolutions of the cutter are between 400-3600 rpm, cutting speed up to 870 mm/min, operating speed of sample slide 30-187 mm/min, and a maximum cutting depth of 2 mm. Two milling heads can be used, 63 mm or 80 mm [4].

## *4.4 Spectrometer*

The "LAB S" Optical emission spark spectrometer instrument is a simultaneous instrument consisting of an energy source (radiation generation), spark stand, optical system (radiation separation), detectors, integrators and central processing unit, for data evaluation which finally produces the analytical result [5].

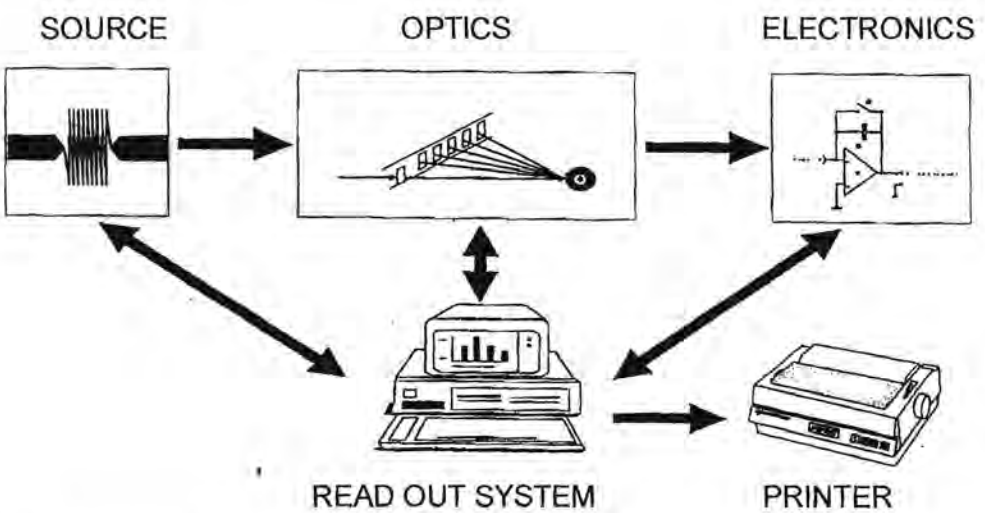


**Fig. 4.3 Instrument lay out [5].**

### *4.4.1 Source*

An electrical charge is generated. The material from the services is vapourised. The atoms in the vapour are excited. Fibre optic is used (in air optics) to transmit light of the chemical elements from the spark stand to the Optics. Argon is used as the discharge atmosphere, for its unipolar discharges and positive polarity. No material

is removed from the counter-electrode [5]. This reduces contamination and simplifies handling, as the tungsten counter electrode can be used for many thousands of measurements before its tip has to be renewed [5]. The path between the radiation source and the optics also has to be made transparent for the UV wavelengths.

Fig. 4.4, 67 show the basic circuit of a spark generator with external ignition. A capacitor, $C_L$ (1 to 20 $\mu$F), is charged by a dc source (400 to1000 V) through the charging resistor $R_L$. As soon as the ignition unit has made the analysis gap, AF, conductive, $C_1$ discharges itself through $R_B$, L and AF. The spark characteristics are determined by the supply voltage, U, and the parameters $C_L$, $R_B$ and L of the oscillating circuit, which is formed by $C_L$, $R_B$, L and AF. The lower the $R_B$ and L values selected, the higher the spark current density (hardness).

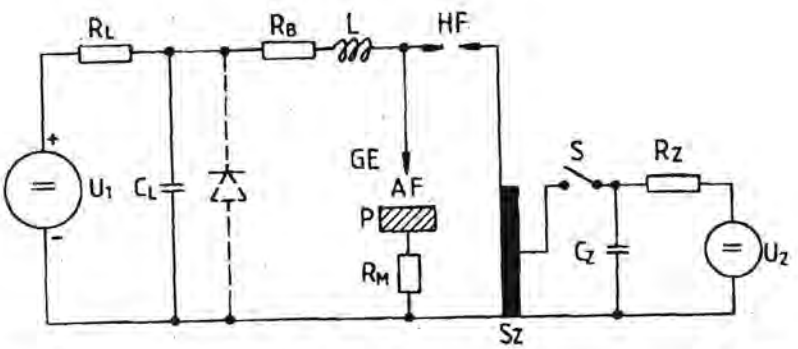


**Fig. 4.4 Principle of a spark generator with external ignition [5]. P=Sample; GE= Counter-electrode; AF= Analytical gap; RM=Measuring resistor; CL=Capacitor; U=Voltage; RL=Charging resistor; RB=Discharge resistor; L=Inductance; Rz=Ignition Capacitor; S=Switch; Sz= Ignition Coil; HF= Auxiliary gap The temperatures generated at the spark are estimated to be between 500K and 10 000K**

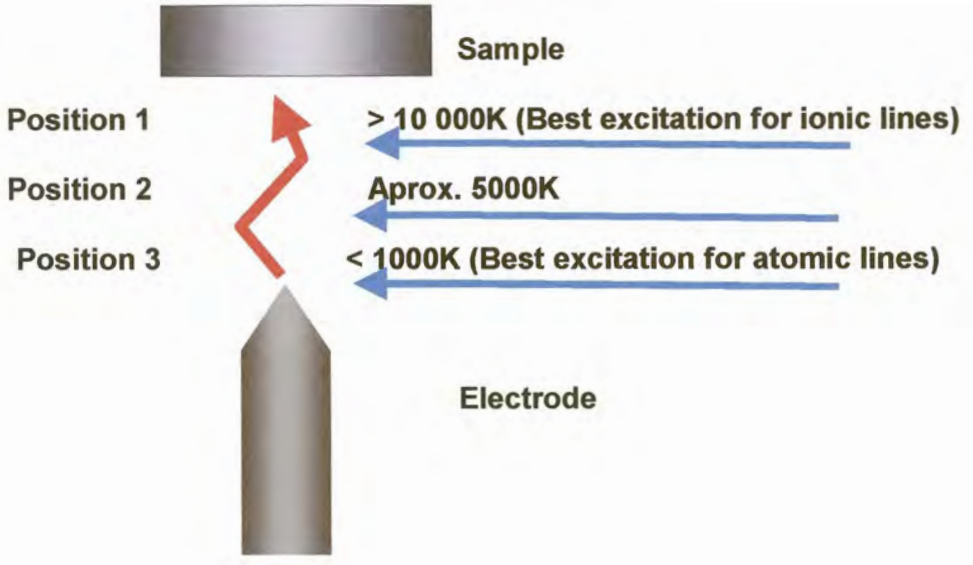


**Fig. 4.5 Temperature and intensity distribution of the spark source. Pos1=Ion lines; Pos 2=Atom lines with high excitation energy; Pos 3=Atom lines with low excitation energy [7].**

### *4.4.2 Sample stand*

The sample table slopes at about 10° to the optical axis. For certain elements the measurements are taken at a higher and for others at a lower lens position. The position of the lens is set to obtain the best signal to background ratio. The stand is coupled to the optical system via fibre optics for elements analysed in the air optics and direct reading for elements in the "UV" range. The spark is discharged in argon to reduce optical interference of the radiation. The argon enters in the front of the side facing the radiation source and is exhausted through the back of the stand. A number of optical fibres can be arranged at different angles on the stand, and depending on distribution in the plasma, the analytical lines can be combined in groups and simultaneously measured.

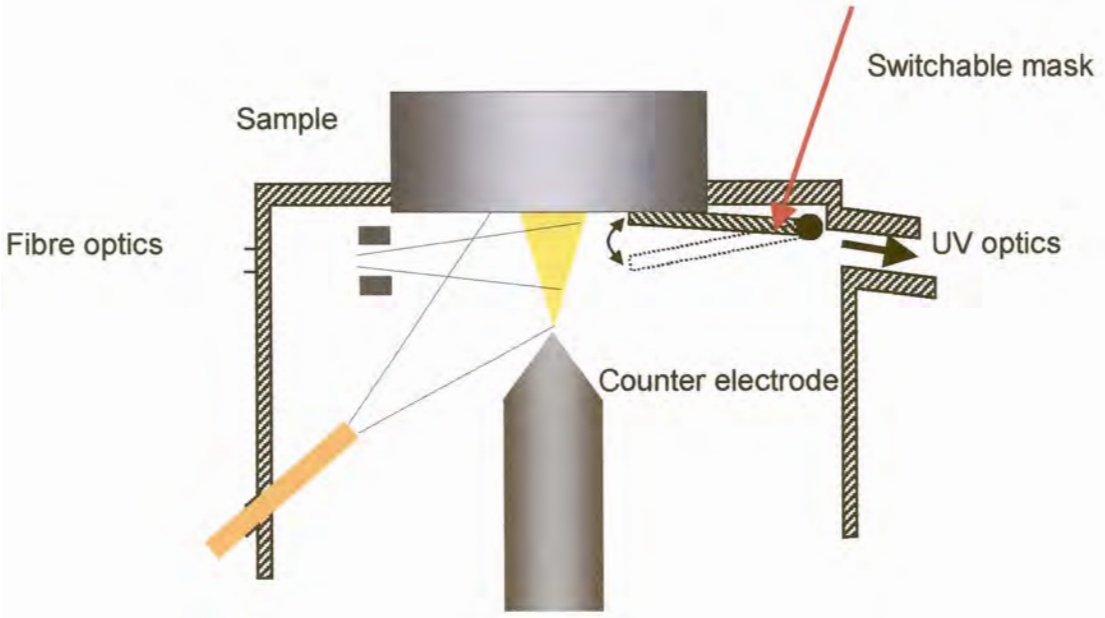


**Fig. 4.6 Radiation off take with optical fibres [7].**

### *4.4.3 Spectrometer optics*

Spectrometer optics is used for spectral dispersion of the radiation produced in the radiation source. The optical system consists of up to five optical systems, of which one is a nitrogen gas-filled system for "UV" range detection of elements.

Radiation produced by the source is passed to the entrance slit of the spectrometer optics were it is dispersed into its different wavelengths. The dispersed radiation is passed through the exit slit to detector and measured. The measured values are converted into concentrations using calibration curves.

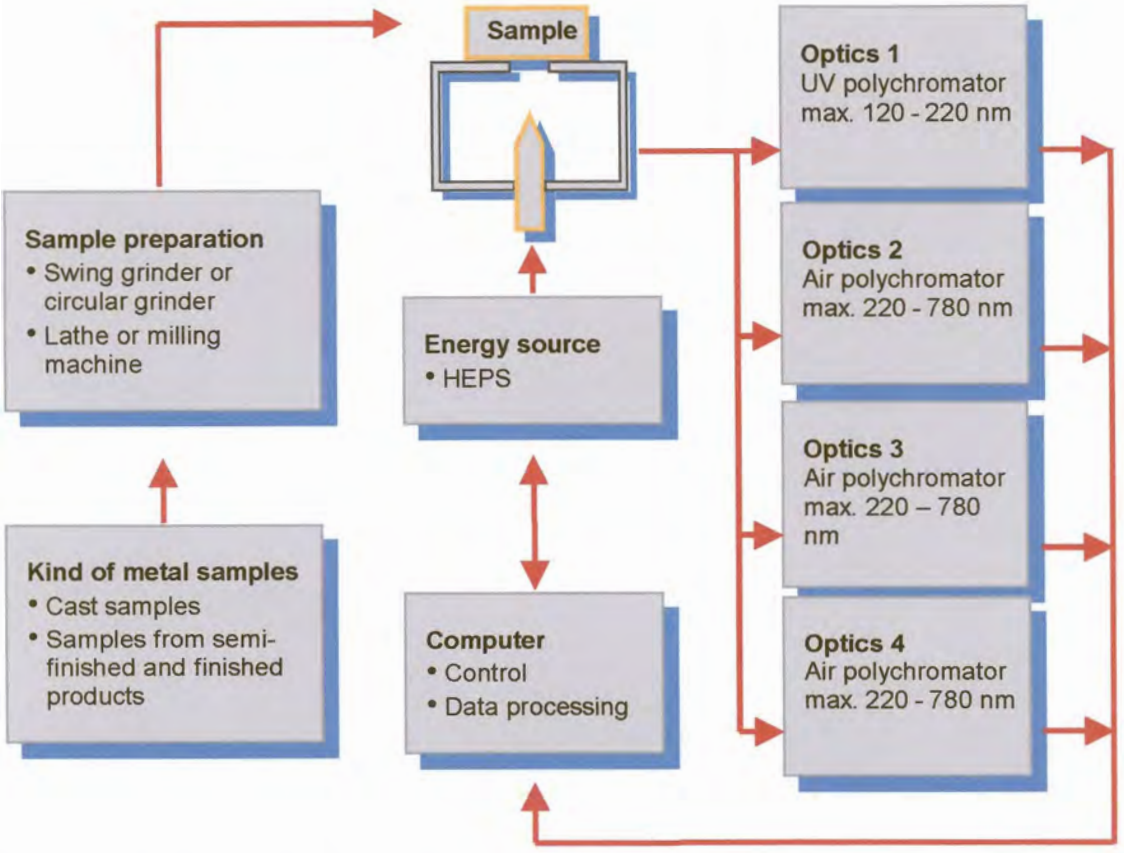


**Fig. 4.7 Schematic diagram of optical system [7].**

#### *4.4.3.1 Optical fibres – light guides*

Fibre optics is used to transmit light from the given light source to the entrance slit of the spectrometer [6]. One end is mounted as closely as possible to the source and the other to the entrance slit. A fibre consists of a transparent core and cladding. Both these are surrounded by plastic material for protection which provides mechanical stability against impact and bending. In fig. 4.8, 71 the angle, $\varphi_A$, is the wavelength-dependent aperture angle at which the incoming radiation, [due to total reflection on the interface between the core (refraction index, $n_1$) and the cladding (refractive index, $n_2$)] is passed along inside the core, emerging at the end of the

fibre and not through the cladding. The aperture angle is calculated from the refractive indexes of the core and cladding: Sin $\varphi_A = \sqrt{n_1^2 - n_2^2}$

Any rays which enter at an angle larger than $\varphi_A$ are not totally reflected and emerge through the cladding.

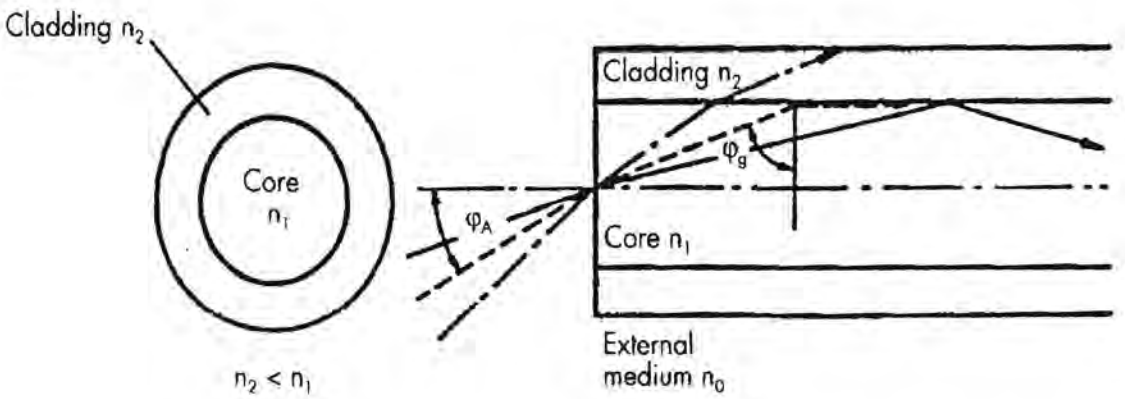


**Fig. 4.8 Cross-section and lengthwise section through a lightguide (fibre optic). φA = Maximum entry angle; φg = Critical angle of total reflection [6].**

The "UV" range of elements makes use of direct reading, with an argon purged light path and air optics using light guides. Using a number of light guides, radiation can simultaneously be measured from a number of observation zones and also at different angles.

#### *4.4.3.2 Spectral dispersion*

A holographic concave grating is used to disperse radiation into its different wavelengths. Gratings are made by ruling equally spaced parallel grooves on a glass or metal plate, using a diamond cutting point whose motions are automatically controlled by an elaborate controlling system. Gratings ruled on metal plates are called reflection gratings because the interference effects are viewed in reflected rather than in transmitted light [8].

The grating equation is defined as [6,9]

$n \times l = d (\sin \alpha + \sin \beta)$ where n = diffraction order

l = wavelength

$\alpha$ = angle of incident ray

$\beta$ = angle of reflected ray

d = grating constant

Commonly gratings are ruled on the surface of a concave mirror, which eliminates the need for lenses. The system makes use of a 3600 lines per mm. grating and 750 mm focal length.

Rowland found in 1882 [6] that a grating ruled into a concave mirror (concave grating, Rowland grating) can disperse light into its individual wavelengths and can also image the slit. The grating itself is then the only optical component in the optics. On a Rowland circle of radius, r, is a grating, Gi, with a radius of curvature, 2r, and slit, Sp as in fig. 4.9, 73. The grating lines run perpendicular to the plane of the circle. The slit is parallel to the grating lines [5]. The grating usually runs from the apex, S, to the centre point of the grating curvature, M. M' is the centre point of the Rowland circle. A beam of wavelength, ll, falling onto the grating through the entrance slit, forms an angle, $\alpha$. The beam diffracts according to the grating equation and forms the angle, $\beta 1$, with the normal. This beam cuts the circle at a point P1. The essential feature of Rowland's discovery is that a divergent bundle of beams emerging from the slit with wavelength 11 are combined after diffraction in P1. Thus a spectral line of wavelength ll is produced in P1. The slit is sharply imaged as a spectral line according to its width but not according to its height. Another bundle of rays with wavelength 12 (12 > 11) is shown to produce a spectral line in P2 [5].

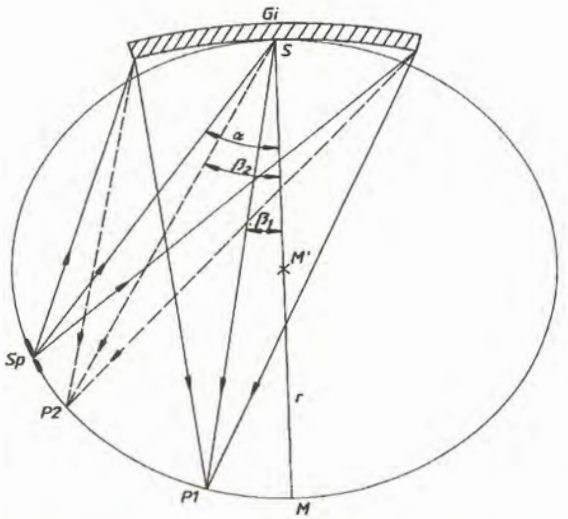


**Fig. 4.9 Spectrometer optics with Rowland concave grating. Sp=Entrance Slit; Gi=Grating;S=Apex; M=Centre point of the circle; r=Radius of circle; P= Points in image plane [5].**

A special version of the Rowland's optical system is the Paschen-Runge mount, (fig. 4.10, 73) which is a Rowland circle configuration with diffraction angles close to 0°, so that dispersion becomes almost independent of wavelength [8]. The system uses a Paschen-Runge mounting for the polychromators, with entrance slits, concave gratings and exit slits situated on the Rowland circle, which has a diameter equal to the radius of curvature of the grating.

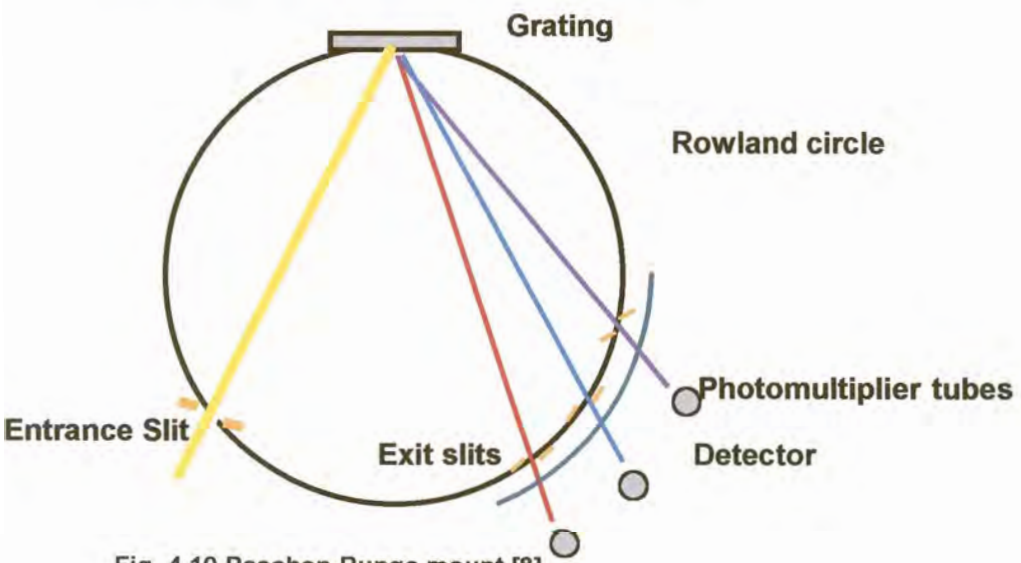


**Fig. 4.10 Paschen-Runge mount [8].**

### 4.4.4 Instrument configuration

#### 4.4.4.1 Polychromators

The instrument contains 48 simultaneous channels but could use as many as 128. Therefore all the lines are measured simultaneously as the radiation from the 10 micron entrance slit is dispersed onto a 3600 grating focused through the exit slits onto the photo multipliers (detection system). Optimum setting of the wavelength peaks is done by profiling using a sample containing the required element. The actual profile adjusts the position of the entrance slit relative to all exit slits. By using the optical fibres to the various spectrometers no element needs to be compromised by using reflection mirrors to fit two photo multipliers in next to each other. These would just be fitted into the alternative optic. Spectrometer optical systems can be optimised for individual wavelength ranges, leading to better resolution. Gratings can be optimised with respect to reflection for a wavelength range (blaze). A number of segments of the Rowland circle are available for installation of exit slits. Therefore the optics can be constructed for a large number of analytical channels.

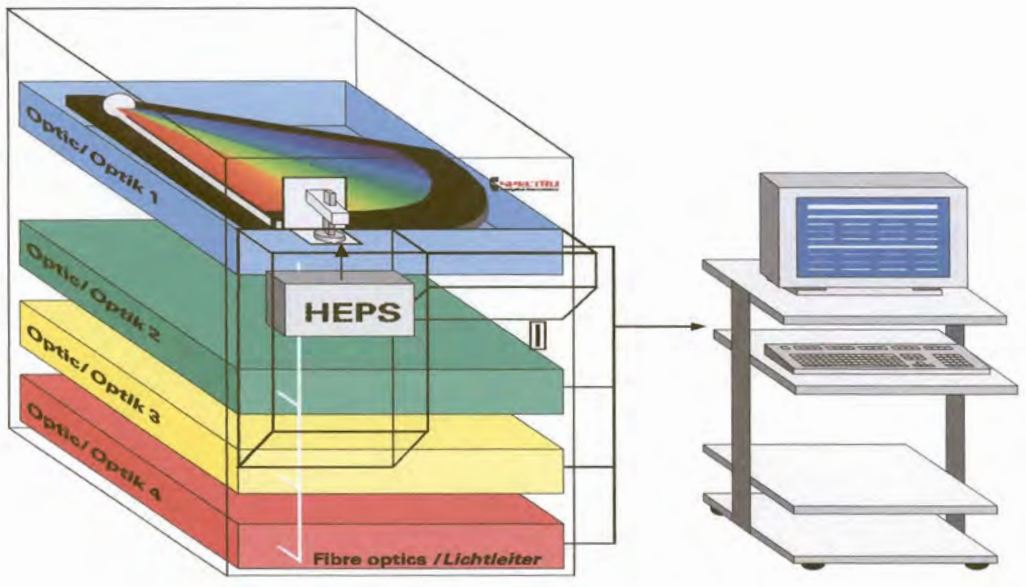


**Fig. 4.11 Spectrometer lay-out of Instrument [7].**

#### *4.4.4.2 Detectors*

Photo multiplier tubes measure photoelectric radiation [5,9]. These are radiation receivers in which the incident radiation releases electrons from the photo cathode to the surrounding vacuum or gas and, after amplification by secondary electron multiplication in a chain of additional electrodes (dynodes), are collected by the anode, and known as photocells and PMT(photo multiplier tube). The PMT can have up to 13 dynodes and $10^6$ - $10^8$ times current amplification. The electron current is taken off at the anode and is linear over large ranges of the incident radiation output. Linearity range is achieved when the current in the dynode voltage divider is at least 100 times the value of the maximum anode current. It is essential for spectrometers to work in the linear range of the PMT to obtain good calibration curves.

Current amplification is the ratio of the current emerging at the anode (the anode current) to the current collected by the first dynode (the cathode current). Current amplification is exponentially dependent on the voltage through the dynode chain. Dark Current is the sum of all the noise currents and possibly contains fluctuating currents due to surface leakages and discharges where there is no useful incident radiation. The signal to noise ratio is the ratio of the measured value of the signal to the measured value of the dark current.

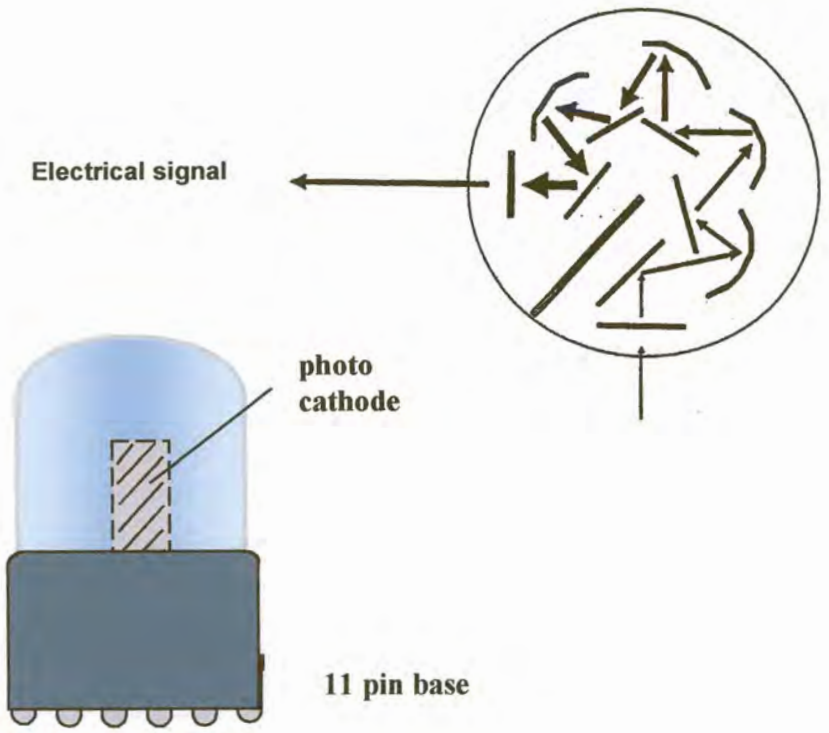


**Fig. 4.12 Principles of photo multipliers [8]**

#### *4.4.4.3 Measurement of photoelectric current*

*Integrator and digital converter:* The anode current from the PMT is integrated in the integrator before being passed to the analogue digital (AD) converter [5]. The integrator circuit consists of the operating amplifier, integration capacitor and a short circuit discharge switch. Negative PMT currents are converted into positive voltages. The discharge switch is used to discharge the integration capacitor at the beginning of each cycle. The maximum output voltage at the integrator is always less than the integrator supply voltage. The integrated circuit works at about 90 % of the supply voltage with a linearity of <0.1 %, i.e. with a supply voltage of 12 V, the range of 0-10.8 V can be used. In order to obtain a large dynamic range, the principle of dynamic integration is used. The capacitor is charged up to 100 times, i.e. 500 times during a five second integration period. The complete multi channel system for simultaneous spectrometer is obtained and controlled by a computer bus. To extend

the measurement range, the required sensitivity and resolution, a 14-bit AD converter with pre-amplifier is used. The pre-amplifier is inserted between the PMT and the integrator. It is possible to integrate the current coming from the PMT for any individual discharge during a pre-set time window as used in the SAFT technique. The output signal from the integrator is switched through to the AD converter and finally to the computer microprocessor. Communication usually takes place by means of a serial interface.

### *4.5 Evaluation of the "burn spot"*

A spark discharge creates the plasma, which contained elements representative of the whole sample. The sample surface is micro-melted in an argon atmosphere during the high energy pre-spark, before the photomultiplier tubes start measuring the radiation. Cooling and recrystallisation occurres rapidly and the surface is uniformly reformed. Any crystalline effects caused by the metallurgical history are partly overcomed. The discharge is divided into pre-spark time and integration spark. The pre-spark time is divided into an initial spark and homogenising time. Inclusion in the sample are attacked during the initial sparking. This leads to diffuse discharges caused by low plasma temperatures. They are indicated by white burn spots and very low intensities for the elements. When all inclusions had been eliminated, the intensities of the individual elements increase to the maximum. The time needed to achieve this state varies according to type and quality.

During homogenising a concentrated discharge occurs. The burn spot surface is refined to produce a shiny metallic surface with homogeneous distribution of craters and a deposit of black condensate on the edge of the burn spot. When the homogenising phase is completed and the sample in the stationary spark condition, vapourised material is replaced by material originating from deeper areas of the sample. There is a balance between evaporated and replaced material. The homogeneous layer is thicker than the dimension of the inclusions. When homogenising had been completed the analytical measuring time starts. The excitation source condition with pre-spark time is selected. The presence of oxygen in the sample or in the spark area cause oxide formation and has a similar effect to

inclusions. Heating in the burn spot increased the intensities of all elements. There are two types of burn spots derived from diffused and concentrated discharges. A comparison can be seen in fig. 4.13, 78.

If metal contained no precipitates there are no preferred points of attack during the spark discharge. Concentrated discharges can be obtained with high purity metal. In the case of diffuse discharges, the energy is distributed through numerous discharge channels. The cathode attack points distributed over a wide area, so that numerous small craters, less than 1 μm deep, were produced. Because of low plasma temperature, the intensity is low. In the case of concentrated discharges, the energy passes through one discharge channel, so that high temperatures are attained in the plasma and a crater 10 μm to 20 μm in diameter produced.

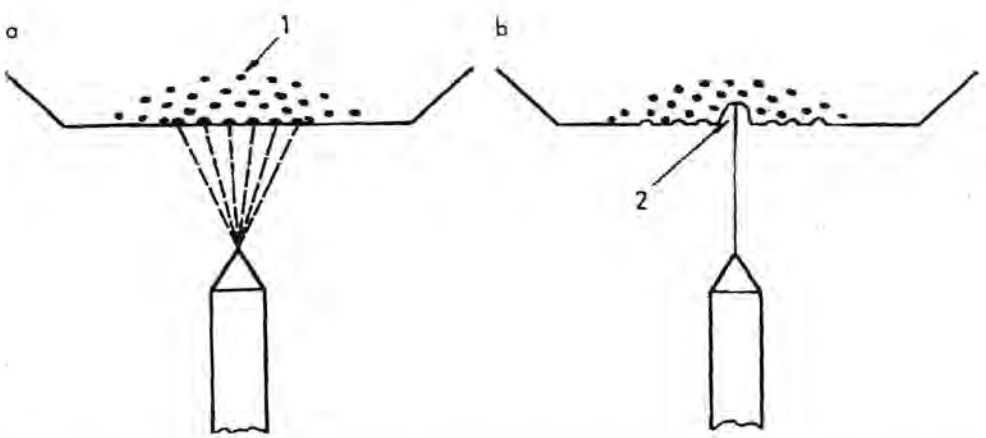


**Fig. 4.13 Illustration of (a) diffuse and (b) concentric discharges. 1 = precipitates; 2 = Crater [5].**

### *4.6 Determination of mechanism of material removal*

Atomic Emission methods are based on the assumption that vaporisation of the constituents in the sample would be proportional to the mean chemical composition, meaning the composition of the plasma was proportional to that of the sample. The burn-off curves of the elements are determined from the beginning of the sparking process by the mechanism of material removal. Equilibrium reached after a certain time of sparking is referred to as "steady sparking state".

The intensity of the base metal and the elements dissolved in it rose continuously after the start of the burn-off curve to become steady at the end of the sparking time. Homogenisation takes place during this time, with concentrated discharges melting and homogenising the sample in the burn spot region. The steady state is reached when all intensities of all elements become independent of sparking time.

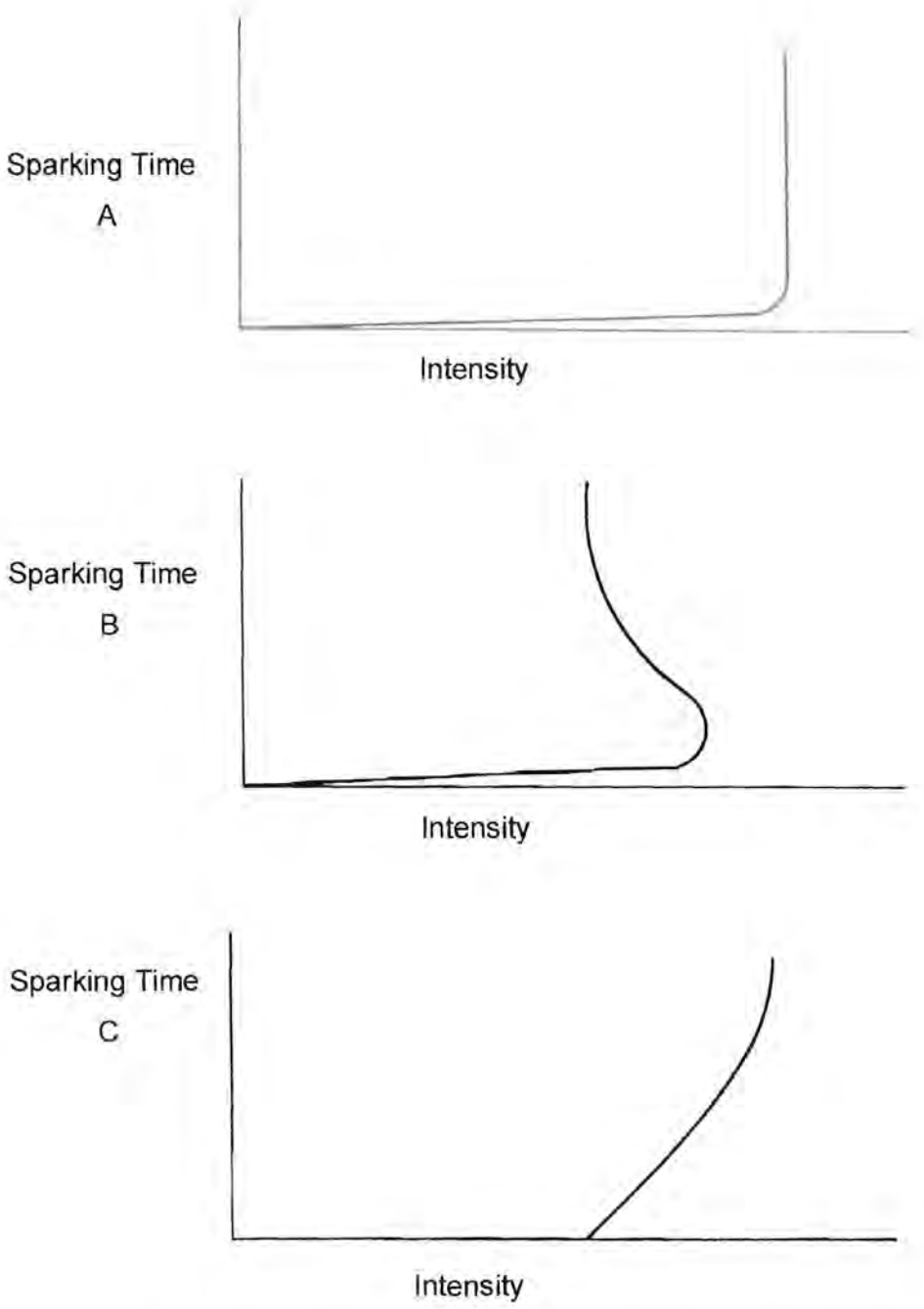


**Fig. 4.14 Typical burn-off curves with spark discharge in Argon [10].**
**A= Base and dissolved elements in a base which was difficult to vapourise e.g. Fe and Ni in Iron Base**
**B= Precipitated elements in a base which was difficult to vapourise e.g. Pb or $Al_2O_3$ in Iron Base**
**C= Elements which were difficult to vapourise in an easily vapourised base e.g. Cu in Zinc Base**

A distinction is made between the following categories with respect to burn-off curves:

- Dissolved elements in a base with high vaporisation temperatures and base metals e.g. in an Iron base [10].
- Precipitated elements or compounds e.g. Pb or $Al_2O_3$ in Iron base [10].
- Elements with high vapourisation temperature in an easily vapourised base e.g. Copper in Zinc Base [10].

In most cases, the intensities of the precipitates increase during sparking. The curves become constant when equilibrium is reached. This is the case when the proportion of concentrated discharges exceeds that of diffuse discharges; the intensity passes through the maximum. Concentrated discharges melt and homogenise the sample burn-spot. During this process, alternative areas of the sample are melted in the burn spot. After each discharge ceases, the minute liquid region around the vapourised crater solidifies on the solid sample. In the melt, the precipitates are present in a finely dispersed distribution, or are brought into forced solid sample. This is due to rapid cooling at 1000 ° C between two discharges; at 10 second intervals the liquid phase freezes. Non-metal precipitates are refined by micro fusion, but neither a sulphide nor an oxide can be dissolved and reach a steady state.

## *4.7 References*

[1] Horst Linn, **Linn High Therm Operating Instructions, Heinrich – Hertz – Platz 1D 92275 Nüremberg: Eschenfelden ,** (1994)

[2] http://www.linn.de, **Sample Preparation Equipment**, (2002)

[3] http://www.breitlander.com, (2002)

[4] **Operating Manual Breitlander Milling machine,** (2000)

[5] Karl Slickers, **Automatic Atomic-Emission-Spectroscopy,** Second Edition, (1993) 125, 137-138, 151-209

[6] H. de Laffolie, Ph. D. **Optical Fibers in ICP Spectrometry, Training notes, Spectro analytical Instruments**, Kleve: Germany,(1992).

[7] **Power point presentation, Stationary Spark Spectrometer, Spectro Analytical Instruments,** Kleve: Germany, (1999)

[8] G.L. Moore, **Introduction to Inductively Coupled Plasma, Atomic Emission Spectroscopy,** Randburg, South Africa, (1989), 108,109

[9] J.R. Dean, **Atomic Absorption and Plasma Spectroscopy, John Wiley and sons**, Second Edition,: University of Greenwich, UK, (1997)

[10] K.A. Slickers, **Automatic Atomic-Emission-Spectroscopy,** Second Edition (1993), 328

# Chapter 5

# Experimental

## *5.1 Introduction*

The aim of the study was to investigate the possibility of an alternative method to Spectrographic techniques for the determination of impurities in Ruthenium. Parameters that could be altered were investigated and optimised to obtain calibration curves for the analysis of the impurities in Ru base matrix. The supply voltage was kept constant at 220 V and the analysis gap (gap between the sample and electrode) adjusted between 3 and 4 mm. The optional parameter settings available were as follows:

Capacitance (μF) 2.2, 4.7, 6.9, 10.0, 12.2, 14.7.

Resistance (Ω) 1, 15

Inductance (μH) 30, 130

Frequency (Hz) 300

These conditions could be applied to the pre-spark and SAFT conditions. The pre-spark or HEPS was to ensure the homogenising process. The pre-spark conditions were determined and remained the same throughout the experiment. The sensitivity of the analytical channels and the background equivalent concentrations were monitored. The capacitance, resistance and inductance were varied where applicable. Calibrations were established for the various analytical elements using optimised conditions. Production samples were measured and compared with the analysis of other techniques. Due to the confidentiality agreement signed with the company supplying standards and samples, results will be presented graphically instead of in tables, in order not to compromise confidentiality.

## *5.2 Samples*

Pure metal salts and purified final metal samples were received for analysis. Salts received for analysis from the plant were ignited and reduced prior to analysis. If the

samples were moist they were placed under an infrared lamp to avoid spitting of the sample before ignition at 900 °C. The sample was placed in a porcelain crucible over a Bunsen burner. A lid placed on the crucible and hydrogen passed over the sample through a glass capillary to replace the oxygen and create a reduced atmosphere. While the sample was cooled to room temperature it was kept in a hydrogen atmosphere. The sample was shaken using a ball type milling action to ensure homogeneity. Loss of ignition was recorded and taken into account in the final analysis. Samples were pressed at 70 tons to prepare them for analysis on the spark spectrometer. The pure, refined metal powder for final analysis was pressed into pellets at 70 tons per square inch.

## *5.3 Optimisation of parameters*

### *5.3.1 HEPS (High Energy Pre-spark)*

Pre-spark used high discharge energy and the analysis was done using lower discharge energy. The capacitance was five times greater during pre-spark than during the analysis. The resistance remained the same. Pre-spark burn spot was larger (6 mm) than during integration (3 mm). This ensured that only material from the region that had been re-melted during prespark to obtain homogenisation was analysed [1].

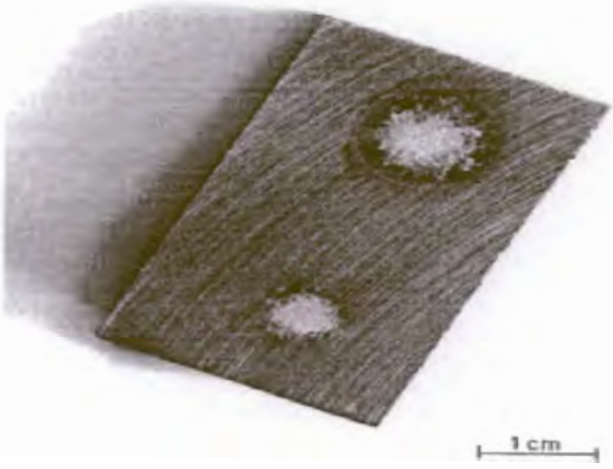


**Fig.5.1 Burn spots on a sample, top – HEPS and bottom – analytical integration [2].**

The duration of the low energy discharge was of secondary importance, as a state of quasi-homogenous layer was obtained and this supported the fact that the solid state does not alter over longer sparking times, which was what the principle of the HEPS was based on. Samples with low conductivity, when heated in the burn spot, caused the surface to disintegrate. Disintegration of the material can cause results to be incorrect. The problem can be overcome by using lower energy per discharge.
The parameters for the HEPS remained constant as per the manufacturers' factory settings. Resistance at 1 Ohm (Ω), Inductance 130 (μH) micro Henry Capacitance at 12,2 (μF) microfarad and Frequency at 300 (Hz) Hertz.

### *5.3.2 Intensity versus integration time*

*Experimental – HEPS*

Samples containing reasonable amounts of impurities were sparked at different integration times until a steady state was reached.
The sample was used for the determination of the pre-spark time. The spark conditions were as follows:

**Table 5.1 R = Resistance Ω Ohm; C = Capacitance Microfarad; L = Micro Henry; F=Frequency Hertz**

| | Pre-Spark | Spark | SAFT |
|---|---|---|---|
| R | 1 | 1 | 1 |
| L | 30 | 130 | 130 |
| C | 12.2 | 2.2 | 4.7 |
| F | 300 | 300 | 300 |

Resistance (R): The ratio of the potential difference between the ends of a conductor to the electrical current flowing in the conductor. All materials except super conductors resist the flow of an electrical current, converting a proportion of the electrical energy into heat. The extent to which a conductor resists the flow of a given current depends on its physical dimensions; the nature of the material of which it is made, its temperature, and in some cases the extent to which it is illuminated [3].

Capacitance (C): The property of a system of electrical conductors and insulators, which enables it to store electrical discharge when a potential difference exists between the conductors. It is measured by the charge, which must be communicated to such a system to raise its potential by one unit. The SI Unit for capacitance is farad [3].

Inductance (L): The property of an electrical circuit as a result of which an electromotive force is generated by a change in the current flowing through the circuit, or by a change in the current of a neighboring circuit with which it is magnetically linked. The SI unit of inductance is henry. An inductance in a closed circuit, such that a rate of change of current of 1 ampere per second, produces an induced electro motive force of 1 volt [3].

*Experimental – intensity versus time*

Sample S8 contained the following concentrations in ppm: Fe 200, Na 200, Ca 200, Si 200, Cu 85, Al 200, Mg 200, Te 100, As 100, Bi 100, Mo 100, Sn 50 and Co 50.
Sample 7 contains the following concentrations in ppm levels: Pt 200, Pd 200, Rh 200, Ir 200, Au 200, Os 120, Ag 200, Zn 200, Pb 100, Sb 100, Mn 100, Ti 100, Cr 100.
Both samples were sparked using the same conditions and the integration time varied from 1 to 10 seconds, increasing the time by 1-second intervals.

### *5.3.3 Effect of different gating parameters*

When a sample is sparked, a background signal is obtained which is synchronous with the discharge current curve. When sparking a sample with concentrations above the background equivalent the intensities of the atom and ion lines differ. The intensities of the ion lines were also synchronous with the current and thus the spectral background. This was due to the high temperatures (current) required for the excitation of the ion lines (15 eV). The number of ions is also proportional to temperature and the intensities of the atom lines appear with a delay time. The intensity curve against time (as described in detail in chapter 3, 3.9.2, 49) is basically

determined by the excitation energy and not by the vapourisation enthalpy. Thus the temperatures for Fe 371.9 nm (3.3 eV) and Cd 228.8 nm (5.3 eV) in a Cu base are very similar against time, although the vapourisation temperatures differed considerably.

The aim was to optimise the delay conditions to reduce spectral interference from ion lines or to eliminate it so that the atom line of the element of interest appeared clearly above the background. The system has to be optimised to produce the best signal to background ratio.

*Experimental – optimising gating parameters*

The test was performed on pressed Ru powder standards. Impurities in solution of the various elements and varied concentrations were added to very pure ruthenium. These samples were dried at very low temperatures and blended mechanically by shaking the mixture in a mixer-mill and then ground it in a rotary mill. Standards were pressed at 70 ton. Five samples were used for the test work. Sample preparation was as has been discussed in chapter 5, 5.2, 83.

Sample 1 was a blank (99.9 % purity).

Sample 7 and 9 contained different concentrations of Ag, Au, Cr, Ir, Mn, Pb, Pt, Pd, Rh and Sb.

Sample 8 and 10 contained different concentrations of Al, As, Bi, Ca, Cu, Fe, Mg, Mo, Na, Ni and Sn.

Two different samples were analysed to confirm any trends.

Ideally I would have liked to have the samples melted but the facilities available could not reach the high temperatures required for melting the Ru standards. Secondly, due to the high value of the material security was tight and the samples were not allowed to be taken from the premises. The standard parameters were; 1Ω Resistance, 30 μH, frequency 300 Hz, Capacitance 4.7 microfarads.

Tests were performed with the 15 Ω and 1 Ω resistor.

The system makes use of a 16-channel integrator board. The times set up for the experiment were at intervals of 16 μs ranging from 16 μs to 176 μs. All the other

parameters stayed constant. The samples were analysed using a 5 second pre-spark and then SAFT parameters for the analysis.

**Table 5.2 Spark Analysis For Traces (SAFT) conditions**

| Parameters | R | L | C | F |
|---|---|---|---|---|
| SAFT Conditions | 1 / 15 Ω | 130 μH | 4.7 Microfarad | 300 Hertz |

### *5.3.4 Internal standardisation*

The internal standard is generally a constant amount of an element, which is added to all samples, blanks and calibration standards used for the analysis. Alternatively, it can be a major constituent of the sample and standards in a large amount, so that it is assumed that the amount is constant throughout. The calibration curve was obtained by plotting the ratio of the analyte signal as a function of the analyte concentration of the standards. Internal standardisation was widely employed in quantitative emission spectroscopy as a way of improving precision and accuracy [4]. The procedure involved calculating the ratio of the intensity of the analyte emission line to that of a second element also present in the sample or added intentionally. Guidelines have been proposed for matching the physical properties of the analyte and the reference elements so that this ratio was insensitive to fluctuation of the experimental parameters.

Greenfield [5] reported a high degree of correlation between two emission signals for elements, which had similar excitation energies, or in the case of ions, a similar sum of ionisation and excitation energy.

In spark emission a reference line is often the base, matrix element. If no element could be found which was suitable as a reference because of variations in the sample composition, a constant quantity of an element not present in the sample (external reference) was added during sample preparation. The reference line is exposed to the same, or similar, changes as the analytical lines, in radiation produced [6].

Changes in the radiation can be due to the composition of the sample itself, changes in viscosity, processes in the discharge gap or faults in the radiation off take.

A suitable reference line should adhere to the following criteria:

- The intensity ratio of the line pair should not be affected by interference from other lines.
- The ratio should be dependant only on the concentration and not on discharge parameters, so that the lines were associated with the same ionisation state, and should have similar excitation energies. Analyte and reference should have similar ionisation energy.
- Vapourisation of the reference element should take place in a manner similar to that of the analytes. This applies particularly for methods with total vapourisation, or if a steady state has not been obtained.

In the case of spark emission, it was found that with elements mainly or entirely precipitated from the base, matrix element (e.g. B, P, S, Pb, Sb in Fe base), the RSD (relative standard deviation) was not improved by relating the analytical line to a reference line [6]. Thus for precipitated elements the sample surface must be heated sufficiently for it to be vapourised. This was achieved by using optimum HEPS conditions. In the case of dissolved elements and the base metal, the crystalline structure must first be destroyed and then vapourised.

In samples where the base metal was close to 100 %, and the intensity of the background at a "clean" (no interferences) wavelength, the total discharge radiation or zero order radiation was used. Since these variables take intensity changes in the spectral background into account, they were suitable as a reference for low concentrations, if the proportion of the spectral background in the total measurement signal was significant. The reference is primarily intended to compensate for changes in the vapourisation behavior and probability of transition, and only secondarily for instability due to absorption or in the geometry of the radiation source with resultant fluctuations in the signal from the photo multiplier tubes due to inadequate radiation off take [6]. Therefore the spectrometer calibrations and the intensity ratio of the analytical line to the reference line are plotted against the

concentration ratio of the analyte to the reference (base material or background position) [6].

### 5.3.5 *Analytical gap 3 mm and 4 mm*

As in Chapter 4, fig. 4.6, 69 the temperature distribution generated at the spark stand can be seen. The electrode, made from tungsten, can be set at either a 3 mm or 4 mm gap (the gap between the sample and the electrode). Under these conditions the temperature generated at the spark is estimated to be between 1000 and 10 000 Kelvin. The best excitation was expected for atomic lines from 5000 to 8000 Kelvin and best excitation for ionic lines at 10 000 Kelvin. The experiment was done using sample 9 and 10. Sample 9 contained Ag, Au, Cr, Ir, Mn, Pb, Pt, Pd, Rh and Sb. Sample 10 contained Al, As, Bi, Ca, Cu, Sn, Mg, Mo, Na, Ni, Si and Fe. The sparking conditions of the instrument remained the same, with only the gap (distance between the electrode and the sample) changing: 3 mm and 4 mm distances were used.

**Table 5.3 Sparking conditions used during 3 and 4 mm gap determinations**

| | Sparking Conditions | | | | | | | |
|---|---|---|---|---|---|---|---|---|
| | C (μF) | R (ohm) | L (μH) | Freq (Hz) | Air Gate(μS) | Air Delay(μS) | UV Gate(μS) | UV Delay(μS) |
| Flush | 0 | 0 | 0 | 0 | 64 | 144 | 64 | 144 |
| Pre-Spark | 12.2 | 1 | 30 | 300 | 64 | 144 | 64 | 144 |
| Spark | 2.2 | 1 | 130 | 300 | 64 | 144 | 64 | 144 |
| SAFT | 4.7 | 1 | 130 | 300 | 64 | 64 | 64 | 64 |

### 5.3.6 *Contamination from another base material*

When a sample is first measured with a high concentration or even another base and then a pure sample, the concentration for the pure sample will most probably be incorrect due to contamination. With repeated sparking, contamination asymptotically approaches zero. If the degree of contamination is not acceptable, it is necessary to change the stand components, which are in contact with the discharge space. It is

inevitable that trace amounts of all the PGM will be analysed in the various base materials i.e. Pt, Pd, Rh, Ir, Au will be measured in Ru. The next sample might be a Pt sample and Ru will then be required as an impurity. Cross contamination must be prevented at all times.

*Experimental – cross contamination:*

To investigate the degree of cross contamination between Pt, Pd, and Ru, samples of 99.9 % purity were used. A pure Ru sample was sparked and without changing plates, a pure Pt sample was sparked and the Ru in the sample monitored, until a stable signal was established. A pure Pd sample was then sparked and the Pt monitored. Then a pure Ru sample was sparked and the Pd monitored.

The same exercise was repeated using the Ru base plate, electrode and chamber accessories when sparking the Ru sample, monitoring the Pd. The Pt sample was sparked using the base plate etc. and monitoring the Ru and the Pd sample sparked with the appropriate base plate monitoring the Pt. Sparking conditions remained the same throughout this investigation. Raw intensities were recorded to determine the extent of cross contamination and to establish operating procedures.

### *5.4 Creating calibration graphs*

Creating standards for analysis was probably the most important aspect of the calibration. Calibration standards were prepared in three different ways. A composite sample was used for the basic standard. This material was very pure (99.99 %) and the impurities were known.

The first set of standards was prepared by using stock solutions of the various impurities. Ten standards were made up in this batch. Twenty grams of material was used for each standard and then the samples were spiked with precious metals and base metals in varying concentrations. The standards were dried overnight at 100 °C in a drying oven or evaporated using an infrared lamp. The standards were homogenised in a sample shaker, which used a ball type milling action, and then pressed at 70 ton.

The second set of standards was prepared by using the Ru composite sample and pressing that at 70 ton. Five grams of a certified reference material from Johnson Matthey was pressed on top of the Ru composite sample at 80 ton. 10 Samples with varying concentrations of impurities were prepared in this way. The third set of standards was prepared by adding the impurities as metal to the ruthenium composite and then melting the material in an inductive or arc furnace. Calibration using optimised conditions as found in varying parameters as well as the mathematical procedure will be discussed in more detail in the next Chapter.

### *5.5 Comparisons of samples analysed*

Ultimately, the new method was required to be used in production. Samples analysed had to be compared with those from other techniques, such as inductively coupled plasma mass spectrometry (ICP-MS) and spectrographic (Spec) analysis. Metal salts were analysed for internal use to control the process. Analysis of the final refined pure metals was analysed by the spark spectrometer and sold to customers on their purity value. Samples from the different mines were analysed by the participating mines and these were referred to as interchange samples.

A composite sample was also sent for analysis internationally and these samples were referred to as a round robin. Various precious metal refineries in South Africa, the United Kingdom and Russia participated in these analyses. Company A (South Africa) was responsible for the analysis done by the Spark Spectrometer, B (South Africa) for analysis done on a Spectrograph, C (South Africa) conducted analysis on ICP, D (South Africa) conducted analysis on a spectrograph and ICP, E (United Kingdom) conducted analysis on ICP, F (Russia) conducted analysis on spectrograph and F (United Kingdom) conducted analysis on a spectrograph. Results of the analyses of these samples were compared to each other.

## *5.6 References*

**[1]** K.A. Slickers, **Automatic Atomic-Emission-Spectroscopy,** Second Edition (1993), 328

**[2]** K.A. Slickers, **Automatic Atomic-Emission-Spectroscopy,** Second Edition (1993), 137-138

**[3]** E.B. Uvarov, D.R. Chapman, **A Dictionary of science,** Maryland, A.S.A. (1943), 329, 61, 196

**[4]** S.A.Meyers, D.H. Tracy, **Improved performance using Internal standardization in Inductively coupled plasma emission spectroscopy. Spectrochimica Acta, Vol. 38B No.9** Norwork, USA, (1983), 1227

**[5]** S Greenfield, **Developments in Atomic Plasma Spectrochemical Analysis,** Heyden, London, Philadelphia (1981), 1

**[6]** K.A. Slickers, **Automatic Atomic-Emission-Spectroscopy,** Second Edition (1993), 226 - 238

# Chapter 6

# Calibration

## *6.1 Introduction*

Calibration comprises the measurement of calibration samples and the determination of the functional relationship between the intensity of the line of an analyte and its concentration in the sample. The functional relationship includes the relations between vapourisation, excitation, radiation off-take, dispersion and the measured value. The slope of the calibration curve is largely determined by the radiation source. The standard error of the calibration and limit of detection is affected by the radiation off-take and dispersion [1]. The final concentration of the unknown analyte is critical and dependent on the calibration of the instrument.

Two commonly employed approaches of calibration are found in emission spectroscopy. These are the methods of direct comparison and standard addition [2]. This study dealt only with the direct comparison method. The accuracy of the calibration was dependent on the selection of standards, the quality of their preparation, the accuracy of their data and the response of the spectrometer used for generating and measuring emission of the required elements.

The instrument signal given by the blank sample will very often not be zero. It is thus wrong in principle to subtract the blank value from the other standard values before plotting the graph [3]. The calibration curve is always plotted with the instrument response on the vertical (y) axis and the standard concentrations on the horizontal (x) axis. This is due to many procedures, which assume that all the errors are in the y values and that the standard concentrations (x-values) are error free [3]. In routine instrumental analysis this statement is justified by the assumption that standards can be made up with an error of 1 % or better, whereas the instrumental measurement might have a coefficient of variance of 1-2 % or worse. The second assumption is that the magnitude of the error in y is independent of the analyte concentration, if the

relative errors in the measurement are constant; the absolute errors will increase as the analyte concentrations increase [3].

Most analytical methods are based on a calibration curve in which a measured quantity *y* is plotted as a function of the known concentration *x* of a series of standards [9]. The best "straight line" is fitted through the points and the most common way of obtaining such a "straight" line is by using the method of least squares regression. In applying this method, we assume a straight line is a good model for the relationship between the area of a peak (*y*) and its analyte concentration (*x*) as given by the equation:

$$y = mx + c$$

Where *m* is the slope and *c* is the intercept of the line. These two parameters form part of the model, which is assumed to be a straight line [4].

### 6.2 *Background Equivalent Concentration (BEC) and Limit of Detection (LOD)*

It is very important to avoid confusion regarding sensitivity and limit of detection. The sensitivity is generally defined as the slope of the calibration graph and provided the plot is linear, it can be measured at any point on it. The limit of detection is calculated with the aid of the section of the plot close to the origin, and utilises both the slope and the intercept [3].

Reference is made to the Background Equivalent Concentration (BEC) and the Limit of detection (LOD). The BEC is the concentration in the sample, which produces the same line intensity as the spectral background, also referred to as the signal-noise ratio. The BEC is the concentration of analyte required to produce the same signal as the background at a given wavelength. It is a fundamental process and variable since it directly affects the limit of detection. If the analyte concentration is zero, the intensity "U" is the spectral background (dark current produced by electronic noise already subtracted). If "U" is doubled and plotted in the direction of the intensity axis and this point "(U+L)" is projected on the concentration axis, the BEC is obtained. A basic feature of the analytical method is its capacity to determine low concentrations. The quantitative information is the limit of detection [1].

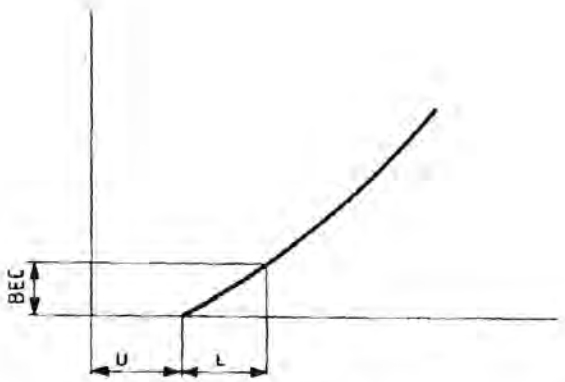


**Fig. 6.1 Representation of Background Equivalent Concentration (BEC) [1].**

Formula for determining the BEC:

$$BEC = \frac{C(H) - C(L)}{I(H) - I(L)} X\ [\ I(L) - DC] - C(L)$$

C(H) = Concentration of high standard

C(L) = Concentration of low standard

I (H) = Intensity of high standard

I (L) = Intensity of low standard

DC = Dark current

The most generally accepted qualitative definition of detection limit is the minimum concentration or mass of analyte that can be detected at a known confidence level [9]. The BEC, LOD and other significant information produced for the calibration on the Spectrolab is based on principles as formulated by Kaiser [5]. The LOD is taken as the equivalent concentration of the absolute standard deviation (ASD) $S_0$ of the precision of the spectral background in the following form [1]:

$$LOD = 3\ X\ \sqrt{2}\ S_0$$

For the simplified version the $\sqrt{2}$ is omitted. The spectral background can only be given by a sample which "does not contain" the analyte. Slickers [1] say: "there is no such thing. If there is a sample, however, containing the analyte at a concentration

far (<2 times) below the LOD, the method of determining the LOD remains "Clean" as the absolute relative standard deviation is then mainly determined by the spectral background and not by the low analyte concentration". The formula for the LOD does not explicitly contain the spectral background (e.g. Expressed as BEC) i.e. if the spectral background were large but infinitely precise ($ASD_0$ towards zero) any number greater than the infinitely stable background could be assigned to a concentration in the sample. The LOD as a function of the RSD can be stated directly, in concentrations incorporating the BEC.

$LOD = 3\ RSD_0 \times BEC/100$

**Table 6.1 The LOD as a function of the RSD**

| $RSD_0$ | 0.50% | 1% | 1.50% | 2% | 3% |
|---|---|---|---|---|---|
| LOD | BEC/60 | BEC/30 | BEC/20 | BEC/15 | BEC/10 |

Usually, the repeatability of the background is 1 % and therefore LOD = BEC/30 is commonly used as an estimate. The LOD for the method can only improve by reducing the RSD or reducing the BEC [1].

## *6.3 Spectral interference*

Spectrometer measurements can be affected by spectral interference effects, which are systematic additive errors and must be corrected.

Spectral interference effects are [6]:

i) Line overlaps: Effects due to line overlaps with inadequate resolution of the spectrometer optics.

ii) Band coincidence: Effects arising from bands of poly-atomic particles (e.g. CN, AlO) forming from the gasses surrounding the radiation source or from incomplete, dissociated compounds.

iii) Background Interference: Effects arising from changes in the spectral background with varying matrix.

iv) Stray light: Effects arising from reflection in the optical system (stray radiation) or from radiation from other orders. It may be element or non-element specific.

Interference effects arising from i), ii), and iii) increase the measured value, whereas effects from background interference can decrease or increase the measured value.

Although most inter-element effects are non-linear, it is often possible to carry out a linear approximation in the concentration ranges present. If the concentration ranges were not greater than those in which a linear approximation of the non-linear correction was permitted [6].
Interelement effects can arise from the sample itself, as well as the discharge atmosphere.

The effects associated with the sample are as follows:

i) Precipitates present in the sample that can change.
ii) Changes may occur in the form of solidification due to differences in the vapourisation rate.
iii) Other elements may be present in the base element, which may dissolve or precipitate partly or completely.
iv) Changes due to elements with high vapourisation temperatures, which were present in a low vapourisation temperature base element.
v) There may be changes in the vapourisation rate due to changes in vapourisation enthalpy. Due to lowering of the melting point by alloy elements, the energy necessary for vapourisation is reduced. Therefore for a given energy conversion in the discharge gap the quantity of sample material vapourised per discharge is increased, which results in increased intensities.
vi) There may be changes in the vapourisation rate due to changes in thermal conductivity. Alloy constituents affect thermal conductivity in different ways. Low thermal conductivity leads to greater localised heating in the burn spot and therefore increased vapourisation of material and increased intensities.

vii) When the analytical line is ratioed to a reference line, the effect of changes in vapourisation rates due to changes in enthalpy and thermal conductivity mostly lose their effect on spectrochemical results. This is because the changes in vapourisation rate affect the dissolved analyte to the same extent as the reference.

The effects associated with the sample and the discharge atmosphere is as follows:

i) Changes in the type of discharge, that is, diffuse or concentrated, may occur due to presence of oxides in the sample.

ii) Changes in the type of discharge due to constituents of the sample and discharge atmosphere other than oxides may occur.

The effects associated with the sample in the plasma.

i) Changes in location of optimum excitation of an atomic line in the plasma may occur due to other elements and differences in the imaging of this location in the optics. This was responsible for discrepancies among interelement effects stated in various texts for the same sample programme. Interferences in the plasma must present a maximum at least one point between the electrodes since it is zero at the electrodes. This effect was lost during analysis where there was uniform radiation from the entire radiation source. This is illustrated in Fig. 6.2, 100 [8].

ii) Changes in the plasma temperature due to other elements with varying ionisation temperatures and resultant changes in excitation probability may also occur. In the presence of elements with low ionisation energy compared to the base element, the plasma temperature dropped so that spectral lines with high excitation energy became stronger. When elements with high ionisation energy compared to the base metal were present together, the plasma temperature increased so that the spectral lines with high excitation energy became stronger and those with low excitation energy became weaker. This interference lost its effect on spectrometric results if homologous lines were used.

Additive correction: Analytical lines, which arise from spectral interferences, can be corrected for if no other wavelength, which is interference free, is available. The

interference factor can be determined by measuring a binary sample (sample that contains the interfering element in rather high concentrations but is otherwise pure). Changes in intensity with respect to the pure sample as a function of the concentration of the interfering element are the basis of the corrections [6].

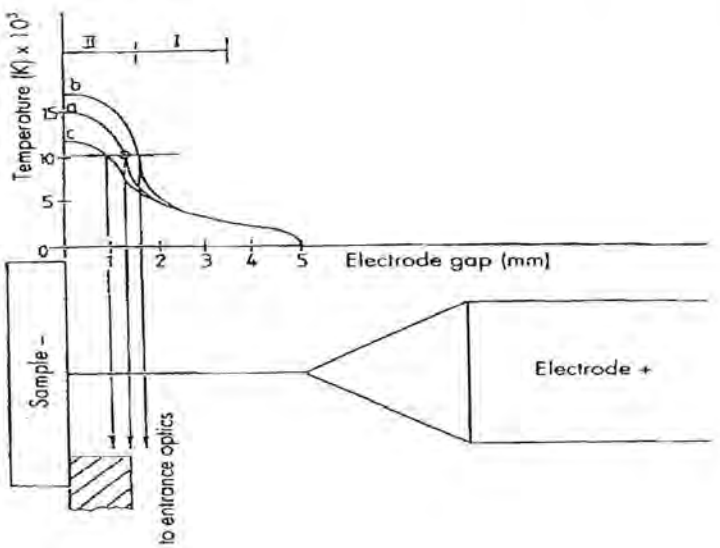


**Fig. 6.2 Displacement of location of optimum excitation 1= Atom lines; 11 = Ion lines [8].**

## *6.4 Background correction*

In optical systems, which only have, one background slit the intensities of the analytical lines and the background were measured simultaneously. In doing so it was assumed that the background in the background below the analytical lines and the background in the background slit could be reciprocally converted by a factor k [6].

The result was:

$I_N = I_{EL} - KI_U$

$I_N$ = Nett Intensity

$I_{EL}$ = Intensity in the channel of the analytical line

$KI_U$ = Background intensity

## 6.5 *Measurement values for the analytical data*

Once all intensities have been measured by the spectrometer, readings of the measurement capacitors for the analytical channels taken, and analogue signals converted into digital forms, the process of calculating concentrations from intensities takes place. These processes are carried out in a number of steps [6].

### 6.5.1 *Intensity ratio*

The intensities obtained are usually ratioed to the reference material. This acts as an internal standardisation. It provides compensation for small changes in the spectrometer during the measuring cycle and from measurement to measurement. These changes could be due to variances in the excitation energy of the source, to condensate collecting in the light path and to the window or lens becoming dirty. The typical intensity of the reference was used as a multiplicator in order to obtain a specific order of magnitude for the intensity ratios, therefore dealing with whole numbers rather than decimals [6]. The typical intensity is the intensity of the internal standard line (matrix element).

$$\text{Intensity Ratio} = (I_{an} / I_{ref}) \times \text{typical } I_{ref}$$

$I_{an}$ = Intensity of the analyte
$I_{ref}$ = Intensity of the reference

In cases of samples that significantly influence the spectrum background, a background correction could be applied. The differences in the sensitivity of the analysis channel and the background channel can be compensated for by using matching variables. In doing so, the difference between the intensities of the analysis channel and background channel is determined.

### *6.5.2 Corrected intensity ratio*

The effect of the inter element interferences are corrected for. These effects are additive, caused by line interferences or multiplicative corrections caused by inter element / matrix effect [7]. The additive effect caused by line interference is due to light from a spectral line of another element entering the exit slit of the analytical line of interest. This occurs if the two wavelengths are very close together. Spectral lines should be carefully selected to prevent this, however this is not always possible. Inter element corrections can be made to overcome the problem if there is no alternative.

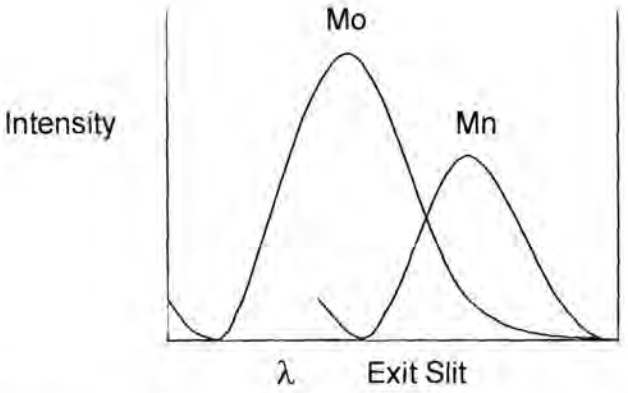


**Fig. 6.3 Light of Mn causing interference at the Mo exit slit [7].**

The multiplicative effect is caused by matrix effects, which are caused by the physical and chemical nature of the sample. In Fig. 6.3, 102 the intensity of the Mn has to be subtracted from the Mo intensity to correct the calibration standards, which contain Mn on to the calibration curve.

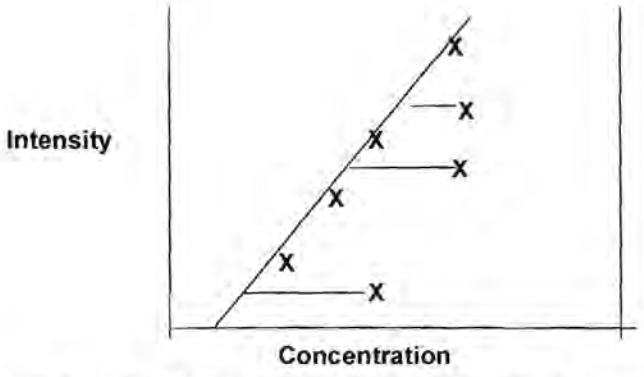


**Fig. 6.4 Corrected Intensity calibration curve[7].**

### *6.5.3 Recalibration*

The additive and / or multiplicative changes in the sensitivity of the spectrometer (drift) brought about displacements of the calibration curves in the linear scale of the co-ordinate system. To avoid the need for regular new calibrations of the spectrometer it is necessary to follow a procedure, which on the basis of a few samples and mathematical calculations, restores the state of the spectrometer by calculations during the calibrations and corrects for any drift correction. This process is known as recalibration, but is also termed standardisation. The samples, known as recalibration samples, were measured during calibration of the spectrometer. The calibration samples were no longer required for daily analysis. The recalibration samples were to adjust the intensity ratios (actual value) measured "today" to those measured at the time of calibration (nominal value) to compensate for any instrumental drift.

For each calibration curve, a low sample (LS) with low concentration and a high sample (HS) with high concentration were measured in a two-point calibration. For back calculation of the data obtained from the recalibration sample to the nominal state of the spectrometer, a factor was calculated from the ratios of the nominal values to the actual values. The offset shows changes in the zero point. On completion of the recalibration / standardisation, the factor and offset for all analysis channels were stored. These were the basis for subsequent corrections of the measurement values with respect to the nominal state of the spectrometer.

$$\text{Factor} = \frac{\text{Int. HS}_{nom} - \text{Int LS}_{nom}}{\text{Int. HS}_{act} - \text{Int. LS}_{act}}$$

$$\text{Offset} = \frac{\text{Int. HS}_{act} * \text{Int LS}_{nom} - \text{Int. HS}_{nom} * \text{Int. LS}_{act}}{\text{Int. HS}_{act} - \text{Int. LS}_{act}}$$

Using the formula:
Factor = change of the slope of the curve
Offset = parallel drift of the calibration curve

The standardisation intensity ratios were calculated as follows:
Standardisation intensity ratio = Intensity ratio * F + offset.

### *6.5.4 Concentration calculation*

In metal analysis with spark discharge optical emission, the matrix / base element is often used as the reference and for this reason concentration and ratio and intensity ratios were used in this study. The concentration of the matrix element / base element was not calculated by the calibration curve, but was obtained by deducting the sum of the analysed elements form 100 % of the matrix element, on the assumption that all the elements present had been determined. The following equation applies [6]:

$$\sum C_{an} + C_b = 100\ \%$$

$C_{an}$ = Concentration of the analysed element
$C_b$ = Concentration of the base element

The concentration of the base element could be obtained by rearranging the equation and taking account of the fact that the concentration ratio of the base to itself was 1 [6]:

$$C_b = 100\ \% \ 1 + \sum C_{an} / C_b$$

The formula to obtain the concentrations of the analyte from the ratios:

$$C_{an} = C_b \cdot C_{an} / C_b$$

If some analytes (usually those precipitated) were calibrated in absolute values, without a reference, the sum of the analytes ($C_{abs}$) must be subtracted from the 100 % calculation for the other analytes. The calculation formula to determine the analyte concentration must therefore be modified [6]:

$$C_{an} = (100 - C_{abs}) / (100/1 + \sum C_{an} / C_b) / C_{an} / C_b$$

The relationship between the Intensity ratio and concentration of the calibration sample was mathematically determined during calibration of the spectrometer. By means of the regression calculation, the optimum mathematical polynomial function (first, second or third degree), for all concentration was automatically calculated. For low concentrations the calibration is usually a linear relationship ($1^{ST}$ degree). To calculate the analyte concentration (c), the recalibrated intensity ratio of the required analysis channel (IR) was introduced into the polynomial function:

$$C = a_3 * (IR)^3 + a_2 * (IR)^2 + a_1 * (IR) + a_0$$

Where $a_3$, $a_2$, $a_1$ and $a_0$ are the coefficients of the polynomial function.

## 6.6 *References*

[1] K. Slikers, **Automatic Emission Spectroscopy,** Second Edition, Germany: Giesen, (1993) 223, 240

[2] J. C. Van Loon. **Analytical Atomic Absorption Spectroscopy, Selected Methods. Toronto, Canada,** (1980) 48

[3] J.C. Miller, J.N. Miller, **Statistics for Analytical Chemistry,** Third edition, **West Sussex, Great Britain,** (1993) 104, 117

[4] R. Caulcutt, R. Boddy, **Statistics For Analytical Chemist, London,** (1983) 79

[5] H. Kaiser, A.C. Menzies, **The limit of detection of a complete Analytical Procudure,** London (1968) 6

[6] K. Slikers, **Automatic Emission Spectroscopy,** Second Edition, Giesen, Germany (1993) 249, 261-269

[7] **Training Schedule**, Kleve, Germany (1999)

[8] K. Slikers, **Automatic Emission Spectroscopy,** Second Edition, Giesen, Germany (1993) 354

[9] D. A. Skoog, F.J. Holler, T.A. Nieman, **Principles of Instrumental Analysis,** Fifth Edition, Stanford University, University of Kentucky, University of Illinois (1997) 13

# Chapter 7

# Results

## *7.1 Optimisation of parameters*

### *7.1.1 High Energy Pre-Spark*

Samples were sparked and parameters were kept constant. During the process samples had to be pressed again as material disintegrated when sparking and created source problems.

**Table 7. 1 Intensities of Sample 7 sparked**

| Seconds | Pt | Pd | Au | Rh | Ir | Os |
|---|---|---|---|---|---|---|
| 1 | 18997 | 16106 | 39217 | 34256 | 314 | 7680 |
| 2 | 19909 | 16183 | 41855 | 84190 | 396 | 7902 |
| 3 | 29316 | 23293 | 60870 | 121982 | 586 | 11893 |
| 4 | 40561 | 31791 | 79022 | 172761 | 866 | 15930 |
| 5 | 52901 | 38745 | 104330 | 204569 | 973 | 21123 |
| 6 | 60255 | 45454 | 123290 | 236265 | 1247 | 25189 |
| 7 | 70256 | 52018 | 143184 | 280135 | 1368 | 30353 |
| 8 | 85281 | 60252 | 162821 | 322111 | 1536 | 32607 |
| 9 | 90587 | 66172 | 182409 | 346259 | 1781 | 35832 |
| 10 | 101370 | 72944 | 204097 | 386193 | 1965 | 40903 |

**Table 7.1 Continued. Intensities of Sample 7 sparked**

| Seconds | Ag | Pb | Zn | Mn | Ti | Cr |
|---|---|---|---|---|---|---|
| 1 | 49677 | 3091 | 48718 | 9552 | 15720 | 30202 |
| 2 | 75034 | 4202 | 58245 | 11875 | 15368 | 30062 |
| 3 | 104766 | 5999 | 73380 | 17825 | 22134 | 43186 |
| 4 | 137110 | 16601 | 90037 | 23392 | 29483 | 58228 |
| 5 | 155139 | 120807 | 101282 | 29851 | 37073 | 72048 |
| 6 | 183697 | 15003 | 112299 | 35145 | 43174 | 82975 |
| 7 | 209639 | 14360 | 128655 | 38434 | 49924 | 92646 |
| 8 | 229709 | 15304 | 126696 | 45591 | 58432 | 108434 |
| 9 | 269770 | 17420 | 148515 | 48088 | 62688 | 118558 |
| 10 | 267941 | 16539 | 146493 | 53314 | 69287 | 128761 |

**Table 7.2 Intensities of Sample 8 sparked**

| Seconds | Cu | Fe | Te | As | Al | Na |
|---|---|---|---|---|---|---|
| 1 | 372068 | 10959 | 454 | 6776 | 26397 | 333936 |
| 2 | 438065 | 21523 | 600 | 9211 | 46730 | 752031 |
| 3 | 440082 | 28497 | 1053 | 11298 | 57393 | 950303 |
| 4 | 496293 | 33889 | 1404 | 16214 | 82204 | 1299000 |
| 5 | 527811 | 42930 | 1532 | 18699 | 83297 | 1398000 |
| 6 | 584068 | 50113 | 1445 | 20414 | 97151 | 1490000 |
| 7 | 629454 | 59901 | 2269 | 24220 | 101184 | 1405000 |
| 8 | 710119 | 73969 | 2129 | 28707 | 138965 | 1509000 |
| 9 | 737609 | 74519 | 2434 | 30993 | 132628 | 1593000 |
| 10 | 798631 | 82210 | 2650 | 34533 | 138393 | 1616000 |

**Table 7.2 Continued. Intensities of Sample 8 sparked**

| Seconds | Ca | Si | Mg | Mo | Sn | Co |
|---|---|---|---|---|---|---|
| 1 | 105613 | 23634 | 105466 | 30587 | 1346 | 4422 |
| 2 | 208713 | 27526 | 200771 | 60413 | 2497 | 13740 |
| 3 | 290214 | 37413 | 250500 | 82441 | 3255 | 20529 |
| 4 | 387243 | 41102 | 313486 | 114349 | 4389 | 29134 |
| 5 | 455269 | 41032 | 352751 | 135354 | 5038 | 37666 |
| 6 | 548502 | 44040 | 396411 | 164889 | 6658 | 45931 |
| 7 | 624099 | 47588 | 421945 | 190052 | 8326 | 56751 |
| 8 | 744912 | 52754 | 477781 | 231268 | 9579 | 65435 |
| 9 | 826967 | 56145 | 522461 | 246024 | 11551 | 73858 |
| 10 | 912861 | 58407 | 546634 | 278720 | 13169 | 84283 |

Four samples were sparked without using the prespark conditions. Two samples containing different concentrations of each element were sparked (elements and concentrations as described in Chapter 5, 5.3.2, 85). Two samples of each element range were used to confirm any trends. The capacitance in each instance was changed and the intensity recorded. In the second instance the inductance, was changed and the sample sparked and the intensities recorded.

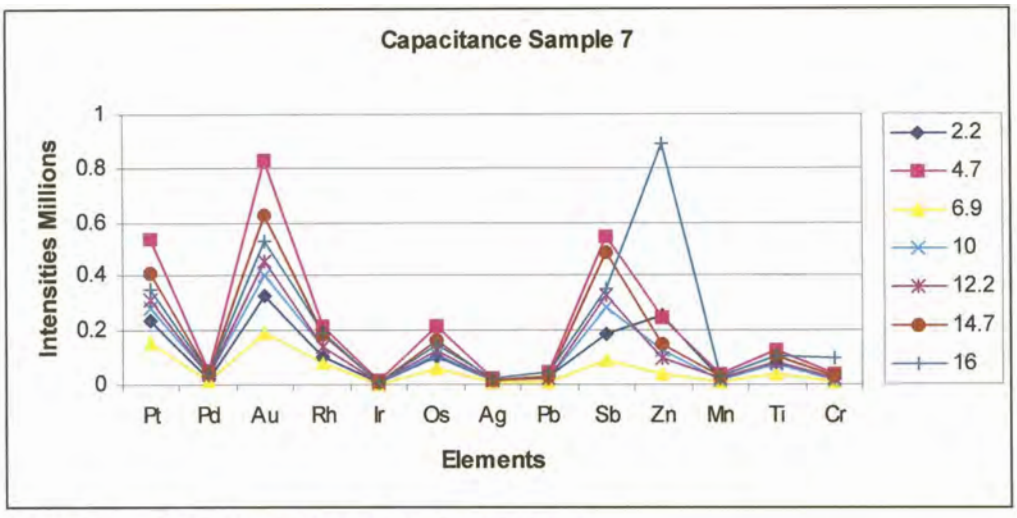


**Fig. 7.1 Sample 7 Capacitance in μF variations**

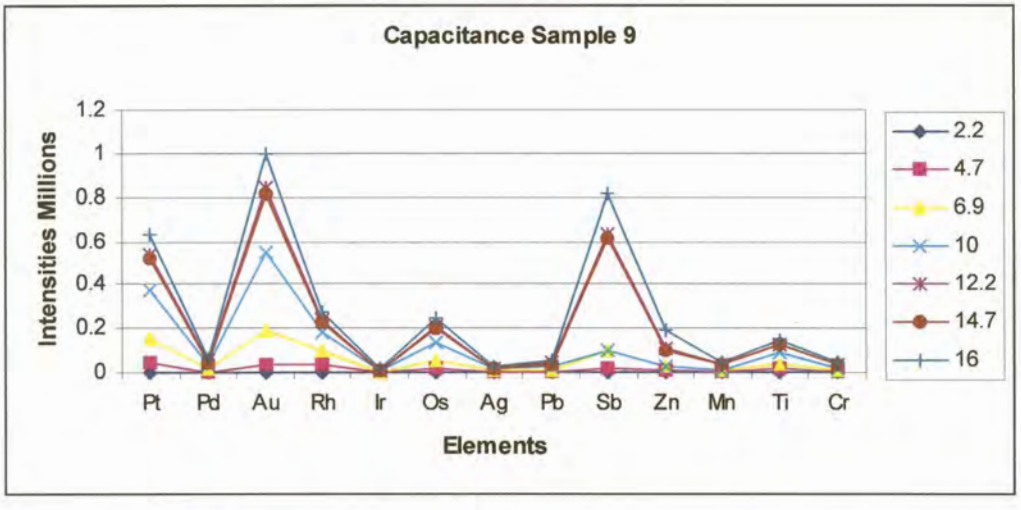


**Fig. 7.2 Sample 9 Capacitance in μF variations**

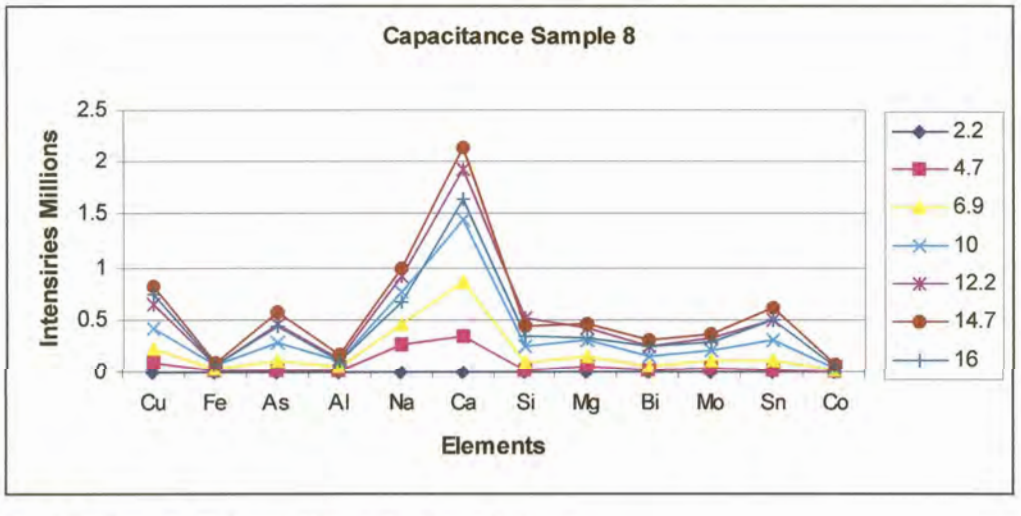


**Fig. 7.3 Sample 8 Capacitance in μF variations**

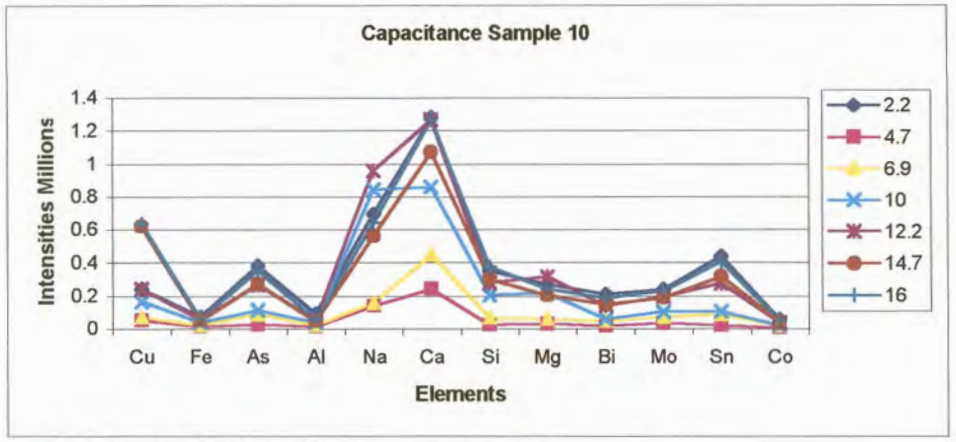


**Fig. 7.4 Sample 10 Capacitance in μF variations**

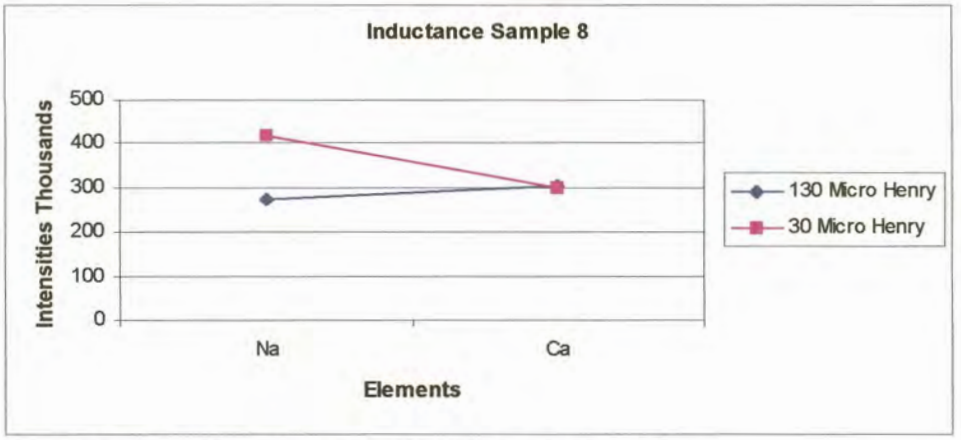


**Fig. 7.5 Sample 8 Inductance in μH variations for Na and Ca**

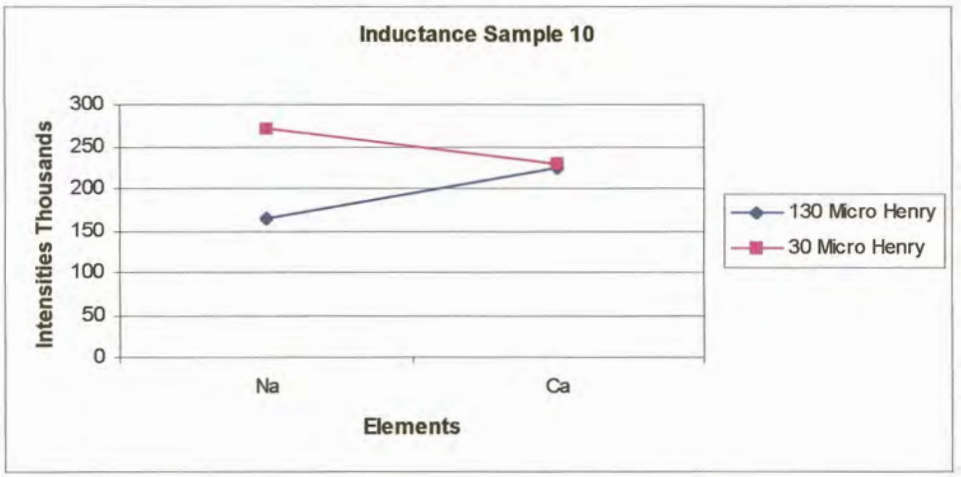


**Fig. 7.6 Sample 10 Inductance in μH variations for Na and Ca**

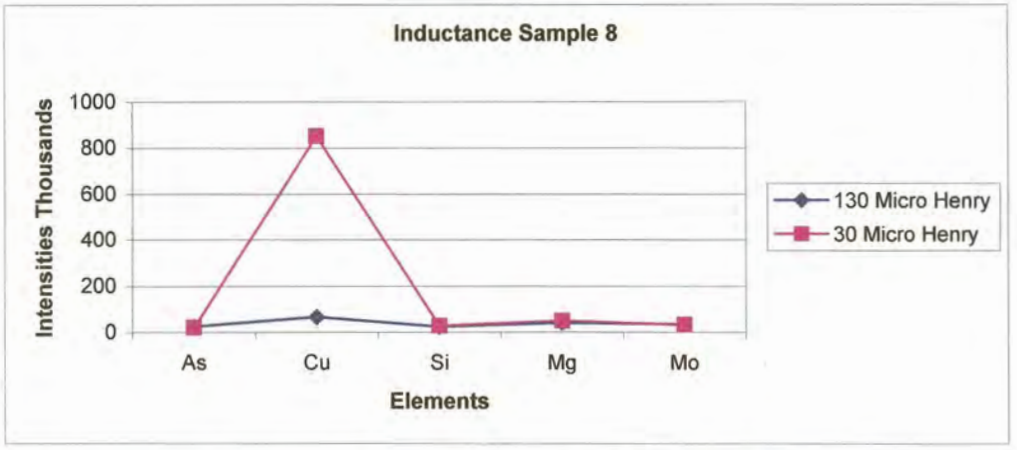


**Fig. 7.7 Sample 8 Inductance in μH variations for As, Cu, Si, Mg and Mo**

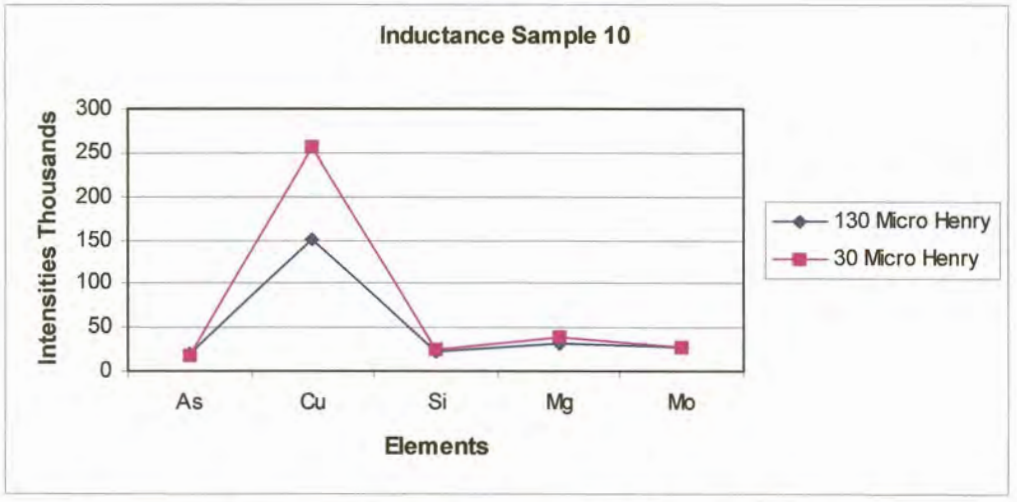


**Fig. 7.8 Sample 10 Inductance in μH variations for As, Cu, Si, Mg and Mo**

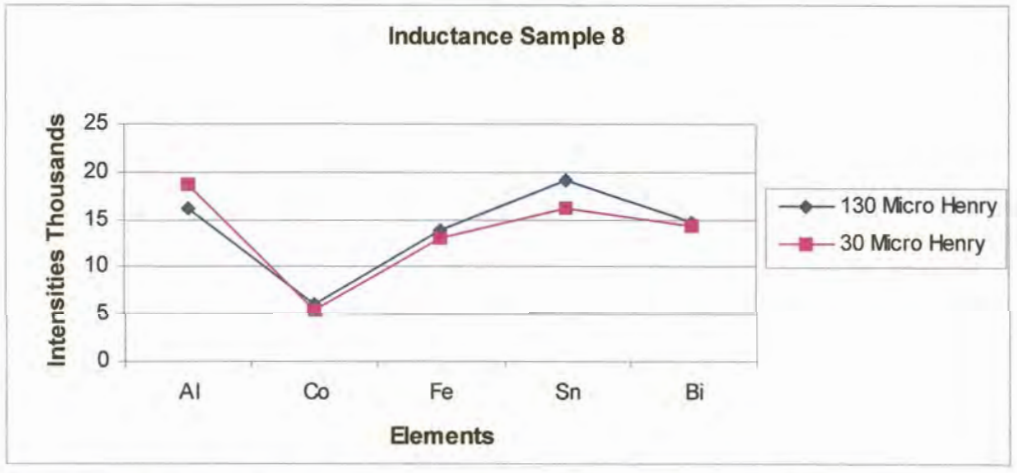


**Fig. 7.9 Sample 8 Inductance in μH variations for Al, Ca, Fe, Sn and Bi**

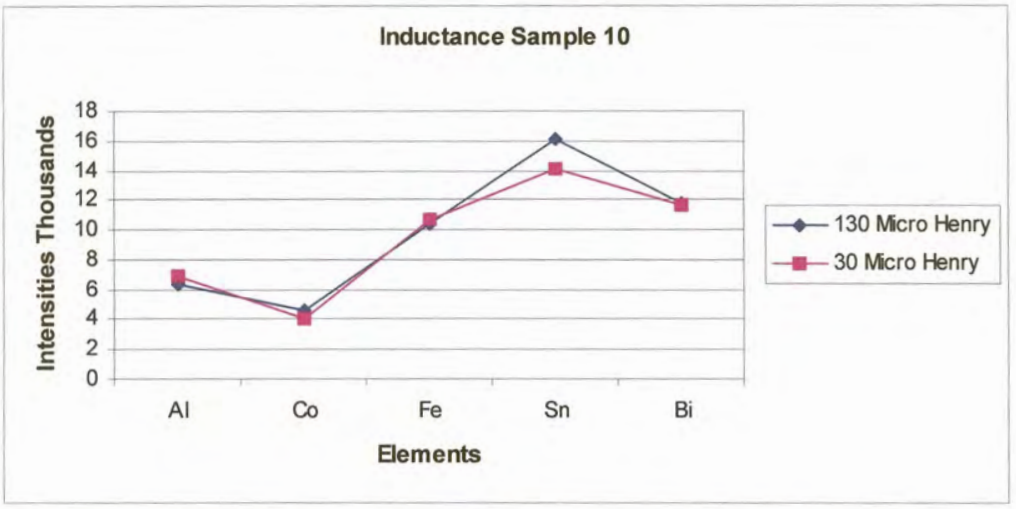


**Fig. 7.10 Sample 10 Inductance in μH variations for Al, Co, Fe, Sn and Bi**

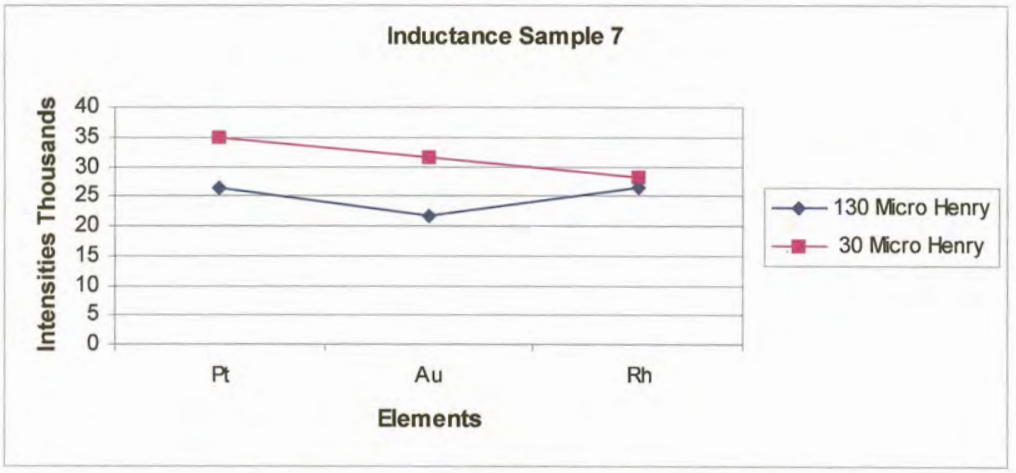


**Fig. 7.11 Sample 7 Induction in μH variations for Pt, Au and Rh**

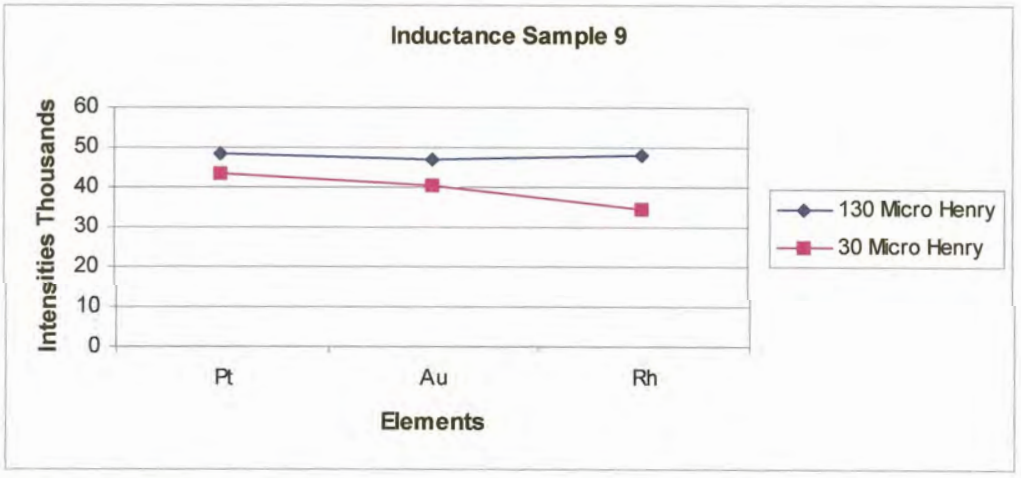


**Fig. 7.12 Sample 9 Induction in μH variations for Pt, Au and Rh**

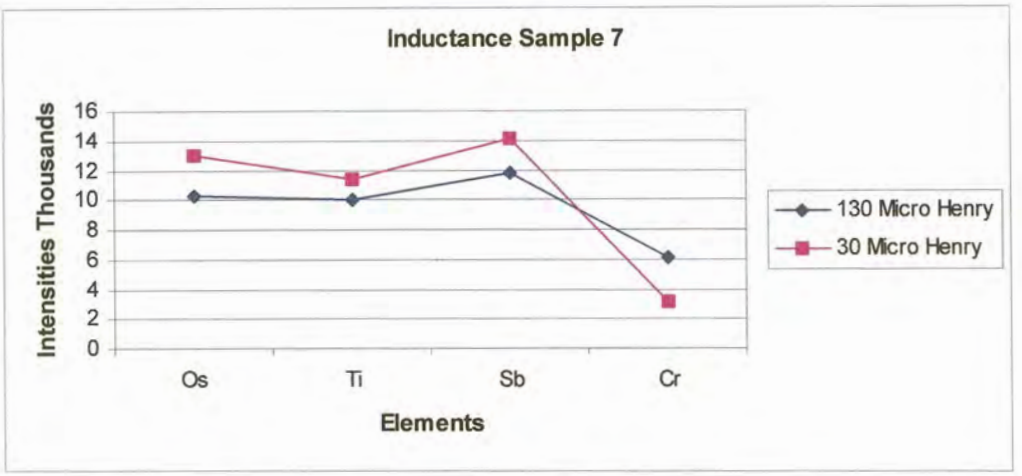


**Fig. 7.13 Sample 7 Induction in μH variations for Os, Ti, Sb and Cr**

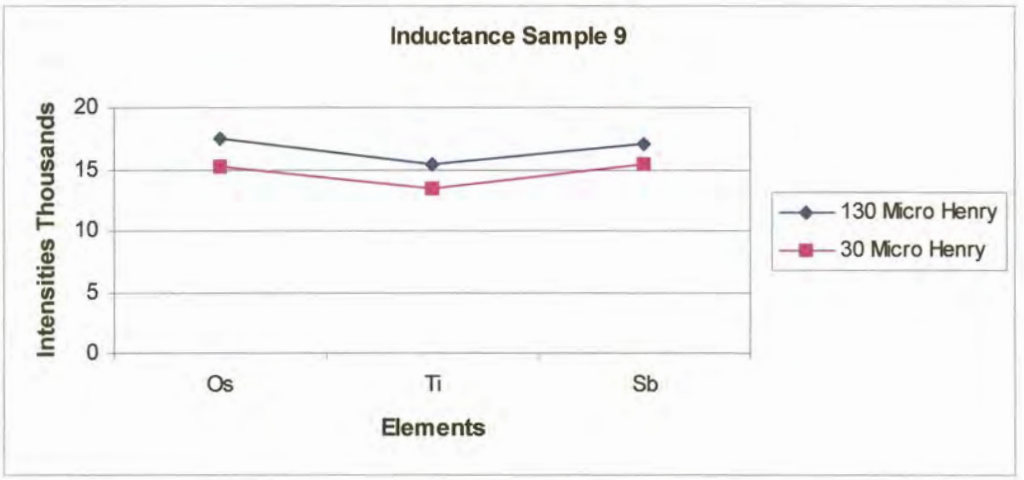


**Fig. 7.14 Sample 9 Induction in μH variations for Os, Ti, and Sb**

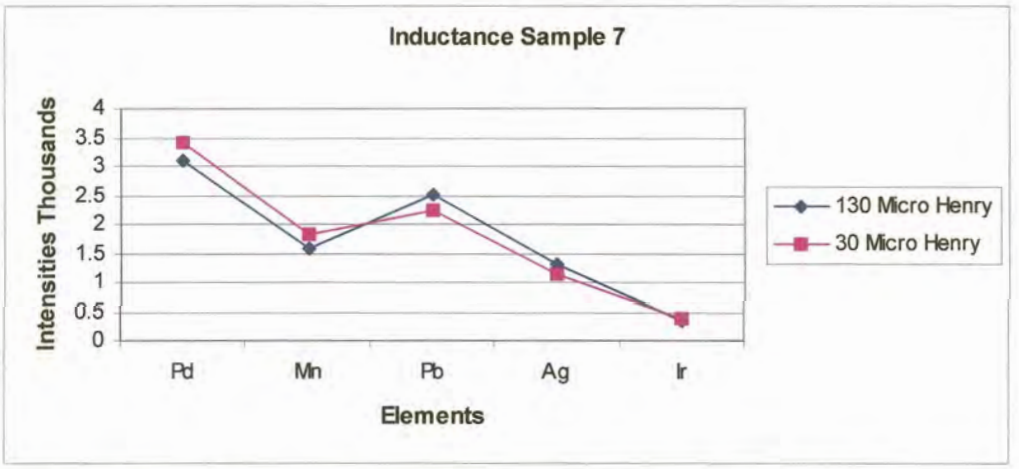


**Fig. 7.15 Sample 7 Induction in μH variations for Pd, Mn, Pb, Ag and Ir**

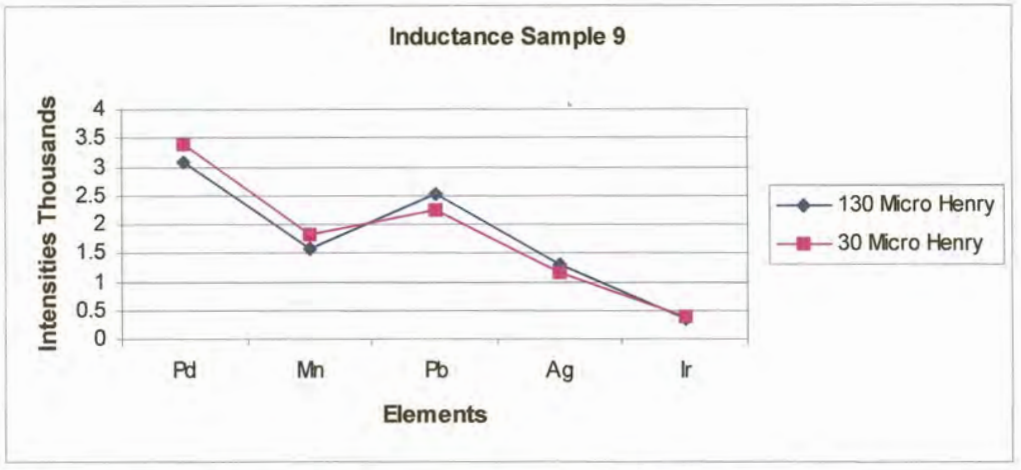


**Fig. 7.16 Sample 9 Induction in μH variations for Pd, Mn, Pb, Ag and Ir**

### *7.1.2 Effect of integration time*

Sample 7 and 8 were sparked using different integration times. Sample 8 was sparked once for 10 seconds, then once for 3 seconds using SAFT conditions, twice for 3 seconds and then three times for 3 seconds integration time. The two and three times integration cycles took place during the same single spark sequence. Sample 7 was conducted the same way; except that the first spark was twice for 5 seconds instead of once for 10 seconds. The square of *s,* is known as the variance: $s = \sqrt{s^2}$ The % relative standard deviation (% RSD) of a set of observations is the positive square root of the variance of the observations and is given by 100 *s/x* (also refer to as the coefficient of variance)

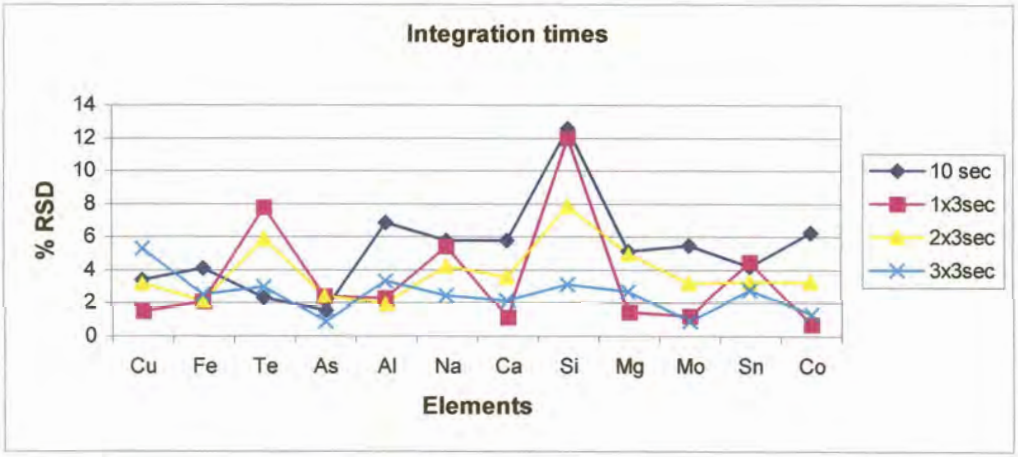


**Fig. 7.17 Different Integration time Sample 8**

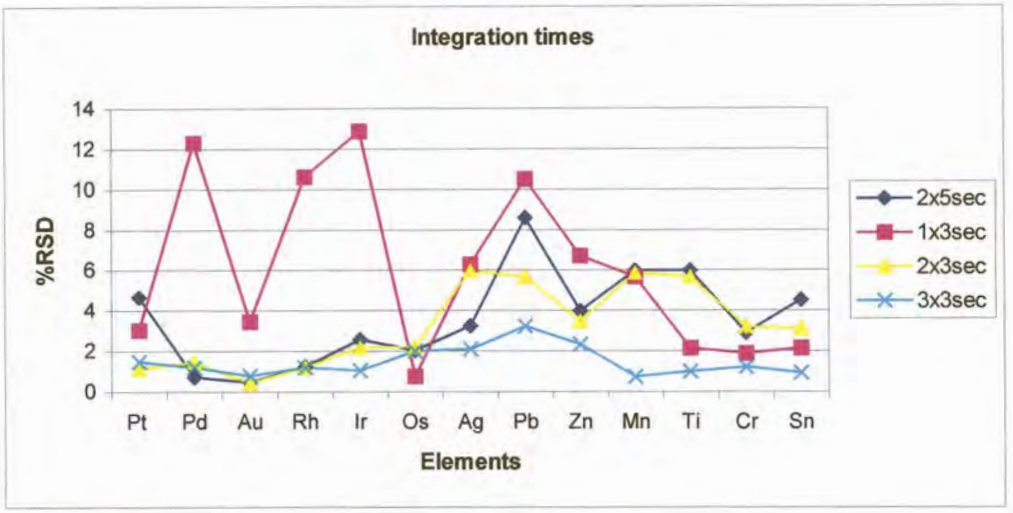


**Fig. 7.18 Different Integration times Sample 7**

### *7.1.3 Effect of different gating parameters*

Sample 7 and 9 contained the same elements in different concentrations likewise sample 8 and 10. Sample 8 contained the following concentrations in ppm: Fe 200, Na 200, Ca 200, Si 200, Cu 85, Al 200, Mg 200, Te 100, As 100, Bi 100, Mo 100, Sn 50 and Co 50. Sample 7 contained the following concentrations in ppm levels: Pt 200, Pd 200, Rh 200, Ir 200, Au 200, Os 120, Ag 200, Zn 200, Pb 100, Sb 100, Mn 100, Ti 100, Cr 100.

Two samples were analysed to confirm any trends. Signal to background ratios were plotted against the "delayed time". The background intensity is subtracted from the sample intensity and divided by the background intensity to obtain a signal to background ratio. Intensities are not plotted against the delay time to ensure that any difference in background at the various delay times are corrected for. Parameter changes of the resistance at 1 Ω and 15 Ω were compared. The delay times are measured in microseconds.

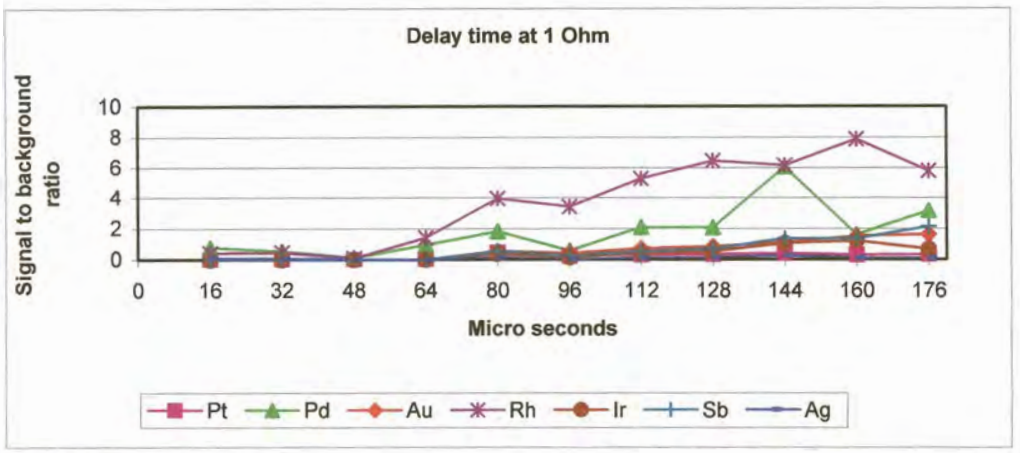


**Fig. 7.19 Sample 7 –1 Ω**

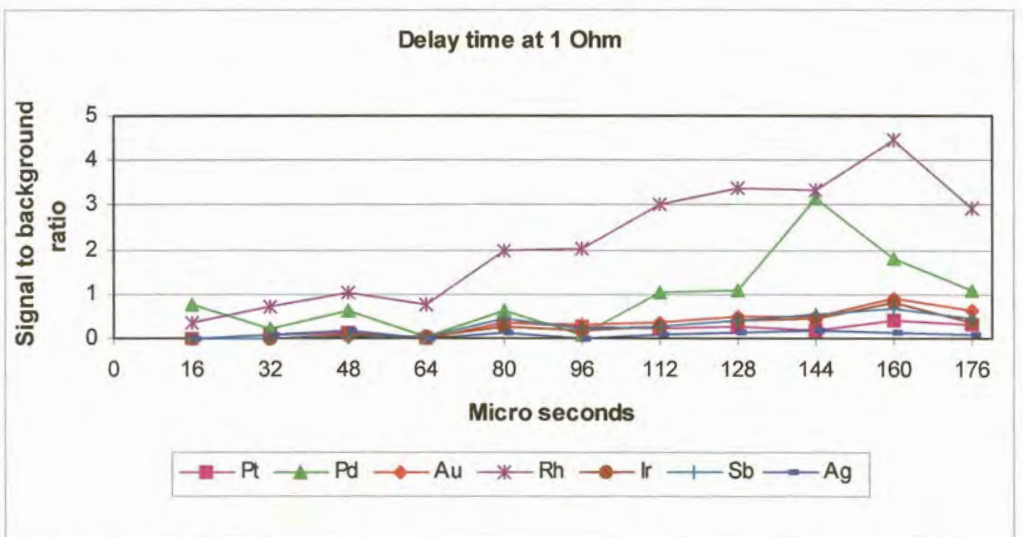


**Fig. 7.20 Sample 9 - 1 Ω**

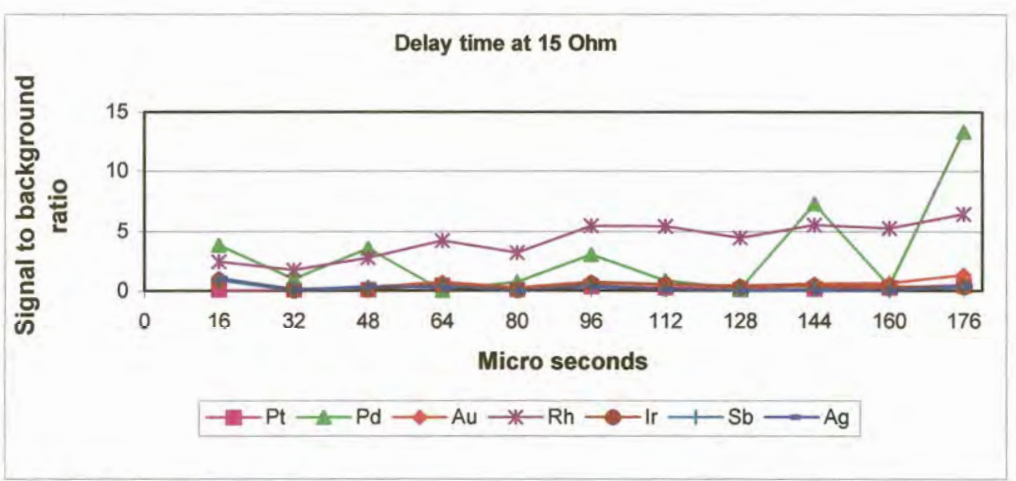


**Fig. 7.21 Sample 7 – 15 Ω**

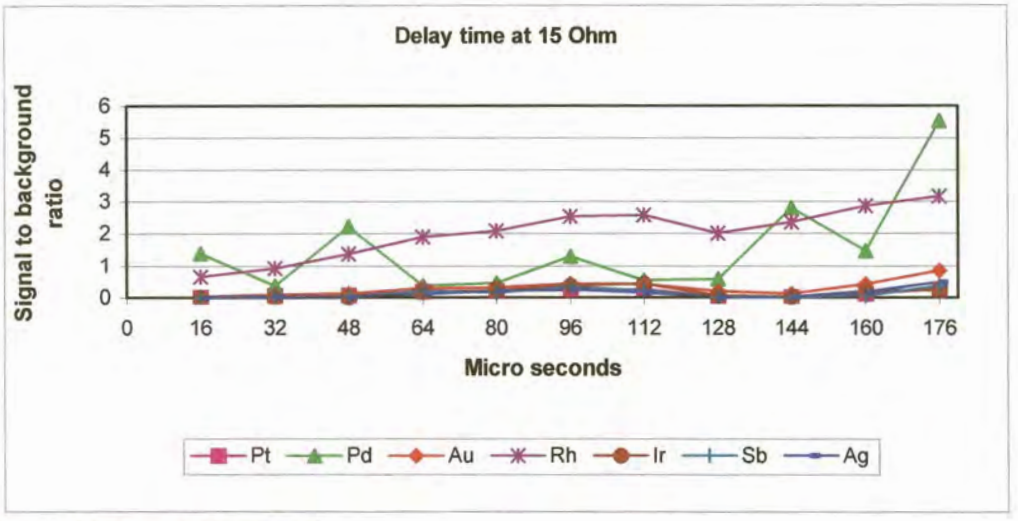


**Fig. 7.22 Sample 9 – 15 Ω**

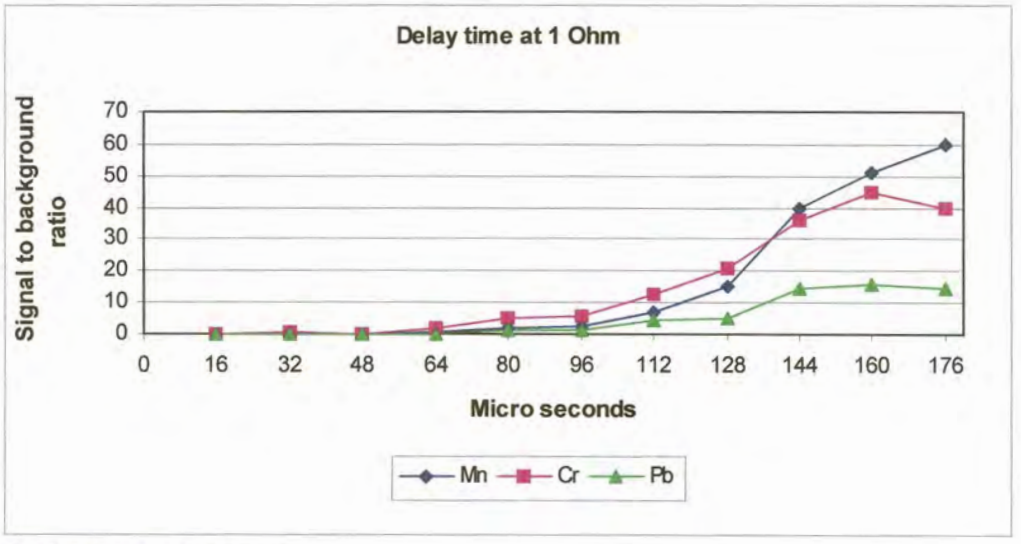


**Fig. 7.23 Sample 7 - 1 Ω**

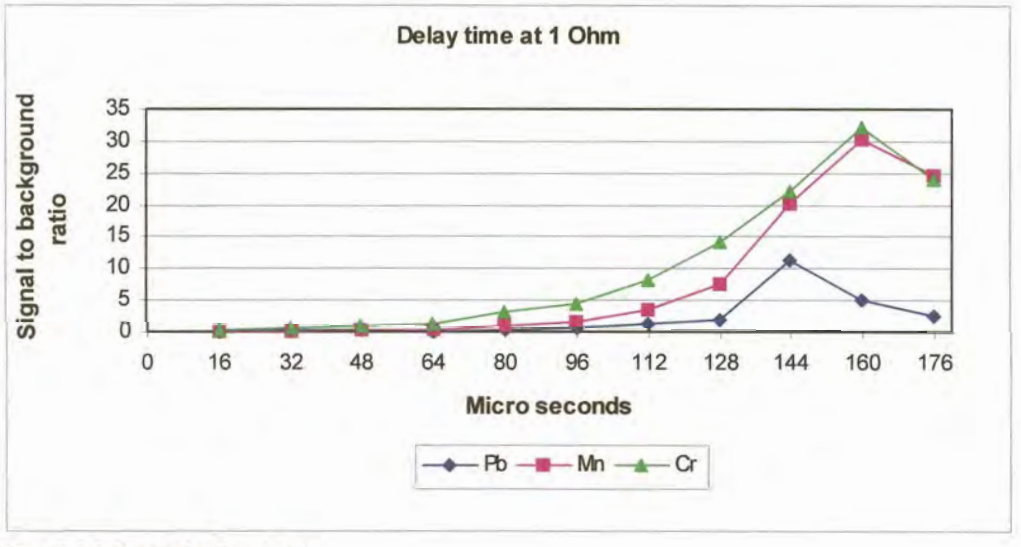


**Fig. 7.24 Sample 9 – 1 Ω**

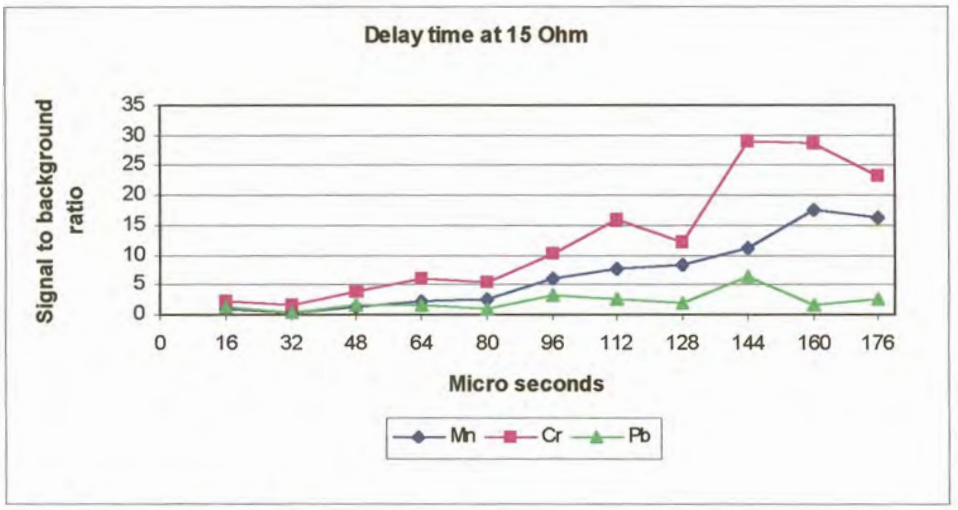


Fig. 7.25 Sample 7 – 15 Ω

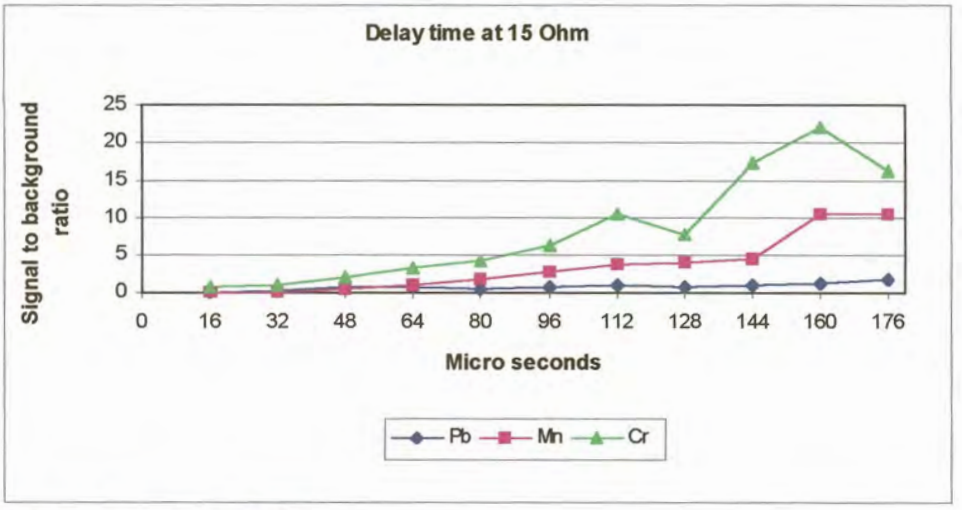


Fig. 7.26 Sample 9 – 15 Ω

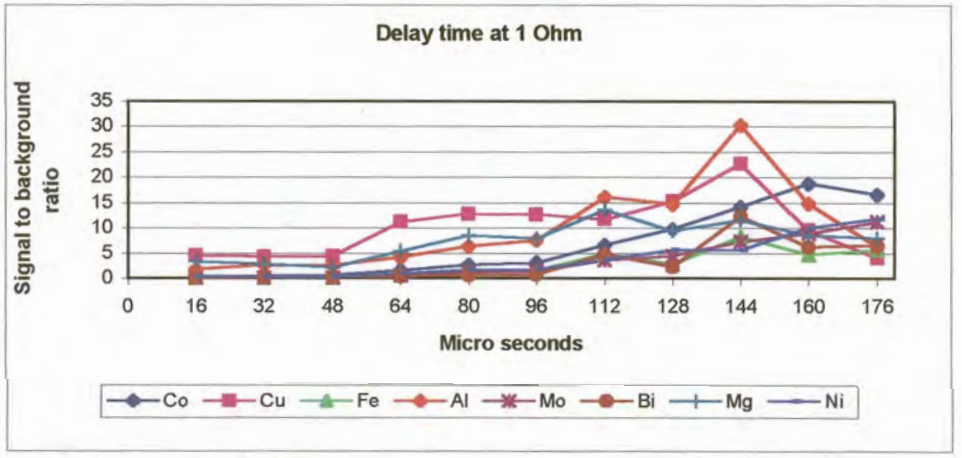


Fig. 7.27 Sample 8 – 1 Ω

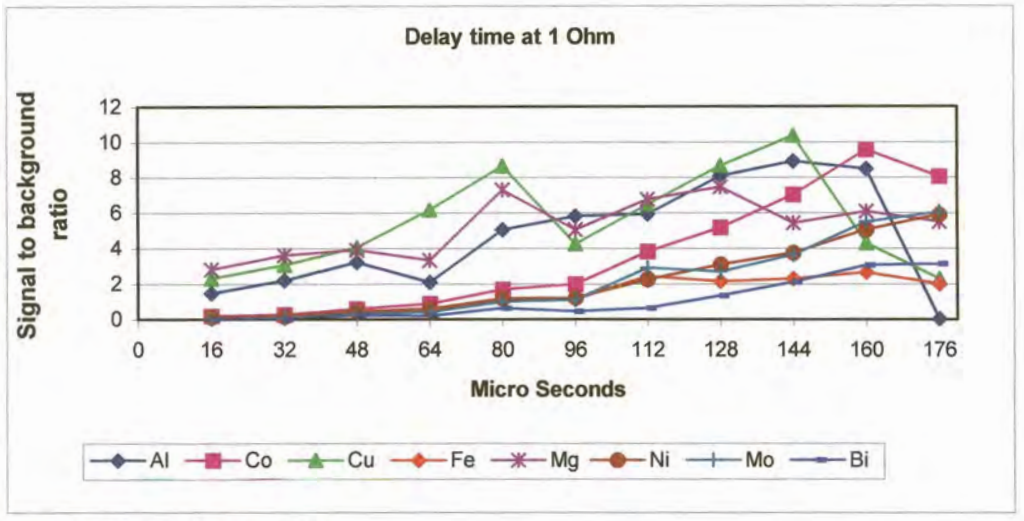


**Fig. 7.28 Sample 10 – 1 Ω**

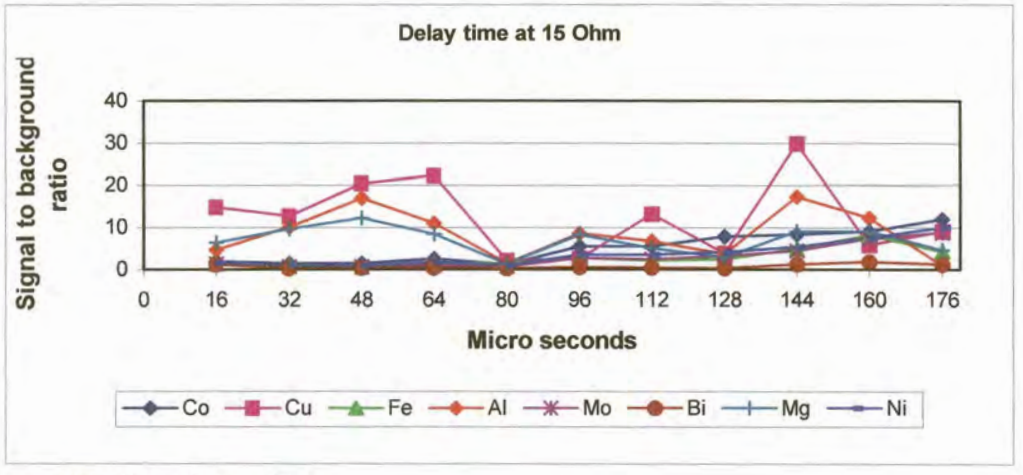


**Fig. 7.29 Sample 8 – 15 Ω**

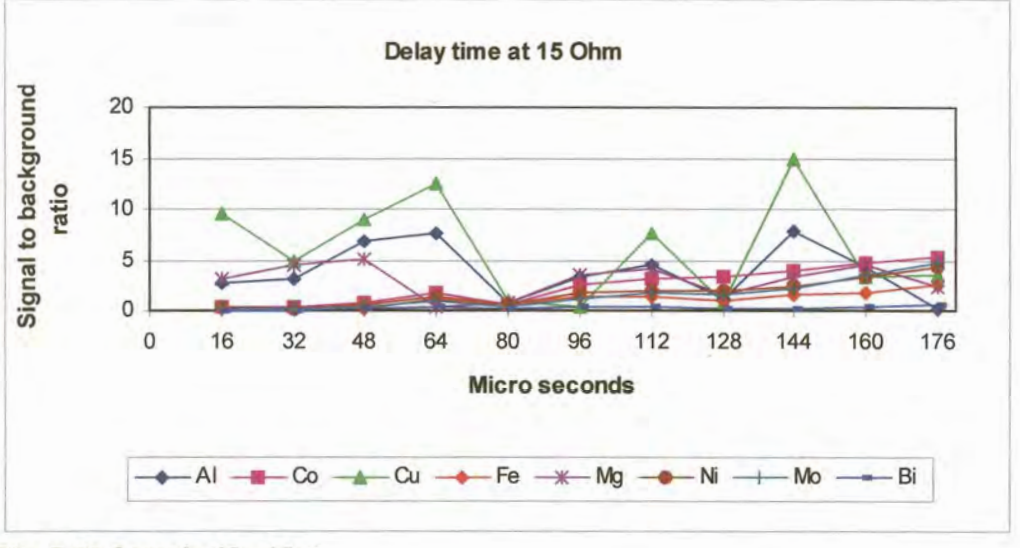


**Fig. 7.30 Sample 10 –15 Ω**

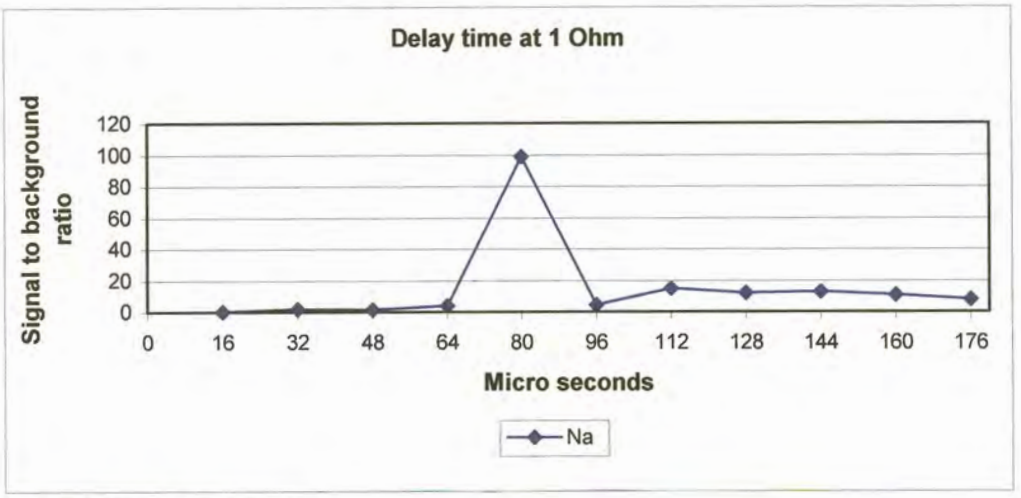


**Fig. 7.31 Sample 8 –1 Ω**

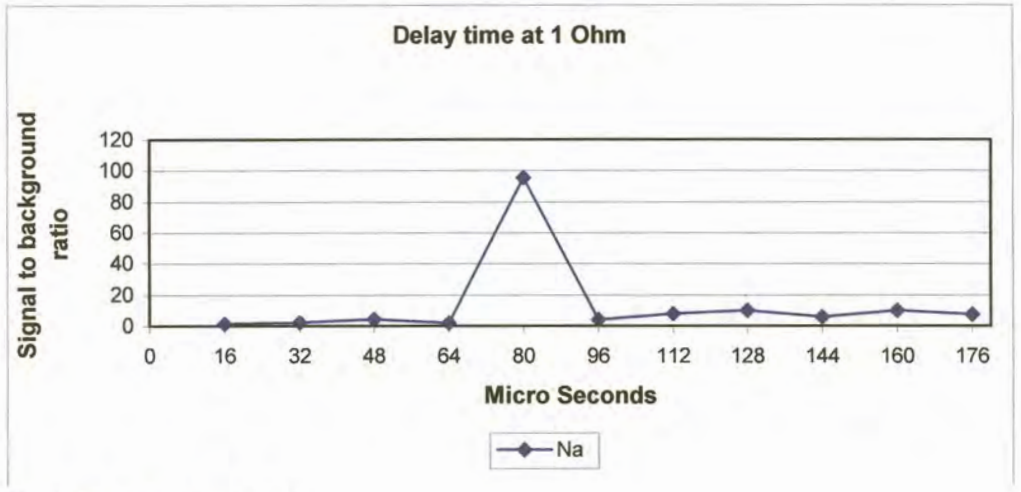


**Fig. 7.32 Sample 10 -1 Ω**

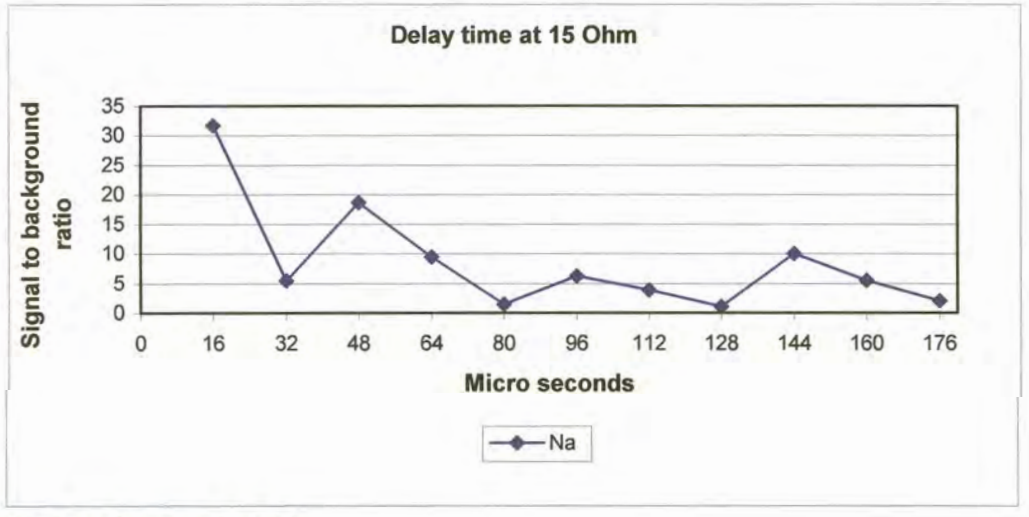


**Fig. 7.33 Sample 8 –15 Ω**

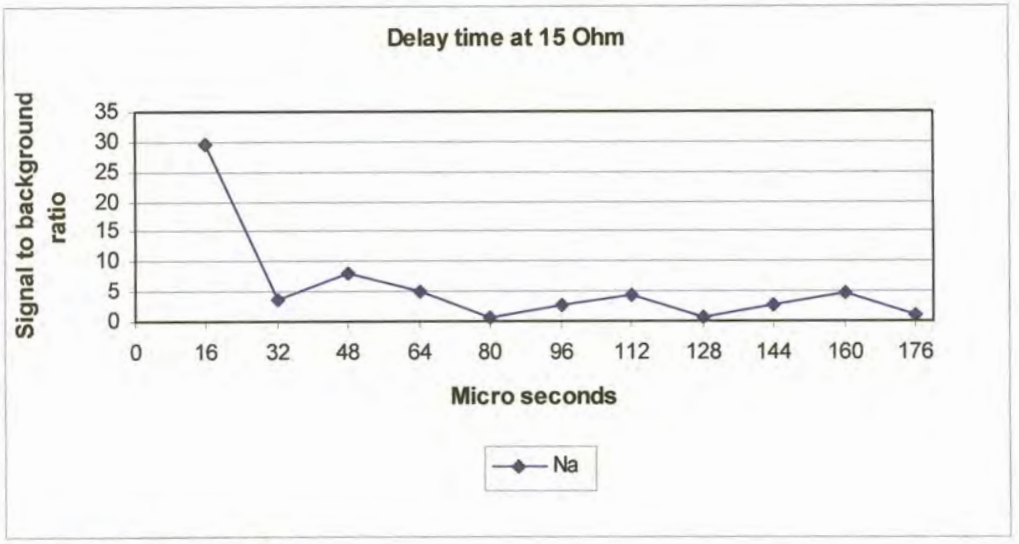


**Fig. 7.34 Sample 10-15 Ω**

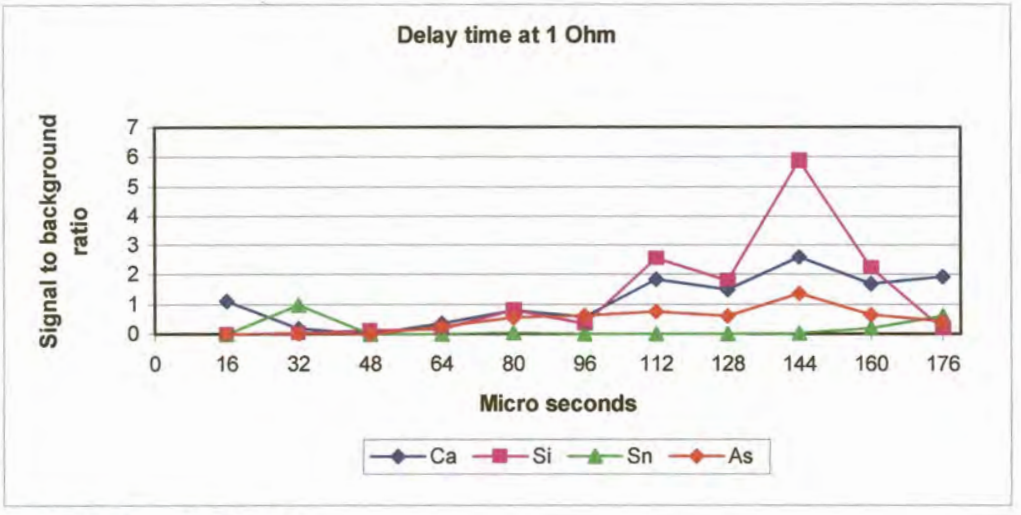


**Fig. 7.35 Sample 8 –1 Ω**

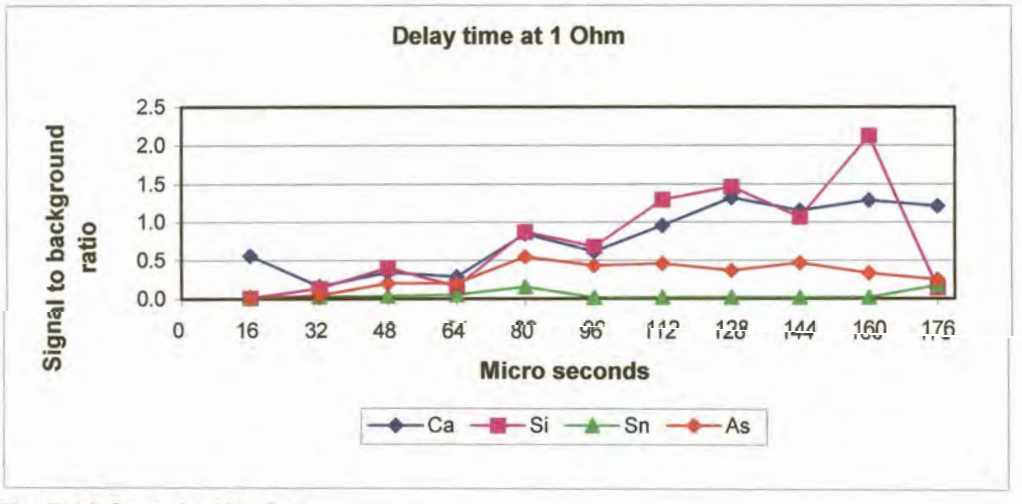


**Fig. 7.36 Sample 10 –1 Ω**

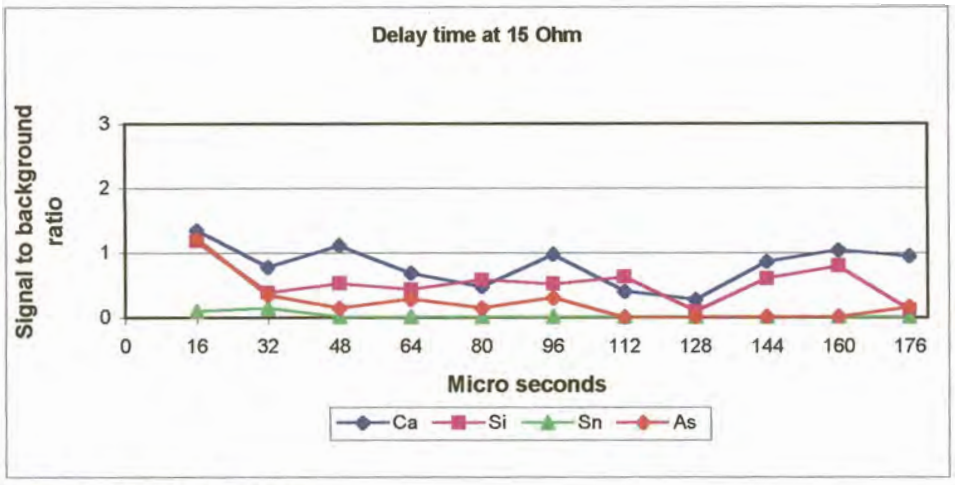


**Fig. 7.37 Sample 8 – 15 Ω**

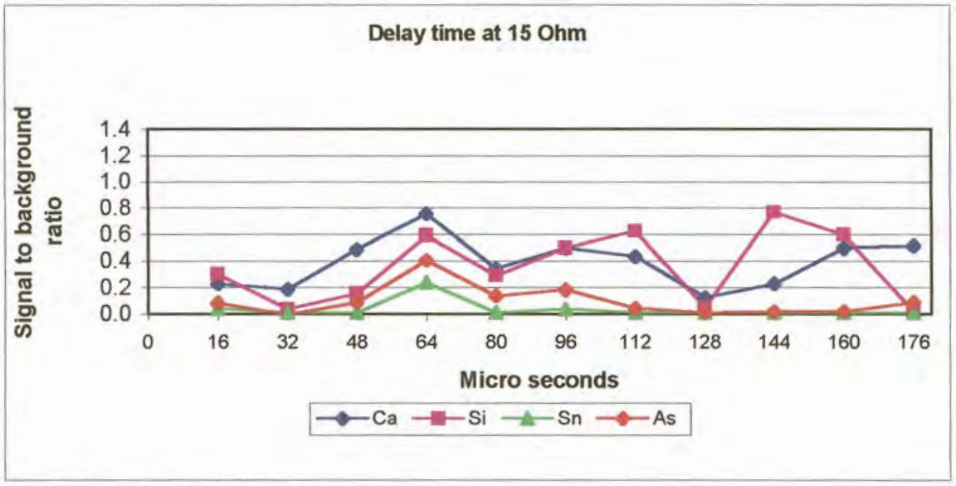


**Fig. 7.38 Sample 10 -15 Ω**

### *7.1.4 Internal standardisation*

The Intensity ratio of the analytical line to the reference line was generally plotted against the concentration ratio of the analyte to the reference element. In this case it was Ruthenium. Ruthenium as a reference line is not available in the in the Ultra violet region, there are no Ruthenium lines available in this region. A background position at the 310-nanometer wavelength is used in this optical system as the internal standard and the analytical line is ratioed to this background position.

### *7.1.5 Analytical gap*

Samples 9 and 10 were sparked using the same conditions changing only the gap between the sample and the electrode to 3 mm and 4 mm. The signal to background ratio was recorded. All the analytical lines are atom lines.

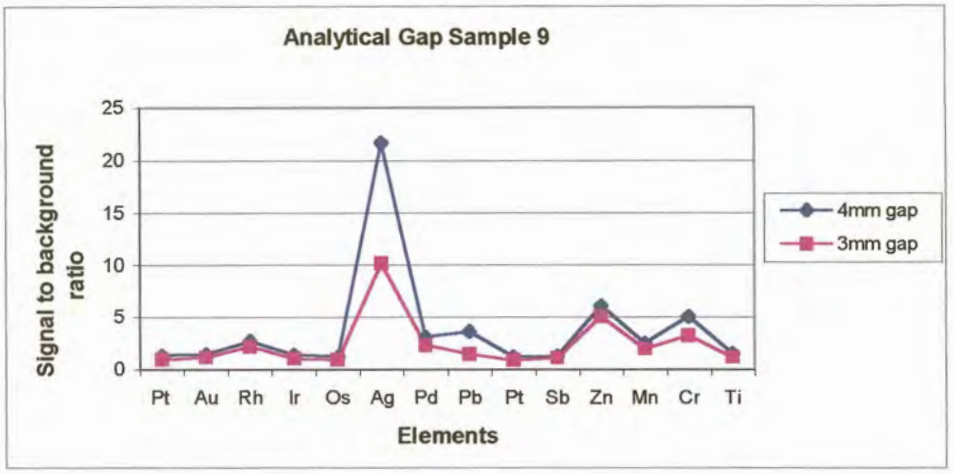


**Fig. 7.39 Analytical gap between the sample and electrode for sample 9**

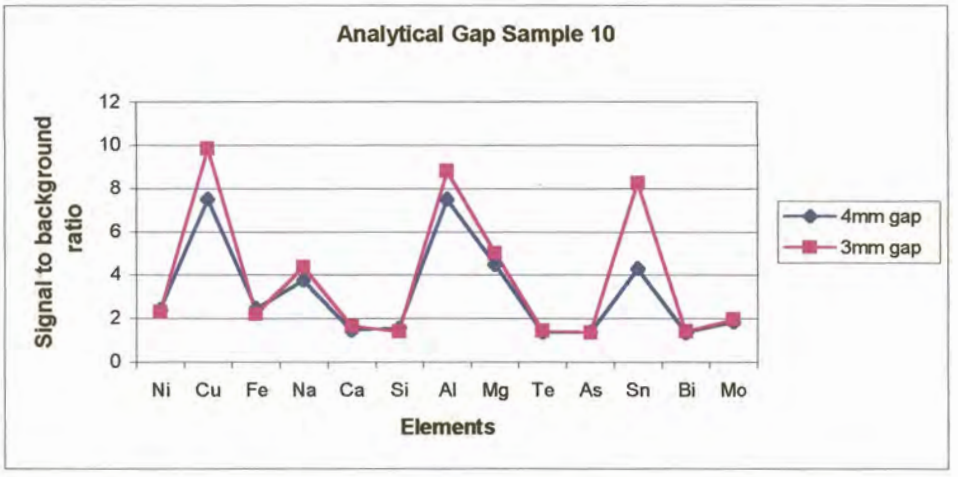


**Fig. 7.40 Analytical gap between the sample and the electrode for sample 10**

### 7.1.6 Contamination from other base material

**Table 7.3**
**Pure Pt, Pd and Ru sample is sparked on the same base plate, monitoring the element of the previous sample to evaluate how many sparks are required before a stable signal is achieved**

| Sample sparked | Pt | Pd | Ru |
|---|---|---|---|
| Base Plate | Ru | Ru | Ru |
| Monitoring element | Ru | Pt | Pd |
| Spark number 1 | 412407 | 577722 | 189787 |
| Spark number 2 | 277828 | 368768 | 120182 |
| Spark number 3 | 241861 | 301456 | 90914 |
| Spark number 4 | 216640 | 300390 | 75427 |
| Spark number 5 | 198708 | 269518 | 77213 |
| Spark number 6 | 96161 | 210648 | 85465 |
| Spark number 7 | 72248 | 194675 | 66175 |
| Spark number 8 | 64843 | 193314 | 63236 |
| Spark number 9 | 68375 | 214059 | 58833 |
| Spark number 10 | 51666 | 214578 | 56065 |
| Spark number 11 | 47458 | 213676 | 56101 |

**Table 7.4**
**Pure Pt, Pd and Ru sample is sparked on a base plate corresponding with the pure sample, monitoring the element of the previous sample to evaluate how many sparks are required before a stable signal is achieved**

| Sample sparked | Pt | Pd | Ru |
|---|---|---|---|
| Base Plate | Pt | Pd | Ru |
| Monitoring | Ru | Pt | Pd |
| Spark number 1 | 83653 | 116059 | 53763 |
| Spark number 2 | 47578 | 114573 | 45847 |
| Spark number 3 | 53027 | 110407 | 36674 |
| Spark number 4 | 52872 | 103172 | 36861 |
| Spark number 5 | 52049 | 115718 | 34057 |

## 7.2 Calibration

The calibration graphs were established for the impurities in Ruthenium base. The elements were calibrated using the wavelength tables as in Table 7.6, 125. The conditions for calibration are recorded in Table in 7.5, 125. All the channels used were in the first order with the exception of Os 581.812, Pt 531.890, which were second order lines. All the wavelengths selected were atom lines.

**Table 7.5 Conditions used for the calibration**

| Calibration Conditions | | | | | | | | |
|---|---|---|---|---|---|---|---|---|
| | Time (s) | C (uF) | R (ohm) | L (uH) | Analytical Gap | Freq.(Hz) | Gate | Delay Time |
| **Flush** | **5** | **0** | **0** | **0** | **4mm** | **300** | **64** | **144** |
| **SAFT** | **3x3** | **2.2** | **1** | **130** | **4mm** | **300** | **64** | **144** |

**Table 7.6 Elements for analytical analysis and their selected wavelengths**

| Elements | Wavelength nm | Elements | Wavelength nm |
|---|---|---|---|
| Ag | 338.289 | Na | 588.995 |
| Al | 396.153 | Ni | 361.939 |
| As | 234.984 | Os | 581.812 |
| Au | 267.595 | Pb | 405.782 |
| Bi | 306.772 | Pb | 283.307 |
| Ca | 422.673 | Pd | 340.458 |
| Co | 345.351 | Rh | 343.489 |
| Cr | 425.435 | Sb | 206.83 |
| Cu | 324.754 | Si | 288.16 |
| Fe | 371.994 | Sn | 317.502 |
| Ir | 351.364 | Te | 214.275 |
| Mg | 285.213 | Ti | 498.173 |
| Mn | 403.449 | Zn | 213.856 |
| Mo | 386.411 | Pt | 531.89 |

## *7.3 Comparison of samples analysed*

Comparison of the round robin sample as analysed by the various techniques by different companies internationally. Discontinuity of the line indicates where companies did not report a result.

- A Spark Spectrometer Method to be evaluated
- B Spectrograph Company A South Africa
- C Inductively Coupled Plasma South Africa
- D Spectrograph Company B South Africa
- E Inductively Coupled Plasma Company C United Kingdom
- F Spectrograph Company D Russia
- G Spectrograph Company E United Kingdom

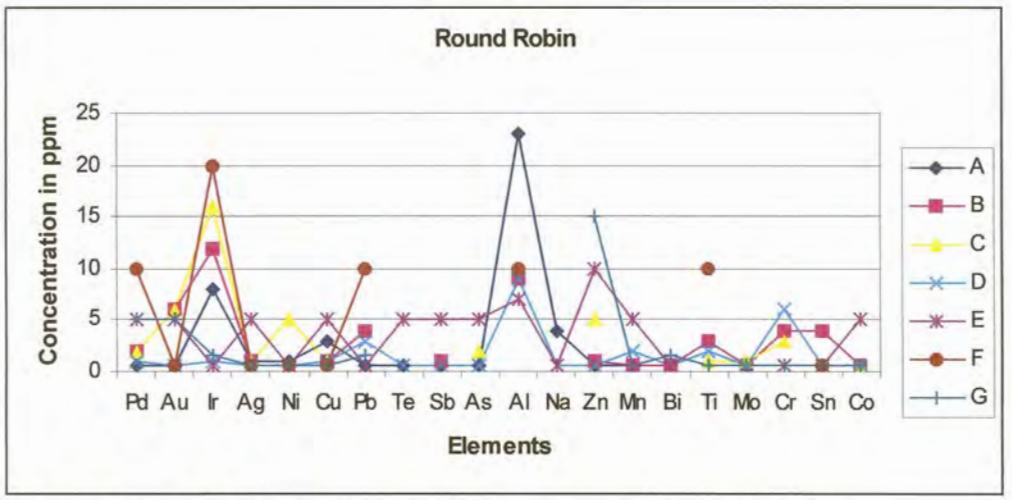


**Fig 7.41 Round Robin sample analysed by seven different companies**

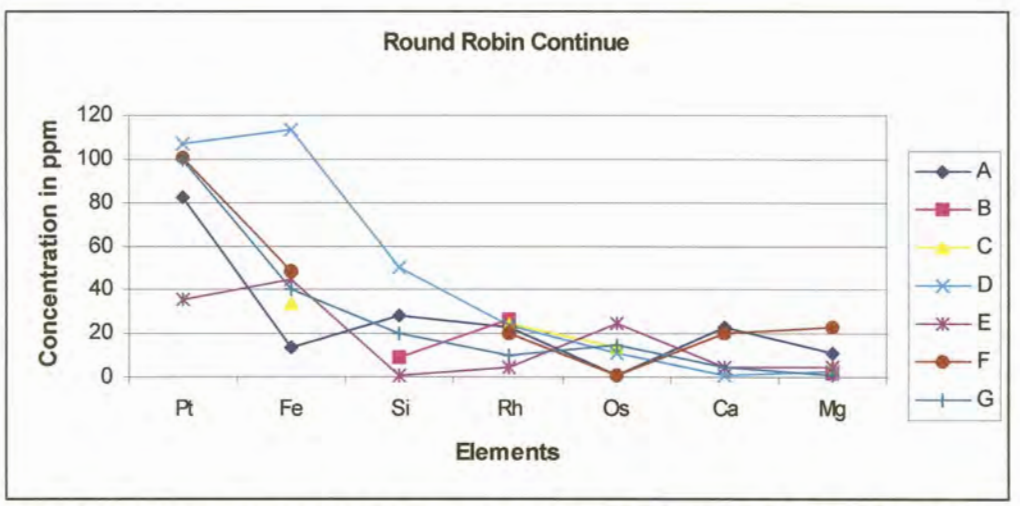


**Fig 7.41 Continue. Round Robin sample analysed by seven different companies**

The purpose of the analysis of ruthenium is to determine the percentage purity of the metal. The Spark spectrometer measures the concentrations of various impurities. These may vary in concentration at various positions in a single sample disc. The sum of the average of three analyses (expressed as a percentage) for all the impurities is taken. This sum is subtracted from 100 % to give the metal purity as a percentage.

The purities were compared for individual samples using the three techniques. The average is recorded and the variance of the sample $s^2$ used to calculate the standard deviation s.

Sample standard deviation: $s = \sqrt{s^2}$

The variance of the sample for $n$ observations $x_1, x_2 \ldots, x_n$ having mean $\bar{x}$ is defined as

$$s^2 = \frac{\sum_{i=1}^{n} (x - \bar{x})}{n-1}$$

**Table 7.7 % Purity of the Round Robin sample and the fourteen-interchange sample, including the average for each sample**

| | Spark | Spectrograph | ICP | Spectrograph | Spectrograph | Spectrograph | Spectrograph | |
|---|---|---|---|---|---|---|---|---|
| No. | A | B | C | D | E | F | G | Average |
| RR | 99.9762 | 99.9912 | 99.9879 | 99.9660 | 99.9813 | 99.9724 | 99.9776 | 99.9789 |
| 1 | 99.9054 | | 99.9129 | 99.8651 | | | | 99.8945 |
| 2 | 99.9775 | | 99.9791 | 99.9823 | | | | 99.9796 |
| 3 | 99.9552 | 99.9817 | 99.9636 | 99.9581 | | | | 99.9647 |
| 4 | 99.9855 | | 99.9898 | 99.9884 | | | | 99.9879 |
| 5 | 99.9842 | | 99.9759 | 99.9730 | | | | 99.9777 |
| 6 | 99.9792 | | 99.9731 | 99.9735 | | | | 99.9753 |
| 7 | 99.9660 | | 99.9564 | 99.9268 | | | | 99.9497 |
| 8 | 99.9748 | 99.9724 | 99.9719 | 99.9899 | | | | 99.9773 |
| 9 | 99.9856 | 99.9865 | 99.9810 | 99.9881 | | | | 99.9853 |
| 10 | 99.9712 | | 99.9625 | 99.9722 | | | | 99.9686 |
| 11 | 99.9852 | | 99.9873 | 99.9898 | | | | 99.9874 |
| 12 | 99.9842 | | 99.9730 | 99.9759 | | | | 99.9777 |
| 13 | 99.9792 | | 99.9736 | 99.9732 | | | | 99.9753 |
| 14 | 99.9649 | | 99.9234 | 99.9580 | | | | 99.9488 |

**Table 7.8 Result of the spark analysis versus the average result from alternative techniques, the standard deviation and two sigma variance of the results**

| No | Spark | Average | Std. Dev. | + 2s | - 2s | Maximum | Minimum |
|---|---|---|---|---|---|---|---|
| RR | 99.9762 | 99.9789 | 0.0087 | 99.9963 | 99.9615 | 99.9912 | 99.966 |
| 1 | 99.9054 | 99.8945 | 0.0257 | 99.9459 | 99.8431 | 99.9129 | 99.8651 |
| 2 | 99.9775 | 99.9796 | 0.0024 | 99.9844 | 99.9748 | 99.9823 | 99.9775 |
| 3 | 99.9552 | 99.9647 | 0.0119 | 99.9885 | 99.9409 | 99.9817 | 99.9552 |
| 4 | 99.9855 | 99.9879 | 0.0022 | 99.9923 | 99.9835 | 99.9898 | 99.9855 |
| 5 | 99.9842 | 99.9777 | 0.0058 | 99.9893 | 99.9661 | 99.9842 | 99.973 |
| 6 | 99.9792 | 99.9753 | 0.0034 | 99.9821 | 99.9685 | 99.9792 | 99.9731 |
| 7 | 99.9660 | 99.9497 | 0.0204 | 99.9905 | 99.9089 | 99.9660 | 99.9268 |
| 8 | 99.9748 | 99.9773 | 0.0085 | 99.9943 | 99.9603 | 99.9899 | 99.9719 |
| 9 | 99.9856 | 99.9853 | 0.0030 | 99.9913 | 99.9793 | 99.9881 | 99.981 |
| 10 | 99.9712 | 99.9686 | 0.0053 | 99.9792 | 99.958 | 99.9722 | 99.9625 |
| 11 | 99.9852 | 99.9874 | 0.0023 | 99.992 | 99.9828 | 99.9898 | 99.9852 |
| 12 | 99.9842 | 99.9777 | 0.0058 | 99.9893 | 99.9661 | 99.9842 | 99.973 |
| 13 | 99.9792 | 99.9753 | 0.0034 | 99.9821 | 99.9685 | 99.9792 | 99.9732 |
| 14 | 99.9649 | 99.9488 | 0.0222 | 99.9932 | 99.9044 | 99.9649 | 99.9234 |

Comparison of interchange samples analysed by South African refineries using different techniques. Discontinuity of the line indicates were companies did not report a result. The graphs are split to accommodate the concentration variations.

- A Spark Spectrometer Method to be evaluated
- B Spectrograph Company A South Africa
- C Inductively Coupled Plasma South Africa
- D Spectrograph Company B South Africa

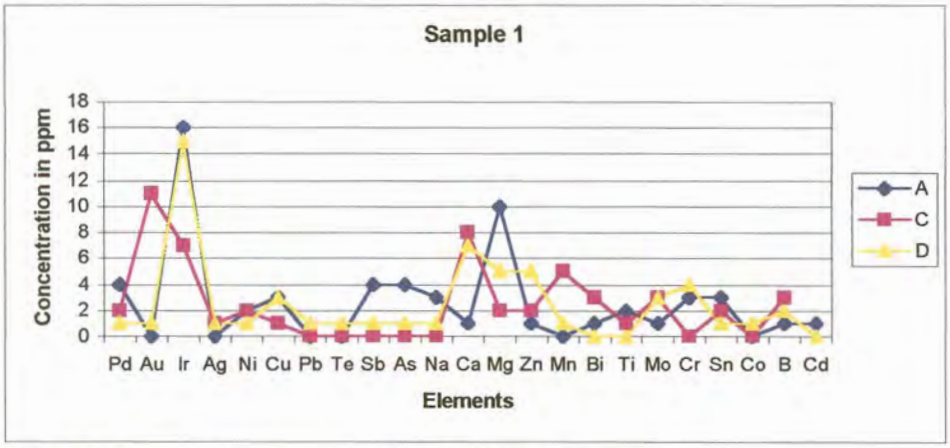


**Fig. 7.42 Sample 1 analysed by three different companies**

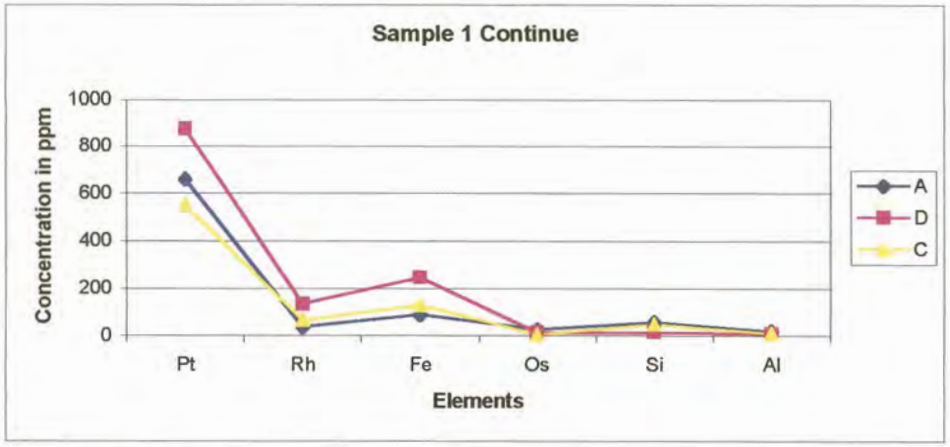


**Fig. 7.42 Continued. Sample 1 analysed by three different companies**

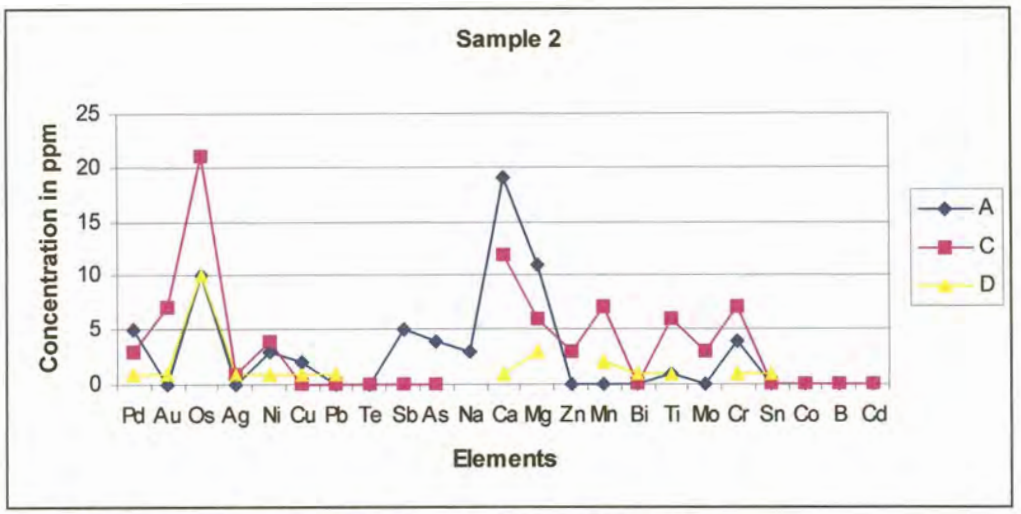


**Fig. 7.43 Sample 2 analysed by three different companies**

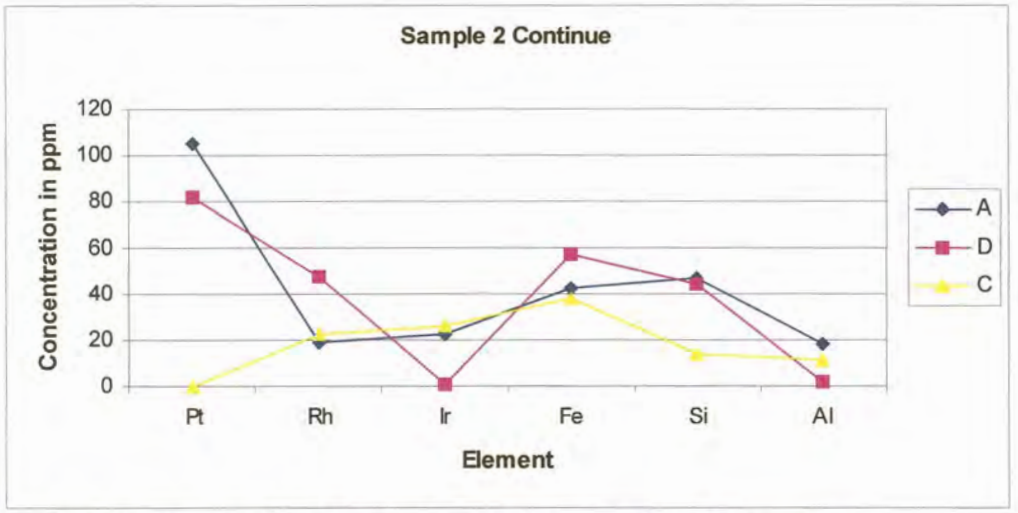


**Fig. 7.43 Continued. Sample 2 analysed by three different companies**

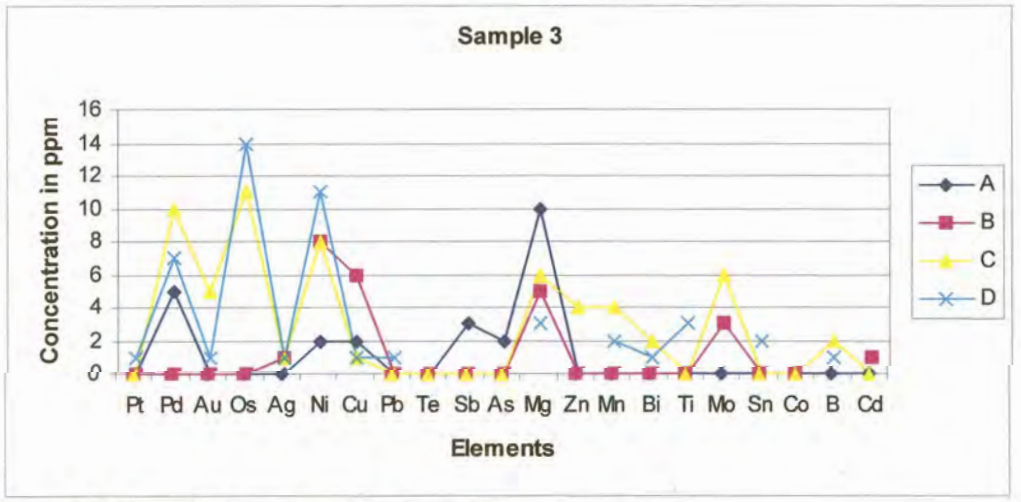


**Fig. 7.44 Sample 3 analysed by four different companies**

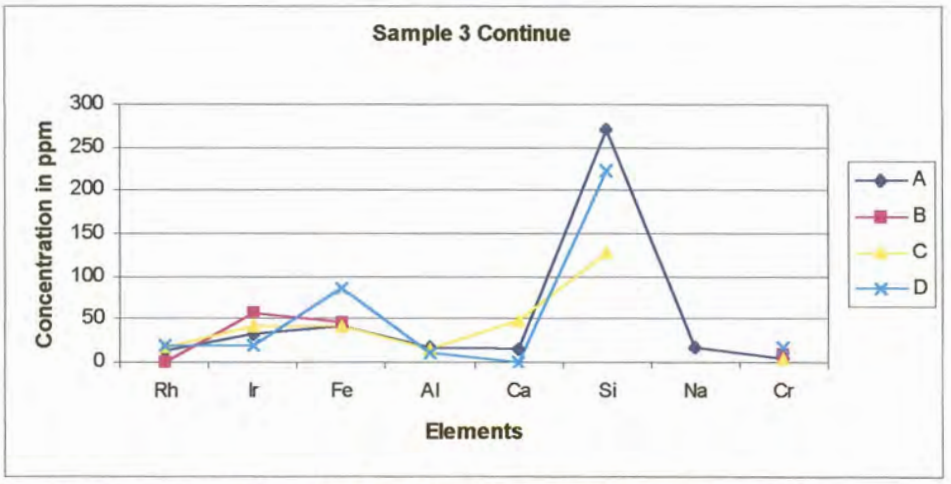


**Fig. 7.44 Continued. Sample 3 analysed by three different companies**

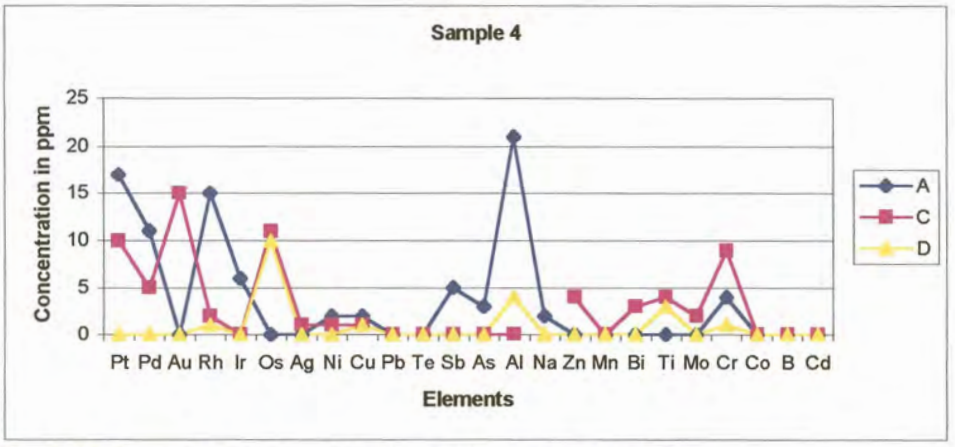


**Fig. 7.45 Sample 4 analysed by three different companies**

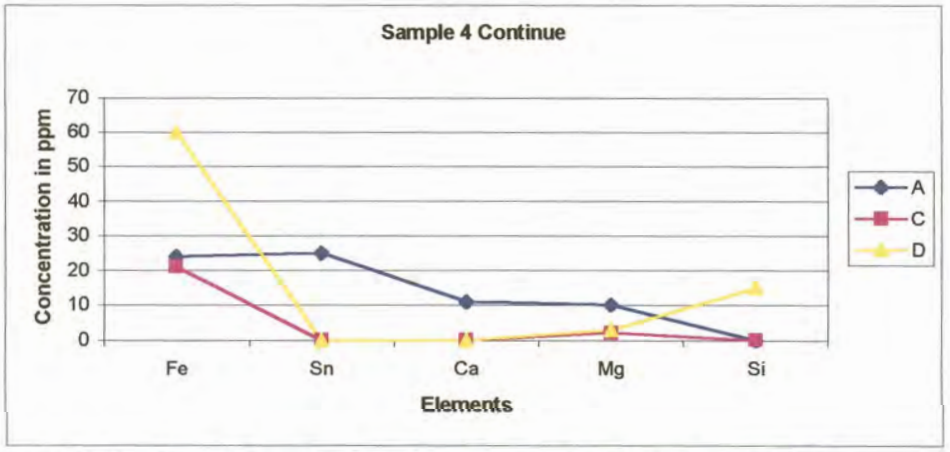


**Fig. 7.45 Continued. Sample 4 analysed by three different companies**

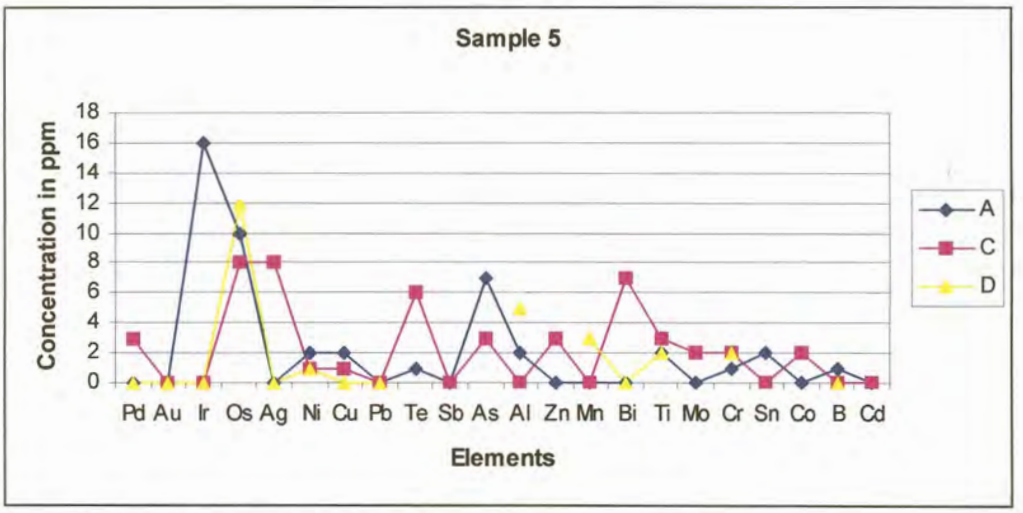


**Fig. 7.46 Sample 5 analysed by three different companies**

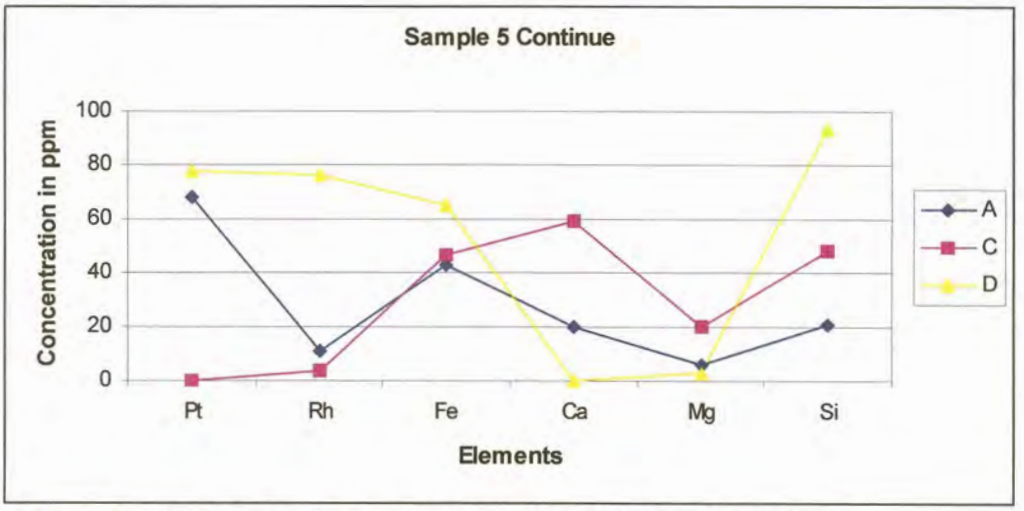


**Fig. 7.46 Continued. Sample 5 analysed by three different companies**

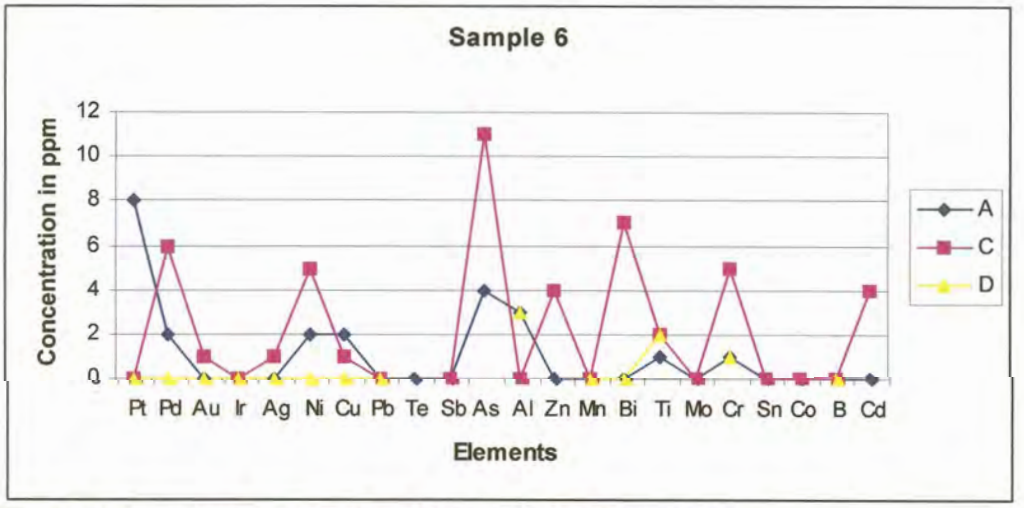


**Fig. 7.47 Sample 6 analysed by three different companies**

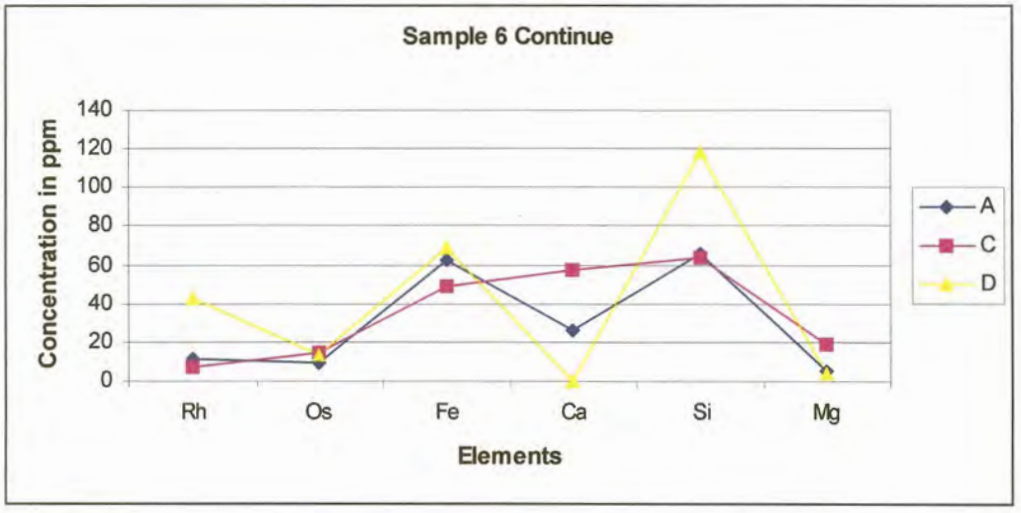


**Fig. 7.47 Continued. Sample 6 analysed by three different companies**

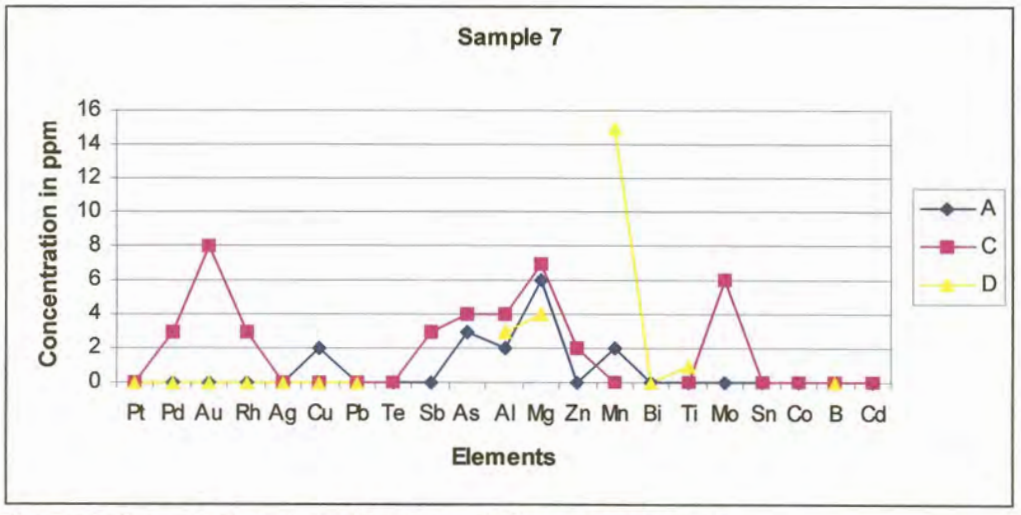


**Fig. 7.48 Sample 7 analysed by three different companies**

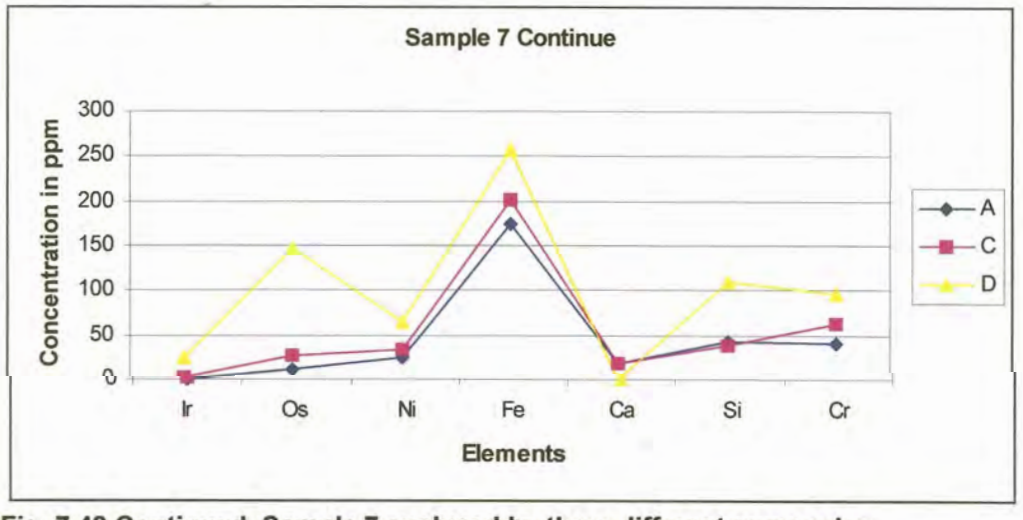


**Fig. 7.48 Continued. Sample 7 analysed by three different companies**

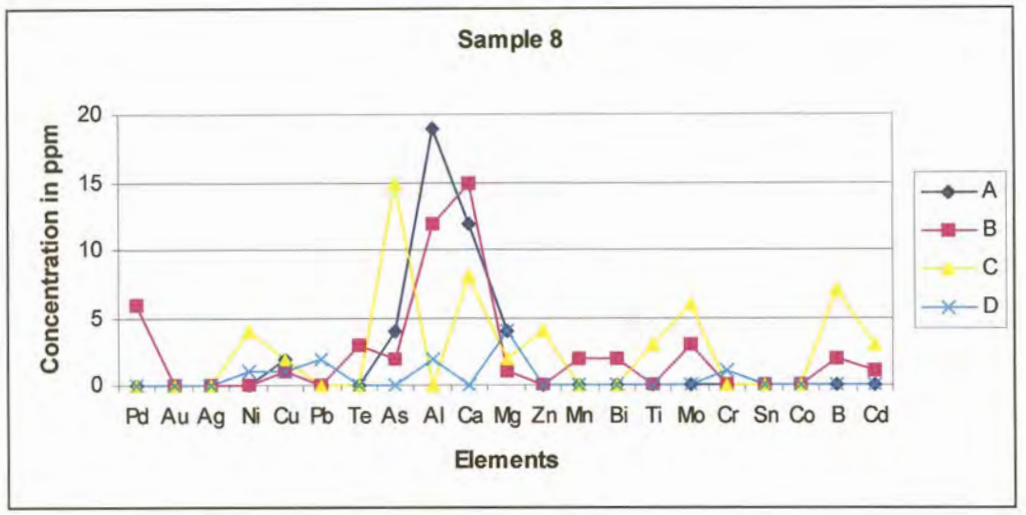


**Fig. 7.49 Sample 8 analysed by four different companies**

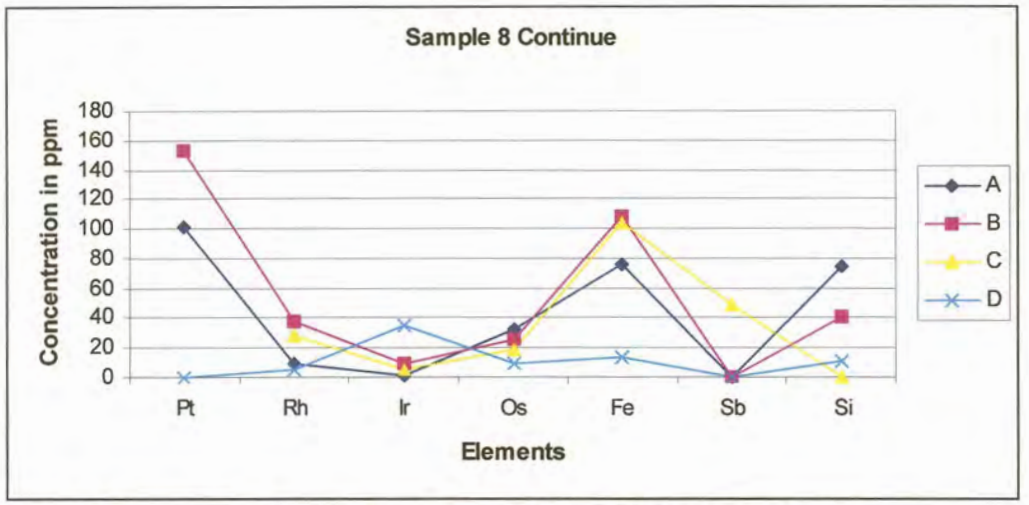


**Fig. 7.49 Continued. Sample 8 analysed by four different companies**

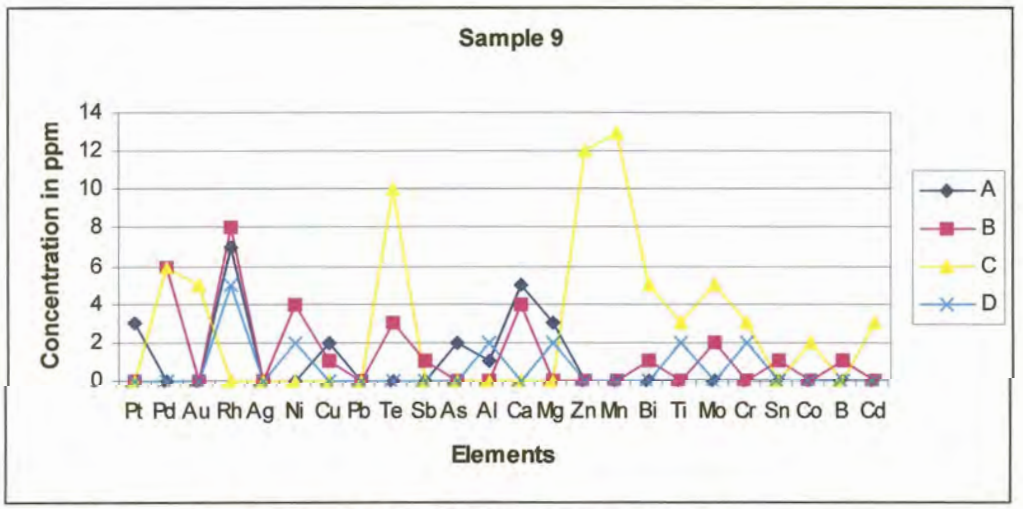


**Fig. 7.50 Sample 9 analysed by four different companies**

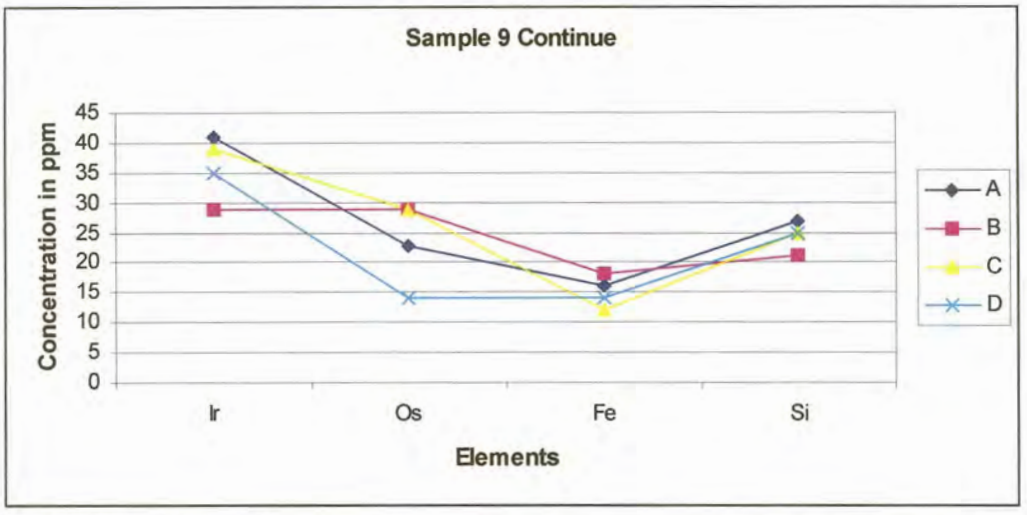


**Fig. 7.50 Continued. Sample 9 analysed by four different companies**

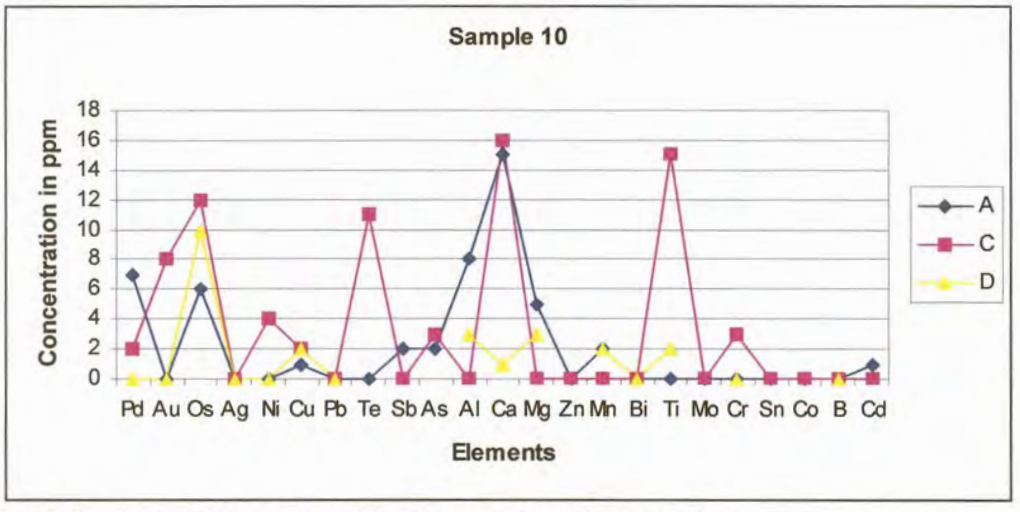


**Fig 7.51 Sample 10 analysed by three different companies**

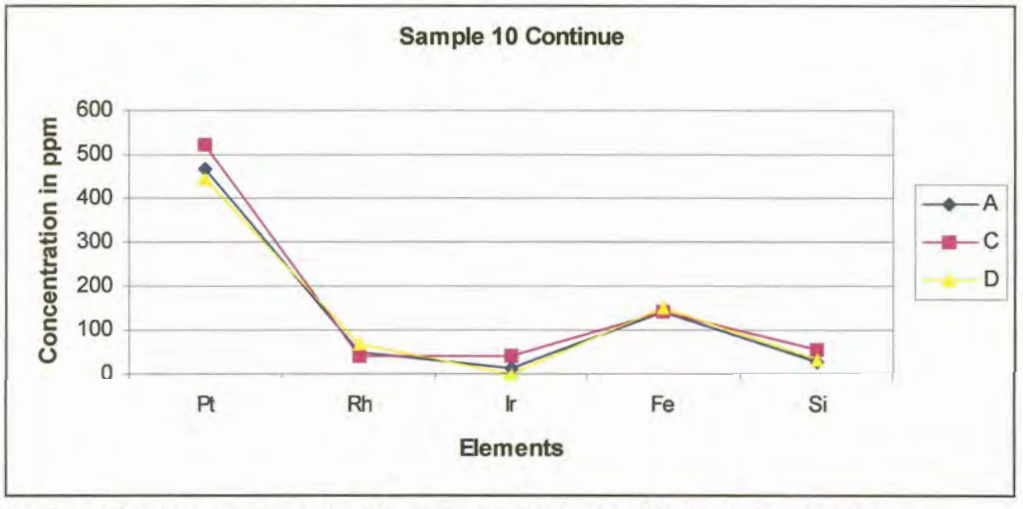


**Fig 7.51 Continued. Sample 10 analysed by three different companies**

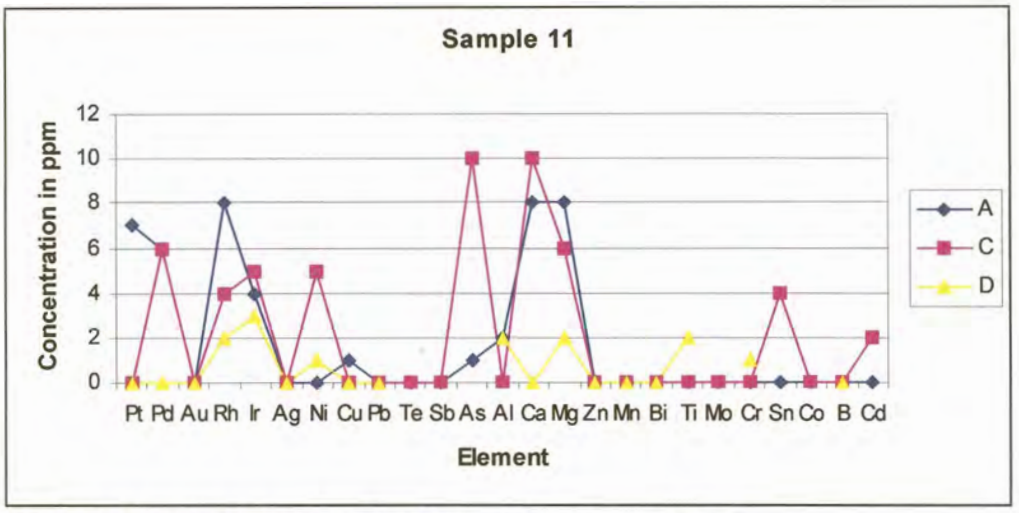


**Fig. 7.52 Sample 11 analysed by three different companies**

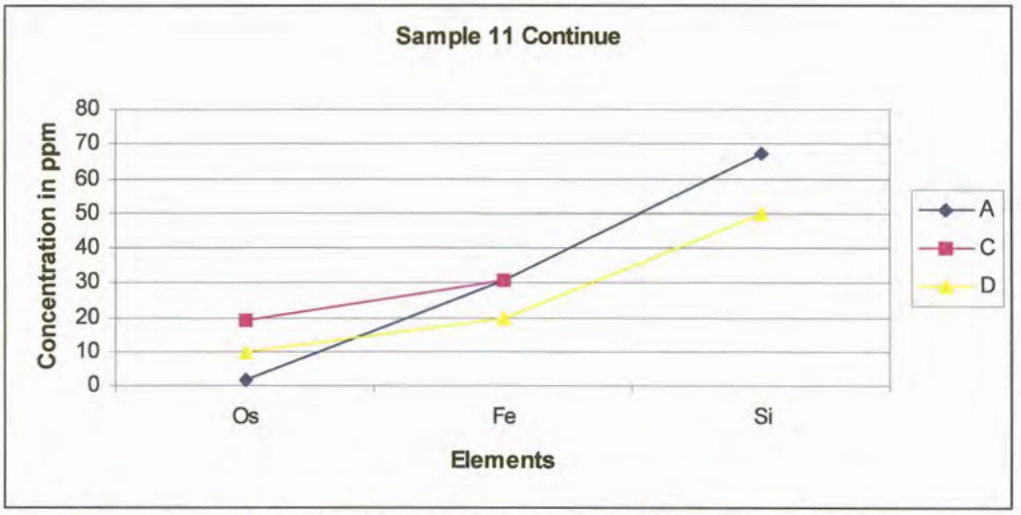


**Fig. 7.52 Continued. Sample 11 analysed by three different companies**

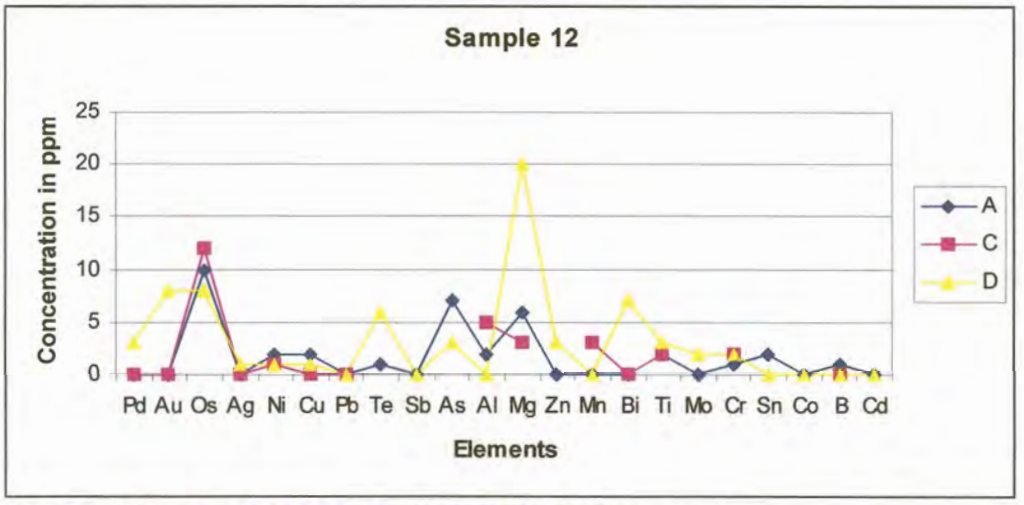


**Fig. 7.53 Sample 12 analysed by three different companies**

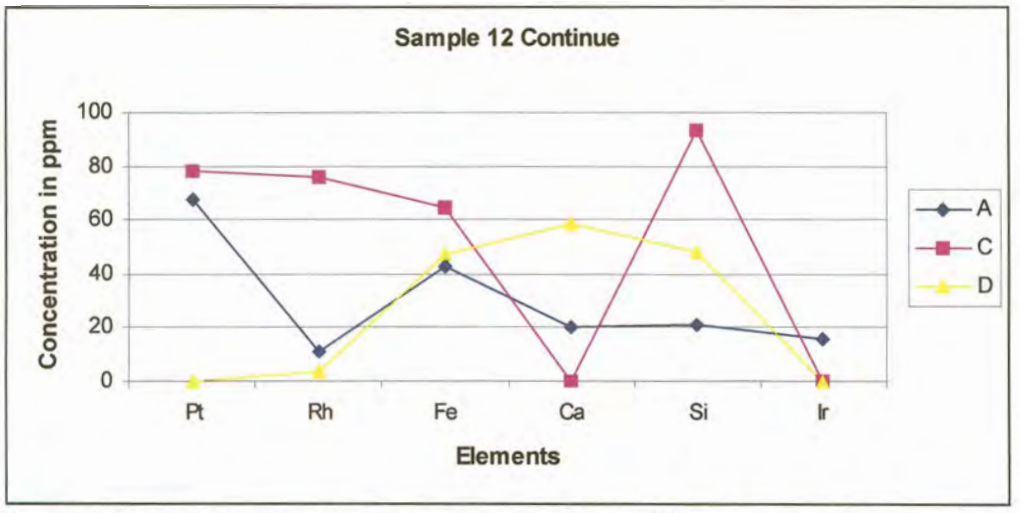


**Fig. 7.53 Continued. Sample 12 analysed by three different companies**

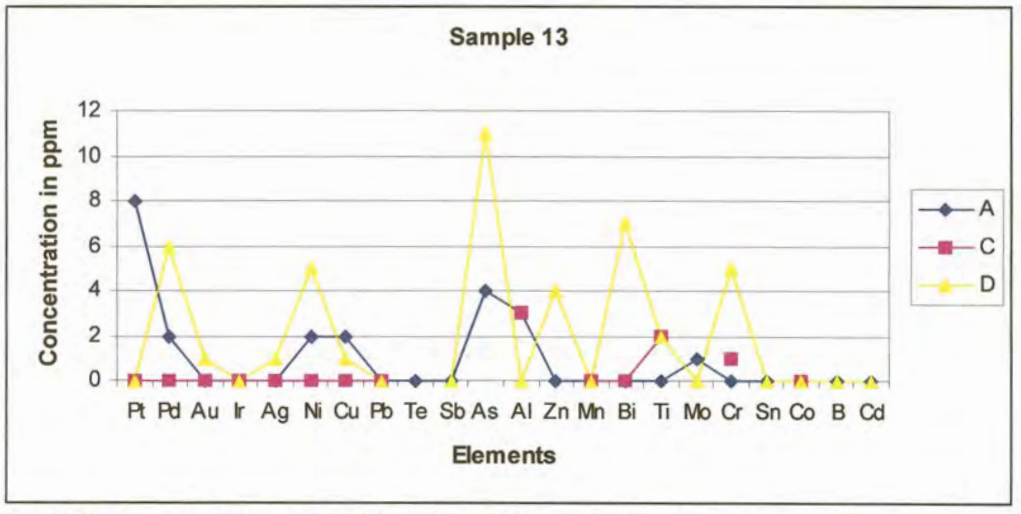


**Fig. 7.54 Sample 13 analysed by three different companies**

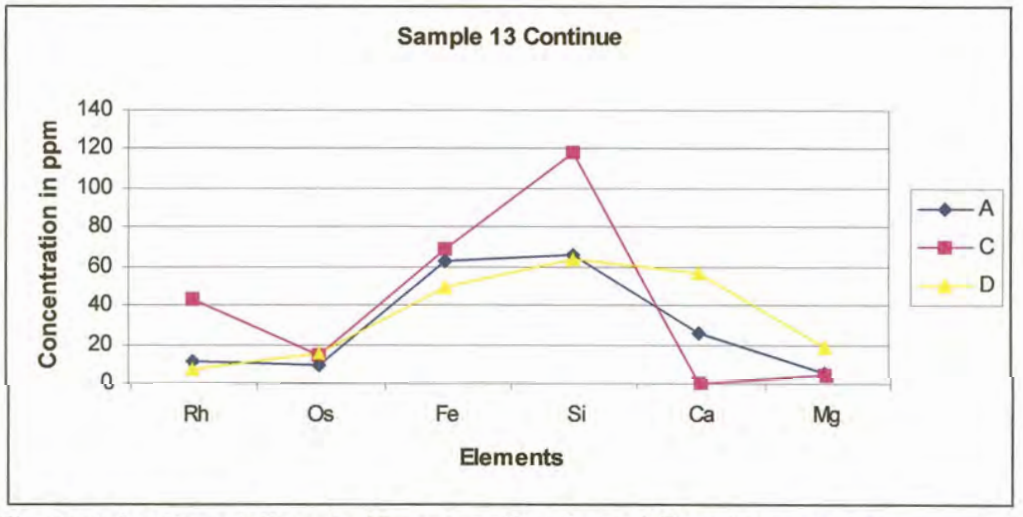


**Fig. 7.54 Continued. Sample 13 analysed by three different companies**

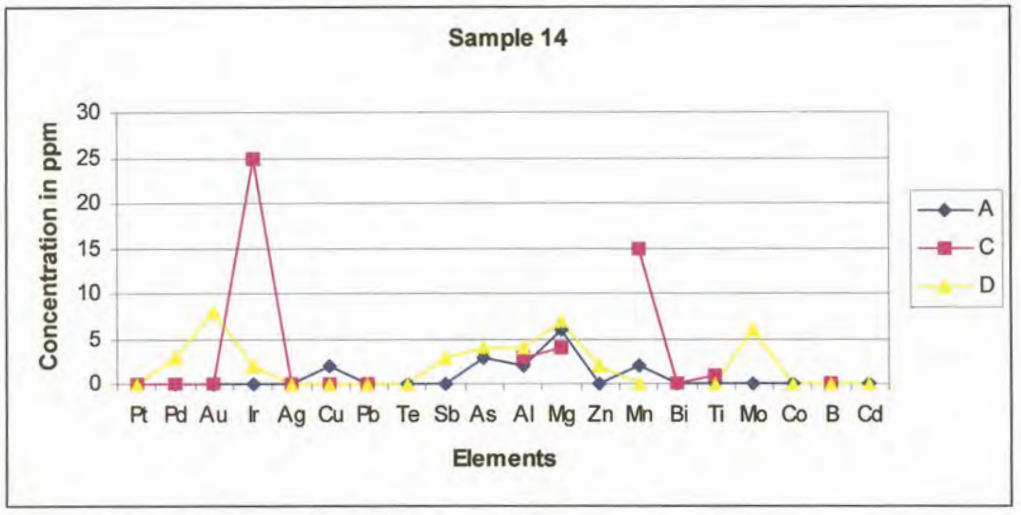


**Fig. 7.55 Sample 14 analysed by three different companies**

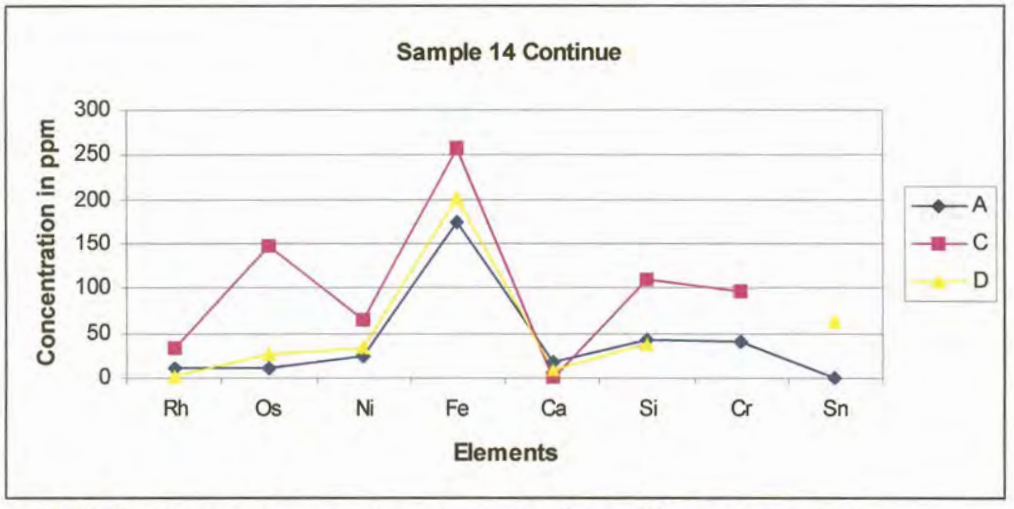


**Fig. 7.55 Continued. Sample 14 analysed by three different companies**

# Chapter 8

## Discussion of results and conclusion

### 8.1 Optimisation of parameters

#### *8.1.1 High Energy Pre-spark*

Two samples, 7 and 8, contained different elements in a Ru matrix. The samples were sparked using a high-energy spark. They were pressed and their surfaces disintegrated during sparking. To obtain a smooth surface for analysis, these samples had to be repressed during the process. The breaking up of the surface could cause a source error. When the spark was directed into an inclusion in the sample, it lead to a diffuse discharge, caused by low plasma temperatures. Equilibrium should be reached after a certain period of sparking and this is referred to as the "steady state".

The intensity of the impurities in the base elements rose continuously and became steadier after 10 seconds of sparking time. The steady state was reached when all intensities of all elements became independent of sparking time. The curve became constant during the first 10 seconds of the spark and equilibrium was reached. With the sample disintegrating, 130 µH could be used which was then similar to that of the analytical spark. If this was used, the analytical spark was extended from 5 to 10 seconds sparking time to ensure a homogenous area for analysis.

*Capacitance:* When the capacitance was investigated, the necessity was borne in mind of selecting parameters that would be suitable for all the elements. Only one parameter could be selected for all elements. It was therefore necessary to consider compromising conditions in both instances. The trends of samples 7 and 9 were evaluated together. The highest intensities achieved for the majority of the elements for

integration gives lower relative standard deviations. The general sparking conditions for the calibration used will be three times 3-second integration time per spark. In general, three sparks are used but in industry samples are sparked between six to ten times to ensure the homogeneity of the samples.

### *8.1.3 Effect of different gating parameters*

The aim was to optimise the delay conditions to reduce spectral interference from ion lines or to eliminate them so that the atom line of the element of interest appeared clearly above the background. The system had to be optimised to produce the best signal to background ratio. It was essential to investigate compromising conditions as only one parameter could be selected for all elements. The instrument made use of a 16-channel integrator board. As seen from Figure 7.19, 116 the delay times set up for the experiment were at intervals of 16 μs ranging from 16 μs (microseconds) to 176 μs. In each instance, the highest signal to background was considered as well as the time delay at 144 μs. and 160 μs. Table 8.1, 141 provides a summary of the best signal to background ratio position. The delay positions at 144 μs and 160 μs were evaluated as follows,

*Yes*: Indicated the position was similar (with in 10 % of the best position) and could be used.

*No*: Indicated this position was not suitable.

*Possible:* This position was a compromising position and could be used but was not optimal.

**Table 8.1 Summary of best and compromised Signal to Background ratio position**

| Channel | Best S/B | Delay 144 μs | Delay 160 μs |
|---|---|---|---|
| Pt 1Ω | 160 | Yes | Yes |
| Pt 15 Ω | 144 | Yes | Yes |
| Pd 1Ω | 144 | Yes | No |
| Pd 15Ω | 176 | Yes | No |
| Au 1Ω | 160 | Yes | Yes |
| Au 15Ω | 176 | Yes | Yes |
| Rh 1Ω | 160 | Yes | Yes |
| Rh 15Ω | 176 | Yes | Yes |
| Ir 1Ω | 160 | Yes | Yes |
| Ir 15Ω | 144 | Yes | Yes |
| Sb 1Ω | 144 | Yes | Yes |
| Sb 15Ω | 144 | Yes | Yes |
| Ag 1Ω | 144 | Yes | Yes |
| Ag 15Ω | 144 | Yes | Yes |
| Pb 1Ω | 144 | Yes | Yes |
| Pb 15Ω | 144 | Yes | Yes |
| Mn 1Ω | 160 | Yes | Yes |
| Mn 15Ω | 160 | Possible | Yes |
| Cr 1 Ω | 160 | Yes | Yes |
| Cr 15 Ω | 160 | Yes | Yes |
| Co 1Ω | 160 | Yes | Yes |
| Co 15Ω | 176 | Yes | Yes |
| Cu 1Ω | 144 | Yes | Possible |
| Cu 15 Ω | 144 | Yes | Yes |
| Fe 1Ω | 144 | Yes | Yes |
| Fe 15 Ω | 160 | Yes | Yes |
| Al 1Ω | 144 | Yes | Yes |
| Al 15 Ω | 144 | Yes | Yes |
| Mo 1Ω | 160 | Yes | Yes |
| Mo 15 Ω | 176 | Yes | Yes |
| Ni 1Ω | 176 | Yes | Yes |
| Ni 15 Ω | 160 | Yes | Yes |
| Bi 1Ω | 144 | Yes | Yes |
| Bi 15 Ω | 160 | Yes | Yes |

**Table 8.1 Continued. Summary of best and compromised Signal to Background ratio position**

| Channel | Best S/B | Delay 144 μs | Delay 160 μs |
|---|---|---|---|
| Mg 1 Ω | 112 | Yes | Yes |
| Mg 15 Ω | 48 | Yes | Yes |
| Na 1Ω | 80 | No | No |
| Na 15Ω | 16 | No | No |
| Ca 1Ω | 144 | Yes | Yes |
| Ca 15Ω | 160 | Yes | Yes |
| Si 1Ω | 144 | Yes | Yes |
| Si 15Ω | 144 | Yes | Yes |
| Sn 1Ω | 32 | Yes | Yes |
| Sn 15Ω | 64 | Yes | Yes |
| As 1Ω | 144 | Yes | Yes |
| As 15Ω | 144 | Yes | Yes |

There was an insignificant difference between 144 μs and 160 μs for Pt.
Pd shows a significant difference between 144 μs and 160 μs. The "No" in Table 8.1, 141 does not mean it could not be analysed at that particular point. It is an indication that the S/B ratio for 144 μs was significantly higher than at 160 μs. Au had a slightly higher S/B ratio at 160 μs. but was very similar to that of 144 μs. Rh overall had a higher S/B ratio at all positions, the best at 160 μs for 1 Ω and 176 μs for 15 Ω, but acceptable at 144 μs. Insignificant differences were found in the S/B ratio for Ir, Sb and Ag.

Mn, Cr and Co had their best S/B ratio at a delay time of 160 μs. There was a significant difference between 144 μs and 160 μs, however, if compromising conditions of 144 μs were to be used, the analysis could be done at 144 μs since the S/B ratio at this position was still higher than the previous eight positions (from 16-128 μs).

Cu seemed to peak at 64 μs and then again at 144 μs There was a significant difference between 144 μs and the 160 μs position for Cu. Fe and Bi had their best S/B

ratio at 144 μs delay for 1 Ω and for 15 Ω at 160 μs. This was, however, very similar and the optimum condition was taken as 144 μs Al, Si and As had their best S/B ratio at 144 μs Mo and Ni tended to have increased S/B ratio's at the longer delay times of 160 μs and 176 μs. The difference between these and 144 μs. was insignificant. Na's best S/B ratio was confirmed to be at 80 μs delay time for 1 Ω and 16 μs. for 15 Ω. The "No" in the table showed a significant difference between the 80 μs and 16 μs delay position and 144 μs and 160 μs however, as compromising conditions had to be considered, there was an insignificant difference between 144 μs and 160 μs.

Ca had its highest S/B ratio at 144 μs for 1 Ω and 160 μs for 15 Ω, but both positions could be used for analysis. Sn had its best S/B ratio at 32 and 64 μs delay, however, this was an insignificant difference from the 144 and 160 μs delay. 144 μs will be used as the compromised conditions for the calibration.

Table 8.2, 144 is a summary of the channels at 1 Ω and 15 Ω to identify the highest signal to background (S/B) ratio. This table indicates the highest S/B ratio or similar if there was no significant difference. The signal to background ratio was evaluated at 144 μs delay time.

The highest S/B ratio gives an indication of the highest S/B at 1 Ω or 15 Ω and "similar" means they were similar in intensities. The "similar" column gives an indication of, the extent to which the S/B ratio differs at 1 Ω and 15 Ω. "Yes", means they are similar, "double" is an indication that the S/B ratio was double at the best position as indicated in the corresponding "Highest S/B ratio" column. In 16 instances, 1 Ω resistance gave the best S/B ratio. Rh, Ag, Mg, Ca, Mg, Si and As gave similar S/B ratios at 15 Ω resistance. The signal to background ratio was double at 1 Ω resistance than at the 15 Ω for Ag, Pb, Mn, Co, Bi, Fe, Al and Mo. Na was about ten times higher at 1 Ω resistance than at the 15 Ω. There was no significant difference for Pt, Au, Ir, Sb, Cr and Sn between the 1 Ω and 15 Ω resistance, their S/B ratios being very similar. The

resistance at 15 Ω gave better S/B ratio for Pd, Ni and Cu. The S/B ratio was similar for Pd and Ni but gave an approximately 40 % better S/B ratio for Cu. Therefore, we could use the 1 Ω resistance for the calibration of the impurities in Ru base.

**Table 8.2 Summary of highest Signal to Background ratio between 1 and 15 resistance used**

| Channel | Highest S/B Ratio | Similar |
|---|---|---|
| Pt | Similar | Yes |
| Pd | 15Ω | Yes |
| Au | Similar | Yes |
| Rh | 1Ω | Yes |
| Ir | Similar | Yes |
| Sb | Similar | Yes |
| Ag | 1Ω | Yes |
| Pb | 1Ω | Yes |
| Mn | 1Ω | Double |
| Cs | Similar | Yes |
| Co | 1Ω | Double |
| Cu | 15Ω | 40% higher |
| Fe | 1Ω | Double |
| Al | 1Ω | Double |
| Mo | 1Ω | Double |
| Ni | 15Ω | Yes |
| Bi | 1Ω | Double |
| Mg | 1Ω | Yes |
| Na | 1Ω | 10 times |
| Ca | 1Ω | Yes |
| Si | 1Ω | Yes |
| Sn | Similar | Yes |
| As | 1Ω | Yes |

### *8.1.4. Internal standardisation*

Where the instrument was not equipped with a Ruthenium reference line in the optic, a background position was selected. There is a background position in the Ultra-violet

optic and the analytical line is ratioed to a background position. Reference lines were used in the air optics and used as the internal standard in the calibration.

### *8.1.5 Analytical gap*

Overall there seemed to be no significant difference between the 3 mm and 4 mm analytical gap (distance between the sample and tungsten electrode), with the exception of Ag where the 4 mm gap gave an increased signal to background ratio (double that of the 3 mm gap). The signal to background ratio of Sn was double using the 3 mm gap and a higher S/B ratio was obtained for Cu at the 3 mm position. Since there was no significant difference and the suppliers installed the instrument with a 4 mm analytical gap, the calibration was performed using a 4 mm analytical gap.

### *8.1.6 Contamination from other base material*

From Table 7.3, 124 it can be seen that when a Platinum (Pt) sample was sparked for analysis immediately after a Ruthenium (Ru) sample, contamination occurred. Ru was monitored as an impurity in the Pt sample. The sample was sparked in excess of ten times before a stable signal for Ru could be obtained. When a Palladium (Pd) sample was sparked immediately after the Platinum and Pt was monitored, the Pt signal only became stable after six sparks. When Ru sample was sparked and Pd monitored as an impurity in the Ru, the signal became stable only after ten sparks. It can therefore be concluded that there was cross contamination between the various bases when sparking pure samples. Between seven to ten sparks were required when changing to another base without changing the spark plate, electrode, electrode spring, glass ring and cleaning the spark chamber.

The results from Table 7.4, 124 indicated much less cross contamination between the samples when the spark stand chamber was cleaned and a Pt base plate, with electrode, electrode spring, and glass ring was used when analysing for impurities in a

pure Pt sample. After three sparks the results became constant. It was therefore standard procedure to clean the spark chamber, change the spark stand plate for the pure samples for analysis as well as all its accessories and to use these when analysing for different pure samples. Each base material (pure sample) must have its own equipment for analysis to avoid cross contamination.

### *8.2 Calibration*

The calibration is performed using the optimal or compromised conditions as determined during the test work. Table 8.3, 147 provides a summary of the limits of detection obtained for the various wavelengths used to determine the impurities in pure Ru (> 99.9 %). This table also indicates typical LOD used for the traditional spectrograph analysis. Elements indicating ND (not detected) are generally too low to be analysed by the technique.

**Table 8.3 Limits of detection (LOD) in parts per million (ppm) obtained from calibration graphs and traditional LOD**

| Elements | Wavelength (nm) | LOD in ppm SAFT | Traditional LOD |
|---|---|---|---|
| Ag | 338.289 | 0.01 | <1 |
| Al | 396.153 | 0.24 | <10 |
| As | 234.984 | 0.26 | ND |
| Au | 267.595 | 0.15 | <1 |
| Bi | 306.772 | 0.93 | <1 |
| Ca | 422.673 | 0.31 | <10 |
| Cd | 228.802 | 0.56 | <10 |
| Co | 345.351 | 0.11 | ND |
| Cr | 425.435 | 0.04 | ND |
| Cu | 324.754 | 0.07 | <1 |
| Fe | 371.994 | 0.93 | <10 |
| Ir | 351.364 | 0.45 | <10 |
| Mg | 285.213 | 0.12 | <1 |
| Mn | 403.449 | 0.11 | <1 |
| Mo | 386.411 | 0.72 | ND |
| Na | 588.995 | 0.27 | <10 |
| Ni | 361.939 | 0.24 | <1 |
| Os | 581.812 | 0.03 | <10 |
| Pb | 283.307 | 1.30 | <10 |
| Pd | 340.458 | 0.72 | <10 |
| Pt | 531.89 | 0.13 | <10 |
| Rh | 343.489 | 0.86 | <10 |
| Sb | 206.83 | 0.85 | <10 |
| Si | 288.16 | 2.00 | <10 |
| Sn | 317.502 | 0.84 | <1 |
| Te | 214.275 | 0.21 | <10 |
| Ti | 498.173 | 0.67 | <10 |
| Zn | 213.856 | 0.05 | ND |

## *8.3 Comparison of samples analysed*

A sample, referred to as a "Round Robin", was analysed by seven different companies nationally and internationally, using different techniques. Due to the confidentiality of these results, they are displayed in a graphical format rather than in a table. The analysis as indicated in Fig. 7.41, 126 is a comparison of all the results.

"A" is the analysis of the spark emission using the time resolved spectroscopy, referred to as the SAFT (Spark Analysis for Traces) technique. Companies A and D did the analyses for all the elements, but the other companies did not, or did not report all the results.

The A analysis for Pt is 20 % lower than D and F, Fe was much lower than the average and Al higher than average. The Ca is higher than D and E but the same as F and Si is the closest to the average. The remaining elements all compared with the other methods, which were used. The results in Table 7.8, 127 show that the maxima and the minima values for each of the samples analysed by different techniques, all lie between +2 standard deviations and -2 standard deviations from the average. This means that, at 95 % confidence levels, there are no significant differences between the results. It is important to analyse as many elements as possible as the technique sums up all the impurities and subtracts this sum from 100 % to determine the purity of the metal. As indicated in Table 7.7, 127 the purity obtained using the SAFT technique compares well with the existing methods of analysis

The results of 14 other samples, which were analysed as interchange samples between Platinum Refineries in South Africa, were compared. The Spark Emission analysis, as indicated by A, is compared to traditional spectrographic analysis, B and D (same technique, different company), and inductively coupled plasma indicated by C.

The analysis of Fe, Ca and Si seems to have scattered values for most of the samples. In comparison to the other techniques, the results obtained for the spark emission technique making use of time resolved spectroscopy, compare very well with the established techniques. This technique takes only a fraction of the time for analysis and there is no dilution or dissolution involved. This technique has been introduced very successfully in the Precious Metals industry for the analysis of impurities in Pt, Pd, Au and Ag. Rh, Ru and Ir are much more complicated due to the lack of availability of reference materials and the high melting point of Ru and Ir.

**Table 8.4 Comparison of interchange samples analysed by four different companies. A = Spark Emission (using time resolved spectroscopy), B = Spectrographic Analysis, Company A, C = Inductively coupled Plasma and D = Spectrographic Analysis, Company B**

| Sample | Variances between the different techniques | | |
|---|---|---|---|
| | Higher Elements | Lower elements | Technique |
| 1 | Rh Fe | Si | D |
| 1 | | Fe Rh | A |
| 2 | | Pt Si | C |
| 2 | Rh Fe | Ir Ca Al | D |
| 3 | Ca | Si | C |
| 3 | Fe | | D |
| 4 | Pt Pd Ir Al Sn | | A |
| 4 | Au Cr | | C |
| 4 | Fe Si | Pt Cd | D |
| 5 | Rh | | A |
| 5 | Ca Si | Pt | C |
| 5 | Rh Fe Si | Ca | D |
| 6 | Ca | Fe | C |
| 6 | Rh Si | Ca | D |
| 7 | Os Fe Si Cr | | D |
| 8 | Pt | | B |
| 8 | Sb | Si | C |
| 8 | Ir | Pt Fe | D |
| 9 | Ni Fe | | B |
| 9 | Au Te Mn Bi Ti Mo Cr Cd | Ca | C |
| 10 | Compares well | | A D C |
| 11 | Si | Os | A |
| 11 | Os | As | C |
| 11 | Si Fe Ca | | D |
| 12 | Ir | Si | A |
| 12 | Rh Si Fe | Ca | C |
| 12 | Ca | Pt | D |
| 13 | Rh Si | Ca | C |
| 13 | Ca | | D |
| 14 | | Cr | A |
| 14 | Rh Ir Os Fe Si Cr | | C |
| 14 | Sn | | D |

## 8.4 Conclusion

The analysis for the determination of the purity of the precious metals was very important, as this has a direct impact on the price paid for the metal (Chapter 1, 1).